CHEMISTRY IN CIRCUMSTELLAR ENVELOPES AROUND EVOLVED STARS

Lecture IV

José Cernicharo
CAB (CSIC-INTA)
Dpt. Astrophysics
Madrid. Spain

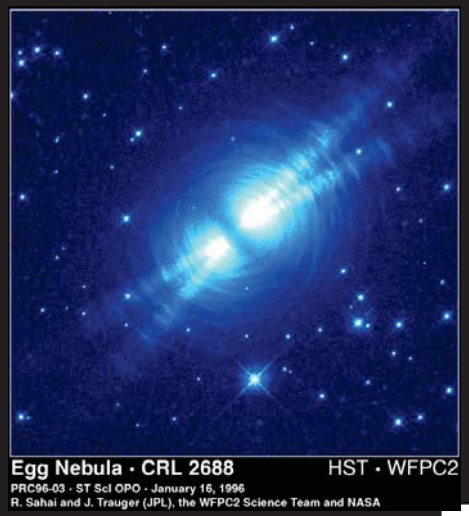

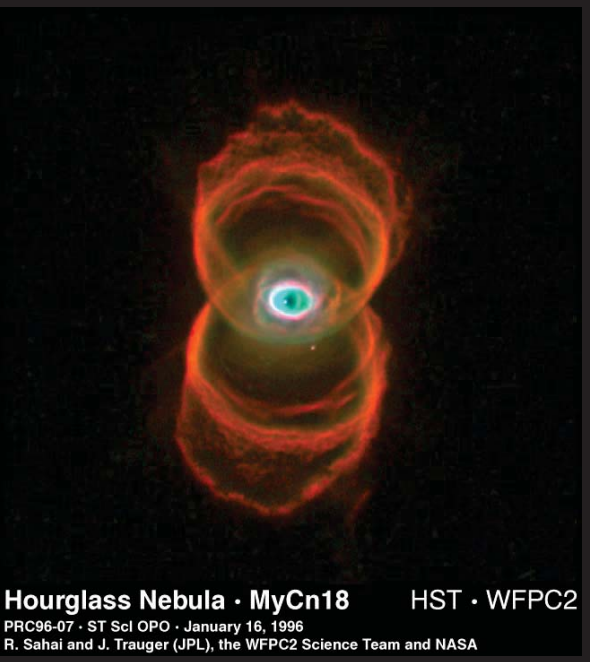

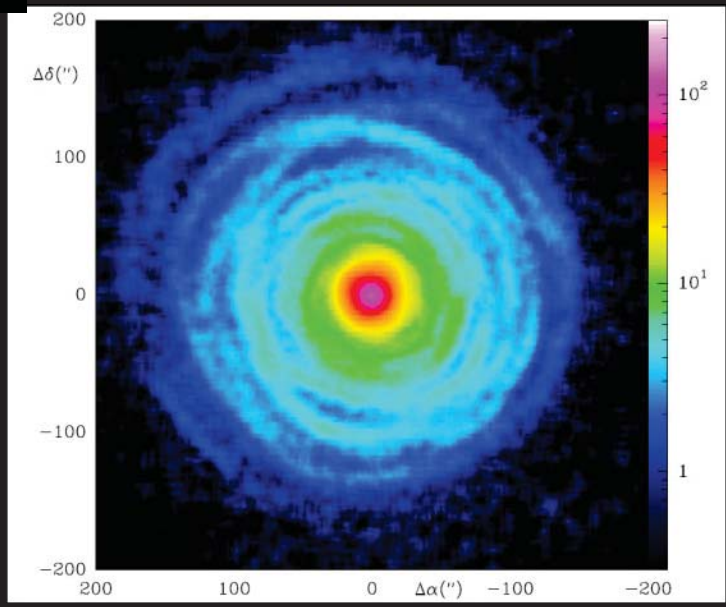

AGBs and Astrochemistry

Why Molecular Astrophysics in AGBs ?

50% of known molecular species in space detected in AGBs (most of them in IRC+10216, but also VyCMa)

Determination of the physical conditions of the gas

Determination of the molecular abundances => Chemical evolution=> Chemical Complexity=>feedback to the ISM

Determination of the dynamical evolution of circumstellar clouds

Main source of dust grains production in space

Water has been found in C- and O-rich CSM.

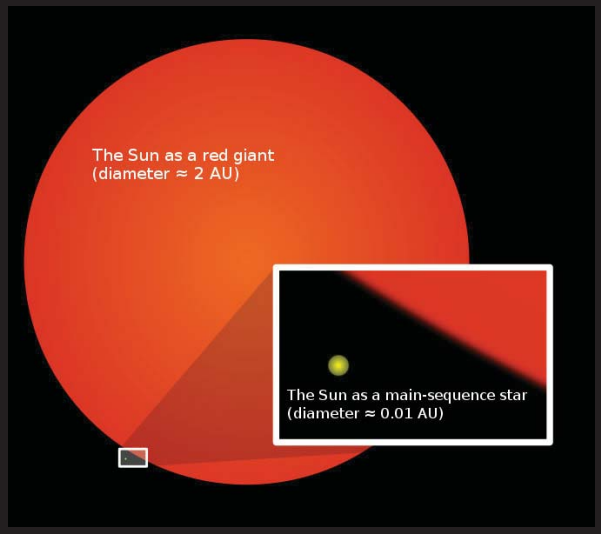

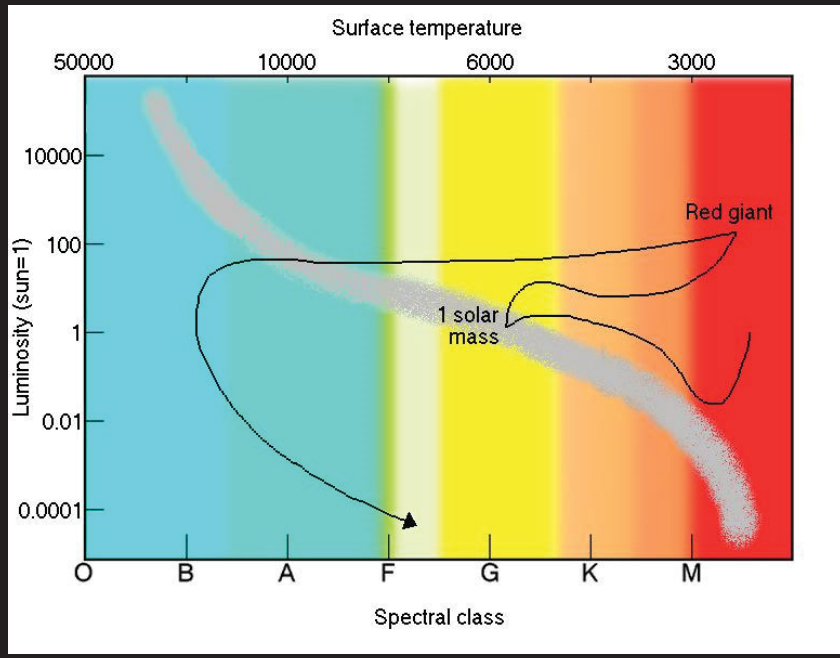

A BRIEF INTRODUCTION TO THE STRUCTURE AND EVOLUTION OF AGB STARS

CHEMISTRY UNDER THERMODYNAMICAL EQUILIBRIUM

THE DUST GRAIN FORMATION ZONE

CHEMISTRY IN THE EXTERNAL SHELLS & THE CHEMICAL EVOLUTION OF THE ENVELOPE

WATER IN C-rich AGBs

WHAT ALMA CAN DO IN THE FIELD OF EVOLVED STARS ?

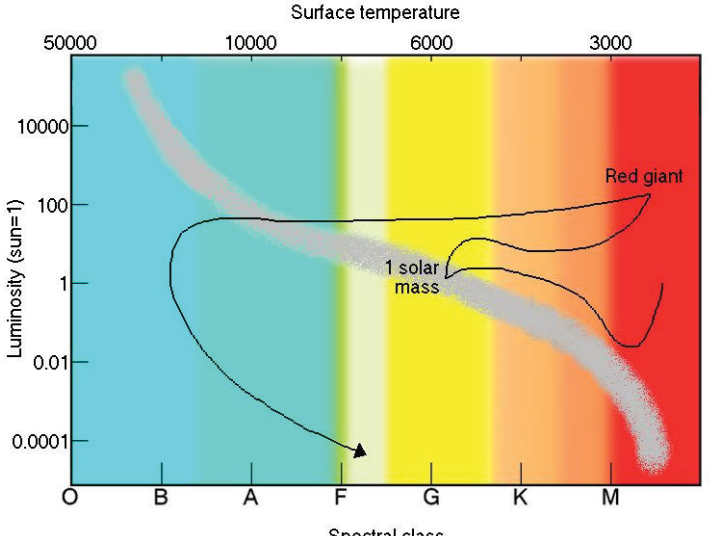

Low-Mass Star = M < 4 M_{sun}

Stages of Evolution of a Low-Mass star:

- Main Sequence star
- Red Giant star
- Horizontal Branch star
- Asymptotic Giant Branch star
- Planetary Nebula phase
- White Dwarf star

Main Sequence Phase

Energy Source: Hydrogen fusion in the core

What happens to the He created by H fusion?

- Core is too cool to ignite He fusion
- Slowly builds up an inert He core

Main-Sequence (H-burning) Lifetime:

- ~10 Gyr for a 1 M_{sun} star (e.g., Sun)
- ~10 Tyr for a 0.1 M_{sun} star (red dwarf)

Core Hydrogen Exhaustion

Inside:

- He core collapses & starts to heat up.
- H burning zone moves into a thin **shell** surrounding the core
- Collapsing core heats the H shell above it, driving the fusion faster.
- More fusion = more heating, so that Pressure > Gravity

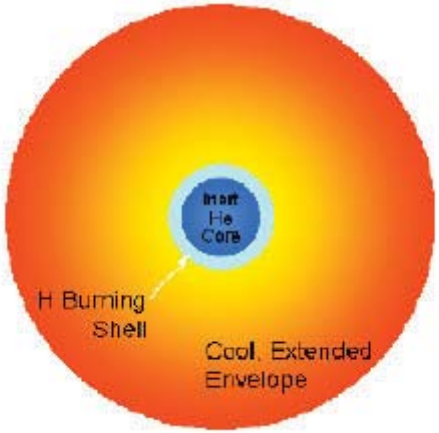

Outside:

- Envelope **expands** and **cools**
- Star gets **brighter** and **redder** & climbs up the Giant Branch.

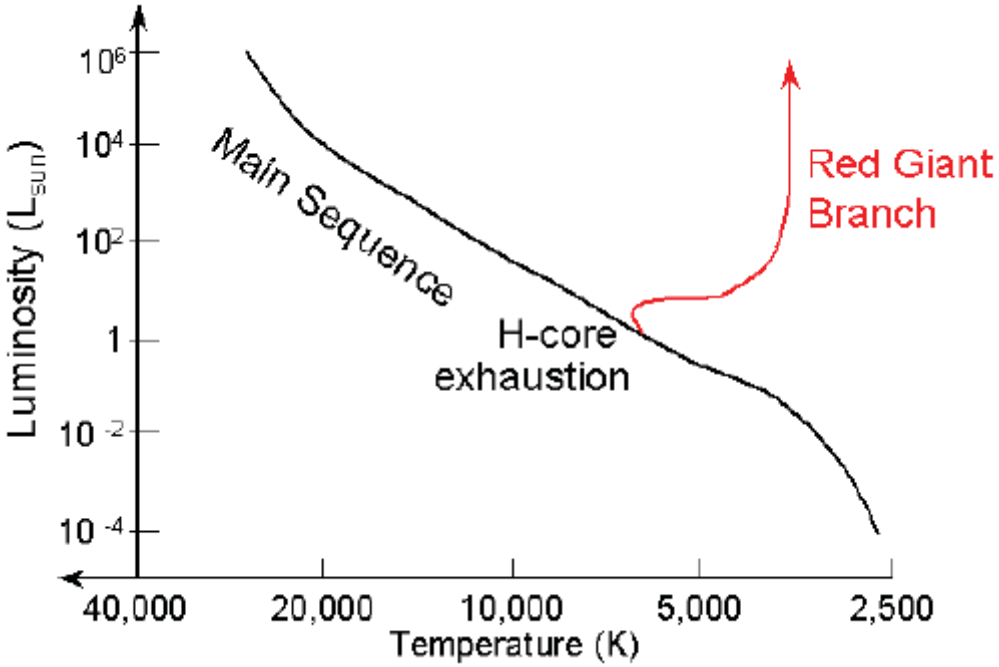

Helium Flash

At 100 Million K, a new fusion source ignites: the **Triple-alpha Process**.

This is the fusion of three ^{4}He nuclei into one ^{12}C (carbon) nucleus:

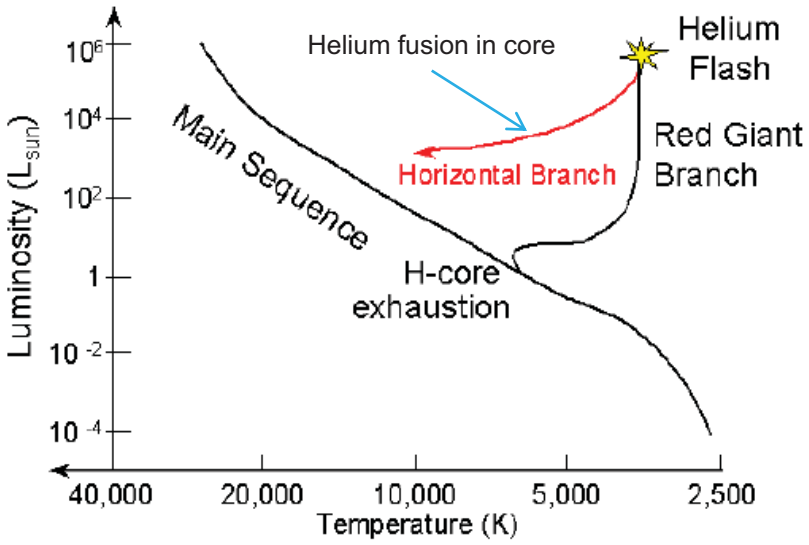

Climbing the Red Giant Branch

It takes a star about 1 Gyr to climb the Red Giant Branch

- He core contracting & heating, but no fusion
- H burning to He in a shell around the core
- Huge, puffy envelope ~ size of orbit of Venus

At the Tip of the Red Giant Branch:

- T_{core} reaches 100 Million K
- Ignite He burning in the core in a **flash**.

When this occurs, the star leaves the Giant Branch.

Inside:

- Starts generating primary energy from He burning in the **core**.
- Gets additional energy from an H burning **shell** surrounding the core.

Outside:

- Gets **hotter** and **bluer**.
- Star **shrinks** in radius, getting **fainter**.

The new energy source helps the star begin to regain Hydrostatic and Thermal Equilibrium. As it does so, it moves onto the **Horizontal Branch**.

Horizontal Branch Phase

Structure:

- He-burning core
- H-burning shell

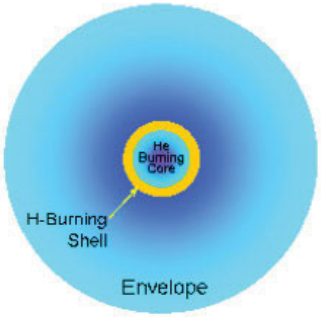

The Triple-alpha Process is very inefficient at producing energy, so it can only last for about 100 Myr.

While it goes on, the star steadily builds up a C-O core, but it is still too cool to ignite Carbon fusion

Asymptotic Giant Branch Phase

After 100 Myr, the core runs out of Helium for Triple-Alpha fusion.

Inside:

- C-O core collapses and heats up
- He burning shell outside the C-O core
- H burning shell outside the He burning shell

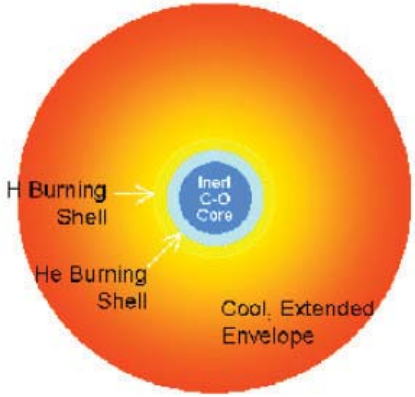

Outside:

- Star grows rapidly in radius and cools

Climbs the Giant Branch again, but at a higher effective Temperature than the Giant Branch, so it ascends with a bluer color, putting it slightly to the left of the original Giant Branch on the H-R Diagram:

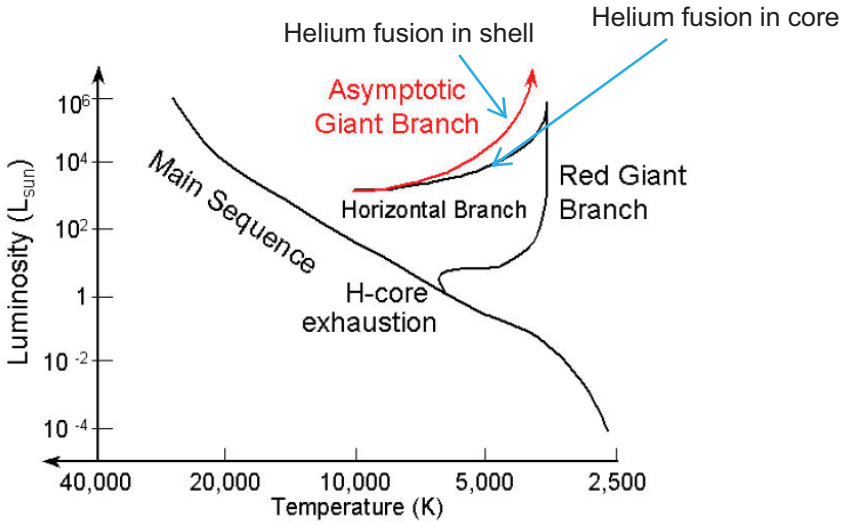

He burning is very temperature sensitive: Triple-alpha fusion rate ~ T^{40}!

Consequences:

- Small changes in T lead to
- Large changes in fusion energy output

Star experiences huge **Thermal Pulses** that destabilize the outer envelope.

Core-Envelope Separation

Rapid Process: takes ~10^5 years

Outer envelope gets slowly ejected (fast wind)

C-O core continues to contract:

- With the weight of envelope taken off, the core heats up less
- It never reaches the Carbon fusion ignition temperature of 600 Million K

Core and Envelope separate physically.

Planetary Nebula Phase

Expanding envelope forms a **nebula** around the contracting C-O core:

- Ionized and heated by the hot central core.
- Expands away to nothing in ~10^4 years.

The star briefly becomes host to a **Planetary Nebula**

The hot C-O core is exposed, and moves quickly to the left on the H-R Diagram at nearly constant luminosity and increasing temperature.

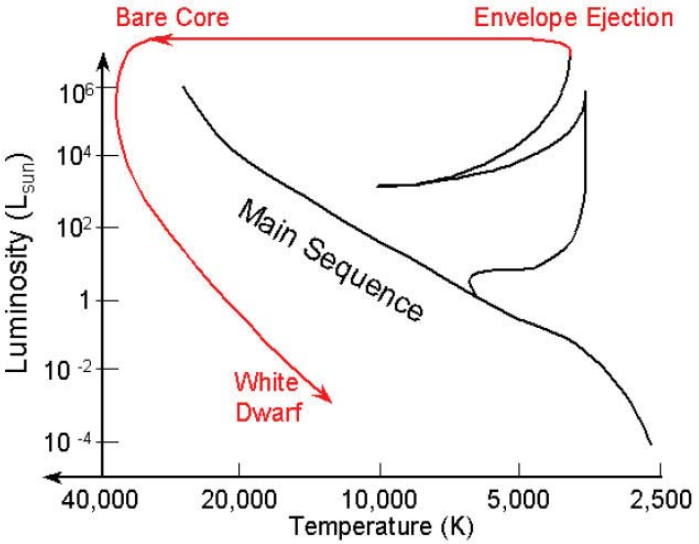

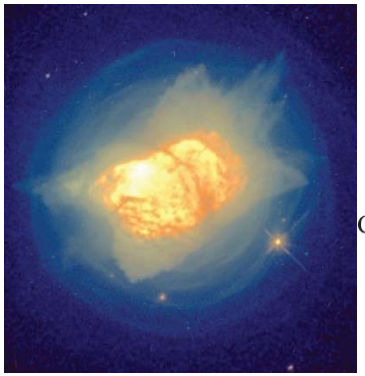

Core Collapse to White Dwarf

The contracting C-O core becomes so dense that a new gas law takes over...

Degenerate Electron Gas:

- Pressure becomes independent of Temperature
- P grows rapidly & soon counteracts Gravity

Collapse halts when R ~ 0.01 R_{sun} (~ R_{earth})

Degenerate core becomes a *White Dwarf*

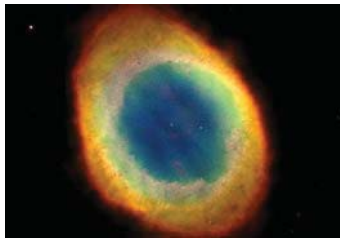

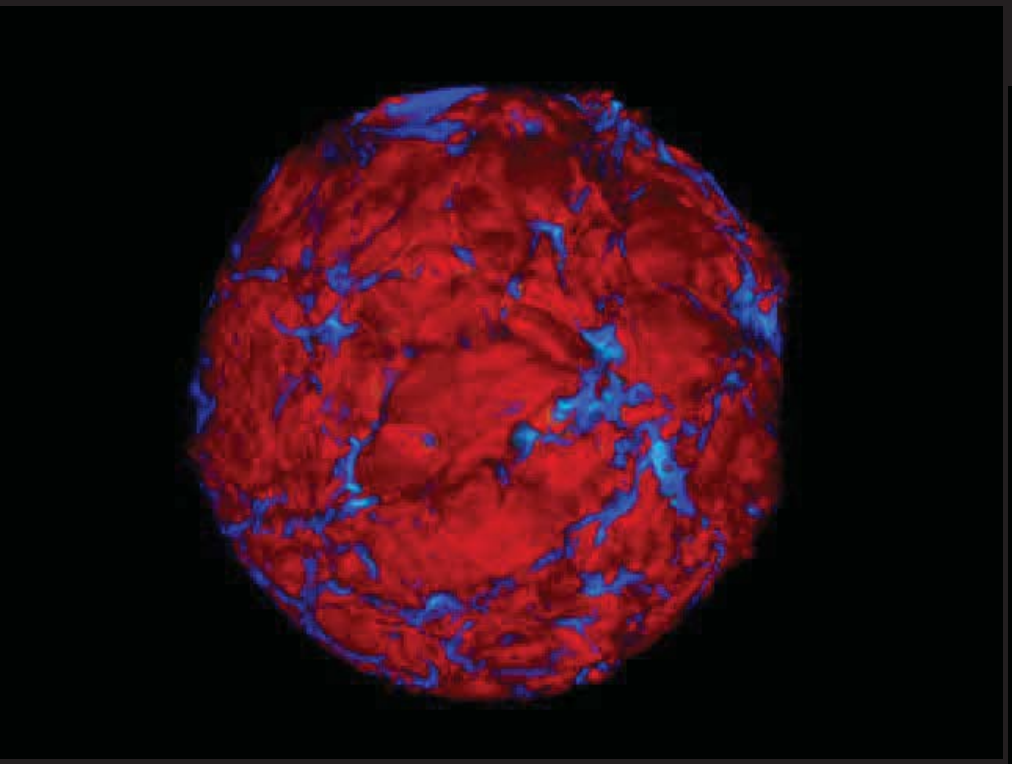

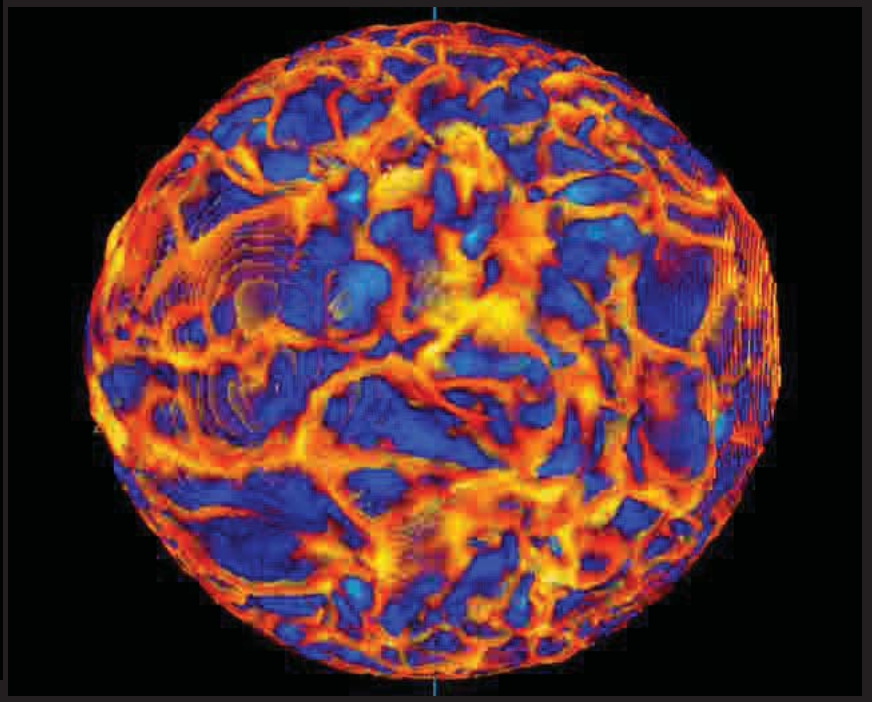

Porter et al. http://www.lcse.umn.edu/research/RedGiant/

Parameters for some well known AGB stars	Max Magnitud	Min Magnitud	Period days
Mira (o Ceti)	2	10,1	331,996
χ Cygni	3,3	14,2	408,5
R Hydrae	3,5	10,9	388,87
R Carianae	3,9	10,5	308,71
R Leonis	4,4	11,3	309,95
S Carinae	4,5	9,9	149,9
R Cassiopeiae	4,7	13,5	430,46
R Horologii	4,7	14,3	407,6
U Orionis	4,8	13	368,3
RR Scorpii	5,0	12,4	281,45
R Serpentis	5,16	14,4	356,41
R Centauri	5,3	11,8	546,2
R. Trianguli	5,4	12,6	266,9
R Leporis	5,5	11,7	427,1
R Aquilae	5,5	12	284,2
R Aquarii	5,8	12,4	386,96
U Cygni	5,9	12,1	463,24

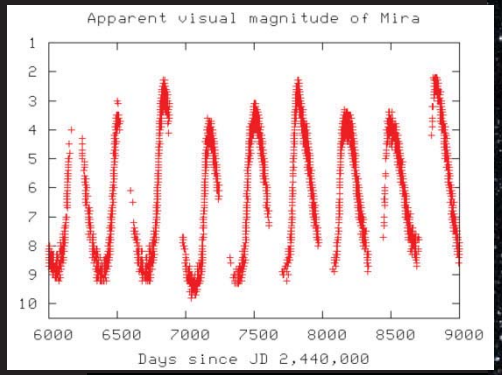

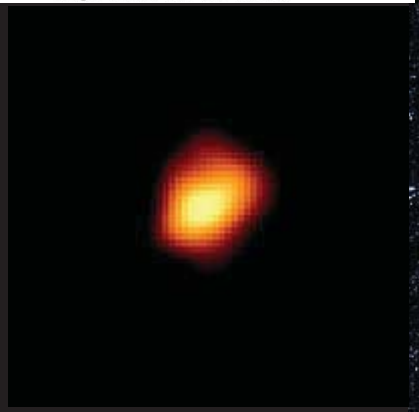

AGB stars loss mass through an isotropic wind

Extended dusty and molecular circumstellar envelope

main source for the reclycing of the ISM

strong absorption of the stellar light

Mass loss rate varies between 10^{-3}–10^{-8}

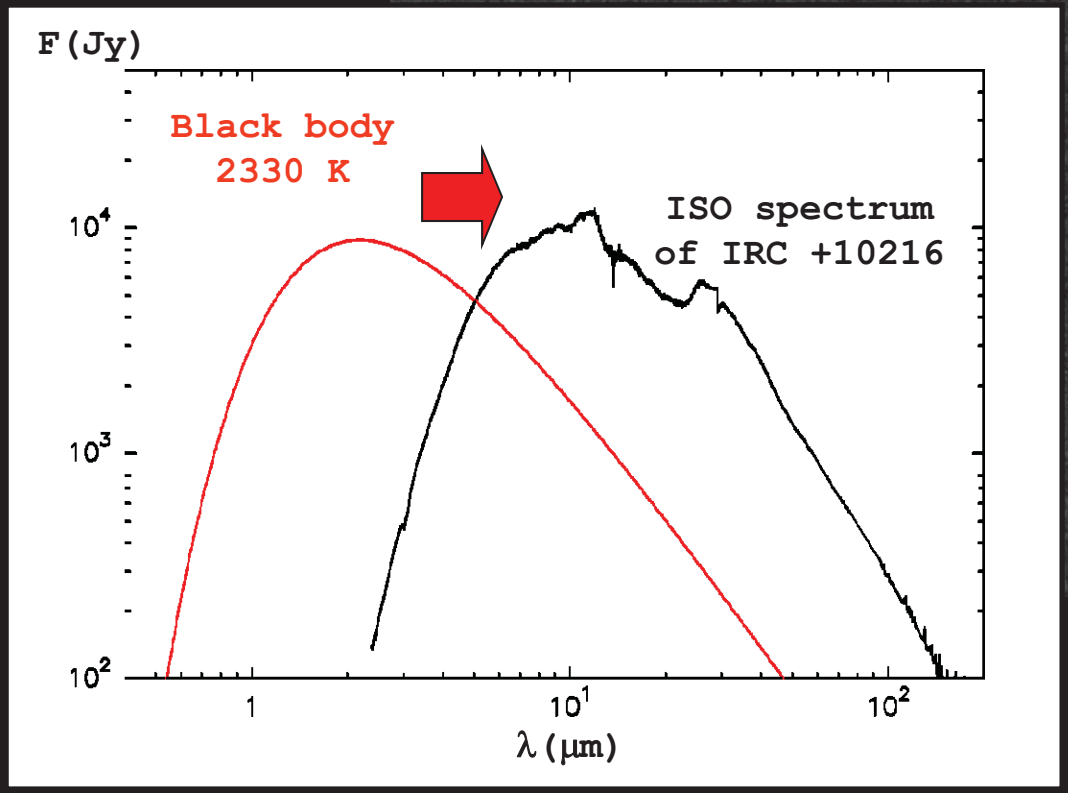

IRC +10216:

- the carbon-rich star nearest to the Earth (~120 pc)

- brightest object in the sky at λ ~5-10 nm

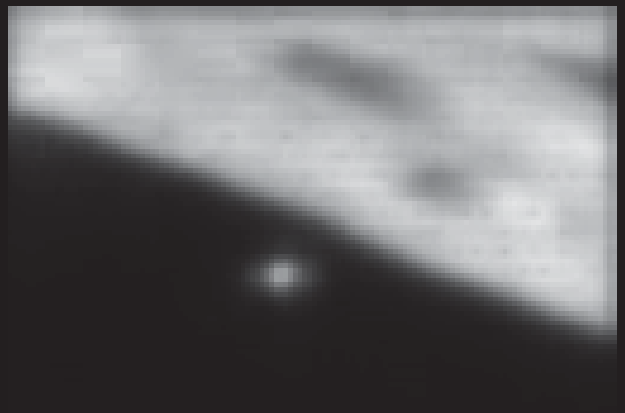

λ@10 μnm; ESO/La Silla
B. Stecklum & H.-U. Kaüfl

Chemical study of the envelope

¿Why is so interesting the study of chemical composition of IRC +10216 ?

- IRC+10216 is a prototype of C-rich stars

- 50% of the molecules known in space have been detected in its CSE

The Extended Molecular envelope : The millimeter domain

Two type of molecules:

I) Species formed under thermodynamical equilibrium near the photosphere

II) Species formed in the photodominated zone (the external shells of the envelope

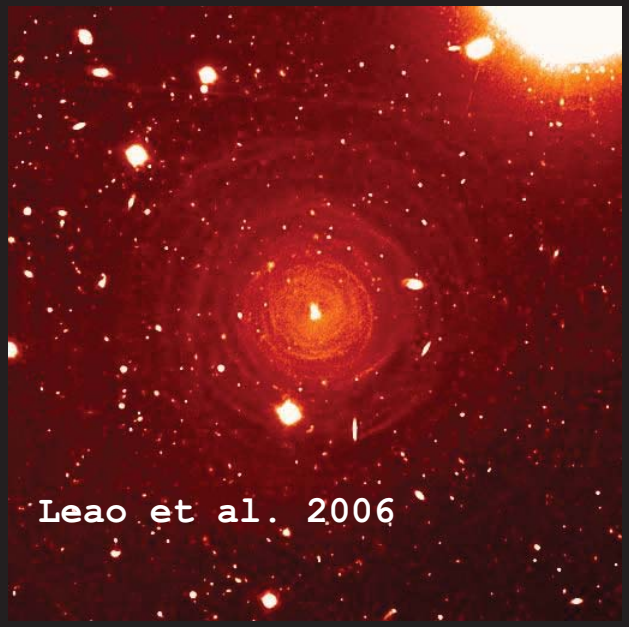

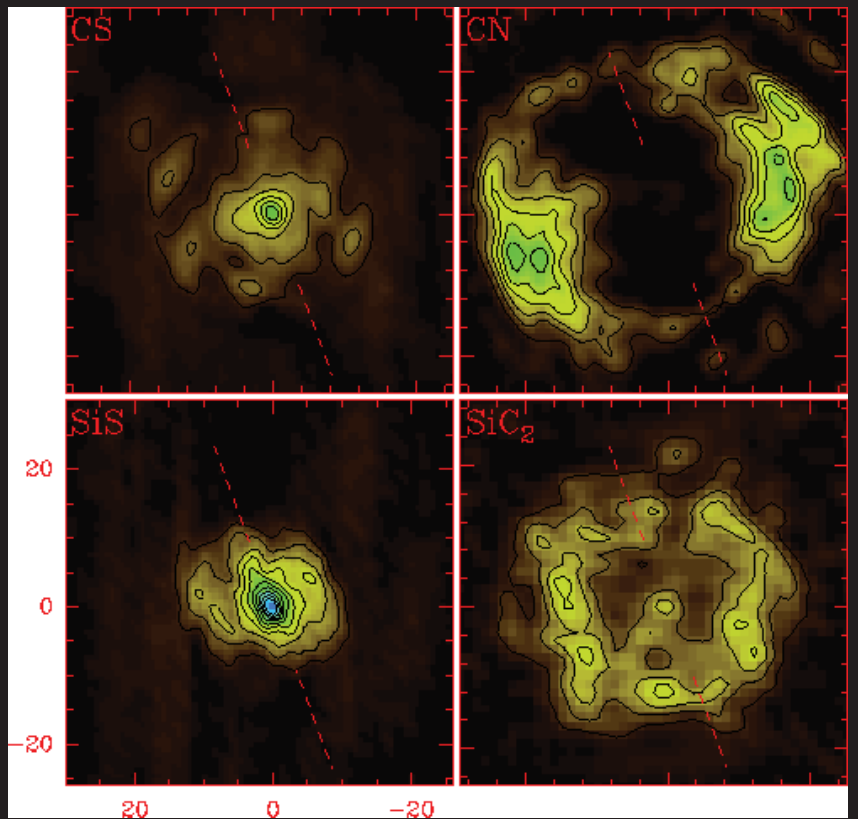

IRC+1021 6 (CW Leo) V=Vsys

(Guélin et al. 1998)

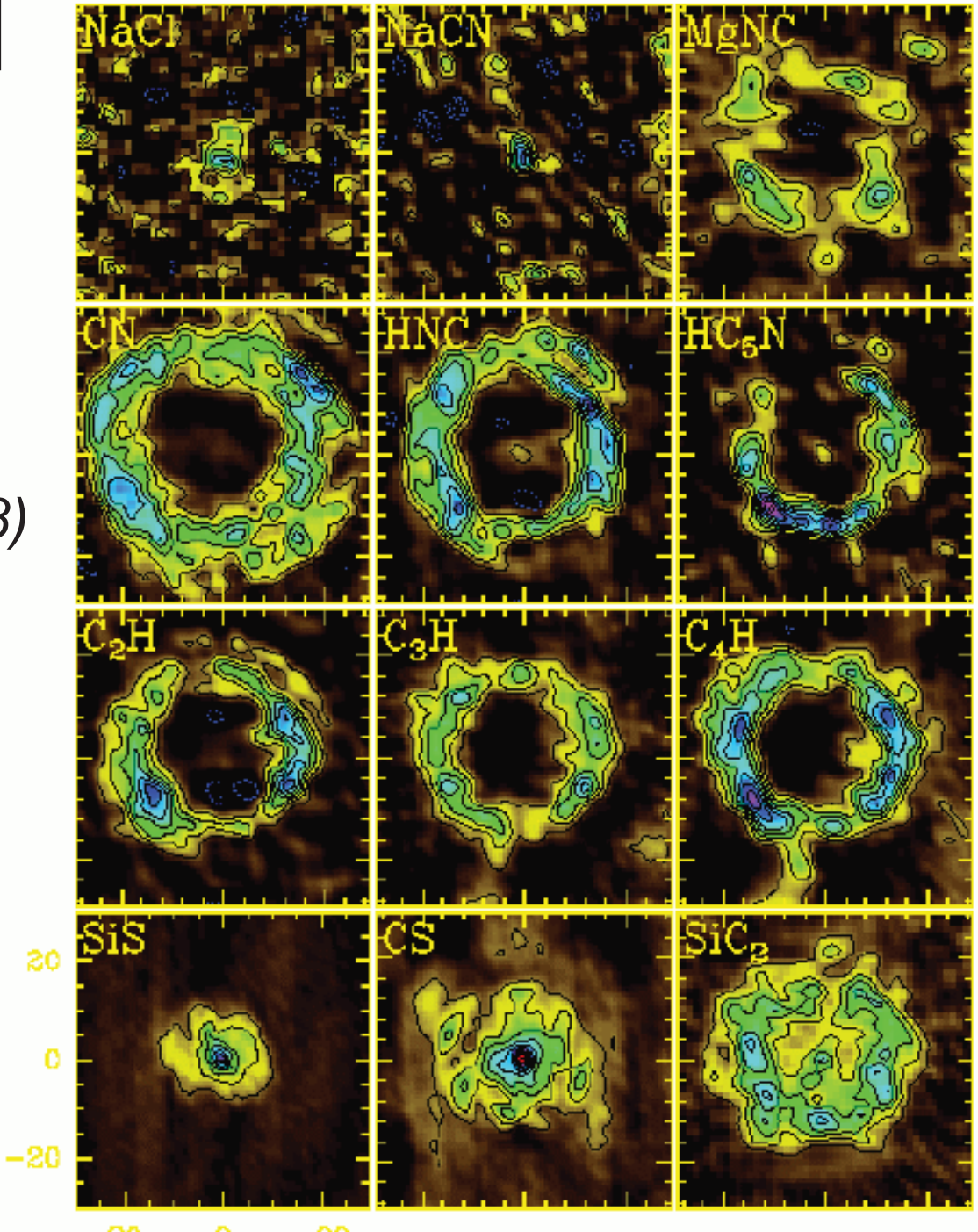

The large scale structure of an AGB star.

CO J=2–1 with the 30m IRAM radiotelescope

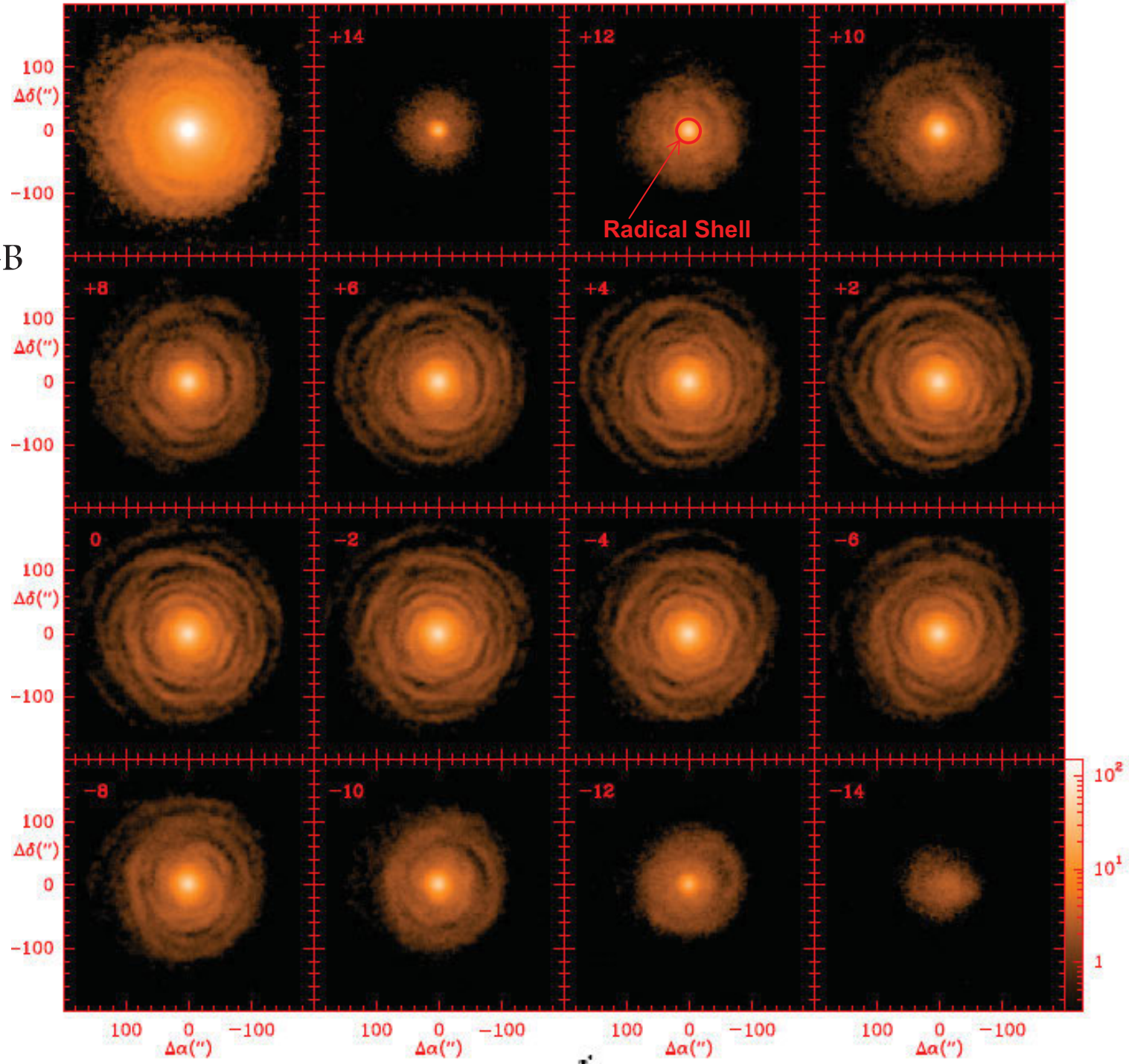

CSE AROUND EVOLVED STARS: BASIC CONCEPTS

* In the last stage of the star evolution stars are submitted to different processes of mass loss.

* The mass loss rate, dM/dt, can be as high as 10^{-4} M_O yr^{-1}.

* AGB stars inject into the ISM dust grains, molecules and heavy elements (^{12}C, ^{13}C, N, ^{17}O, ^{18}O,...)

*AGB stars inject momentum and energy into the ISM. O and B stars play a much more important role in this context but not in the chemical aspects.

* ¿ Which is the structure of an evolved star ?

The structure of the envelope depends on the distance to the star. The chemical composition will depend on the relative abundance of the atoms.

In the inner layers the abundance of C/O could be very different from the external layers because the gas is continuously enriched by the ejection of matter from the central object.

if C/O > 1 stars rich in Carbon
if C/O < 1 stars rich in Oxygen
if C/O ≈ 1 stars S

Photosphere : Temperature < 3000 K.
Very complex physical processes. Pulsation. Shocks

Theoretical values for isotropic mass loss rate :

Mass loss

$$\dot{M}(r) = n(r)\mu 4\pi r^2 V(r)$$

Density

$$n(r) = \frac{C}{r^2}(V_\infty / v(r)) \qquad \mathrm{cm}^{-3}$$

$$C = 3 \cdot 10^{37} \frac{\dot{M}_{-5}}{V_6} \qquad \mathrm{cm}^{-1}$$

Temperature

$$T \sim 100 \left(\frac{r}{10^{16}}\right)^{-0.7} \mathrm{K}$$

Velocity field

$$v(r) = V_\infty \left(1 - \frac{0.984 r_\circ}{r}\right)^{1/2}$$

R (cm)	T °K
$6\ 10^{14}$	450
10^{15}	370
10^{16}	140
10^{17}	60

At 10 stellar radii ($R_* \approx 6.7\ 10^{13}$ cm) the temperature is 450 K while in the zone of 1-2 stellar radii the gas must be at a temperature close to 1500 K. The density in innermost zone is of the order of $10^{10\text{-}12}$ cm^{-3}.

However, at 10 stellar radii is only of $10^{8\text{-}9}$ cm^{-3} and at 100 stellar radii of 10^{6} cm^{-3}.

The evolution time scale for the envelope is given by

$$\tau_{din} = r/v = 10^9 \left(\frac{r_{15}}{V_6}\right)$$

r_{15} and V_6 are the distance and velocity (units of 10^{15} cm, 10^{6} cm/s) For r_{15} = 1-100 and V_6 = 1 the dynamic time scale varies between 30 and 3000 years

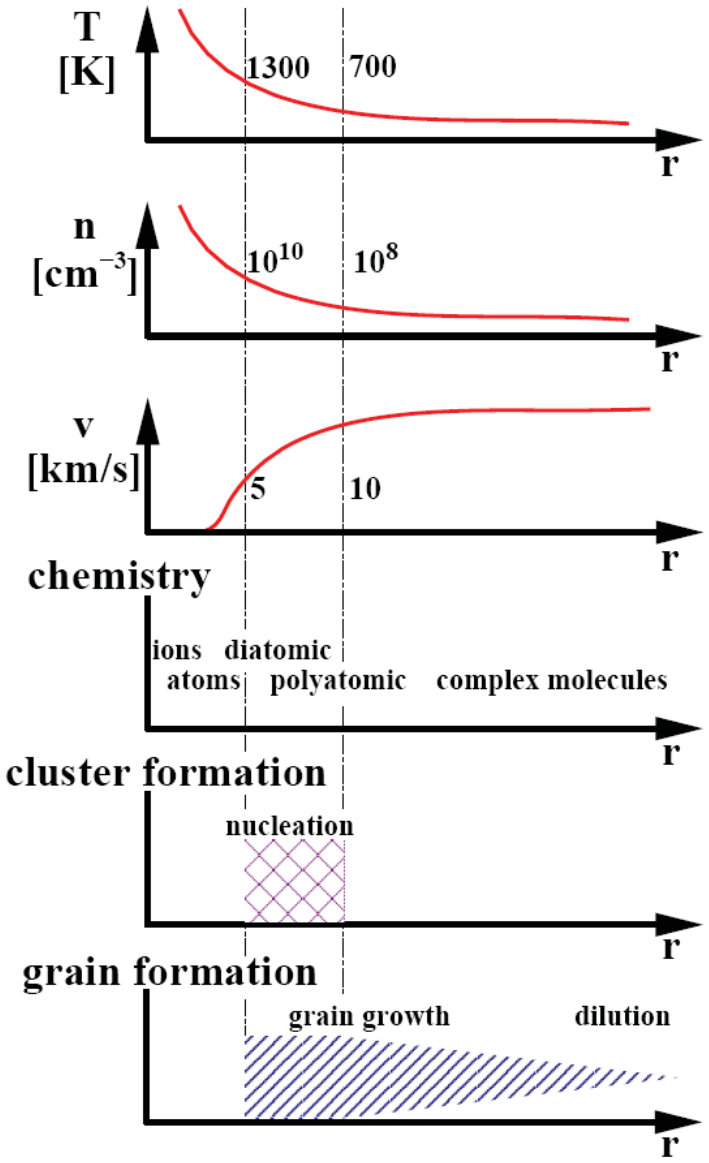

Figure 1. Schematic structure of a dust forming circumstellar shell. Dust nucleation is well confined to a region approximately between 1300 K and 700 K while the region of dust growth extends much farther outwards.

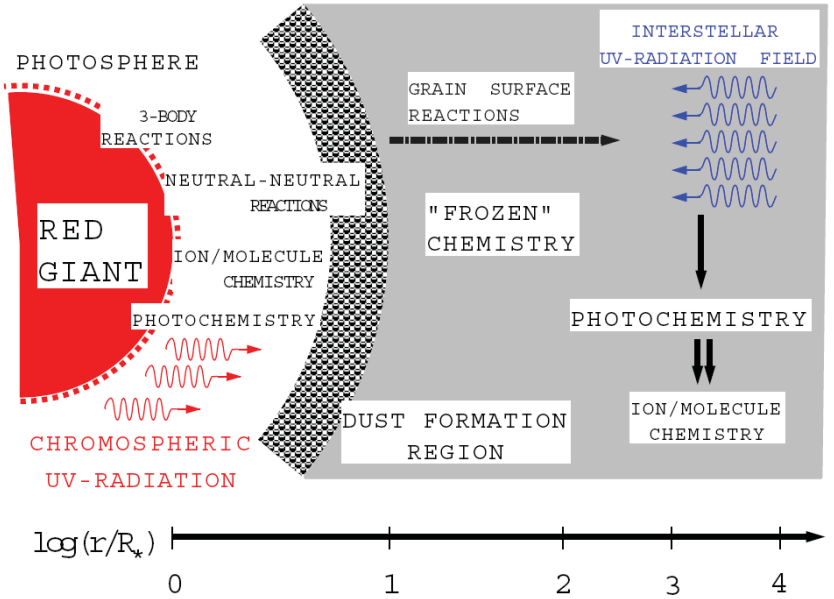

Figure 2. Chemical processes in different regions of the circumstellar shells around re giants (adopted from Patzer (1996))

From Sedlmayr and coworkers

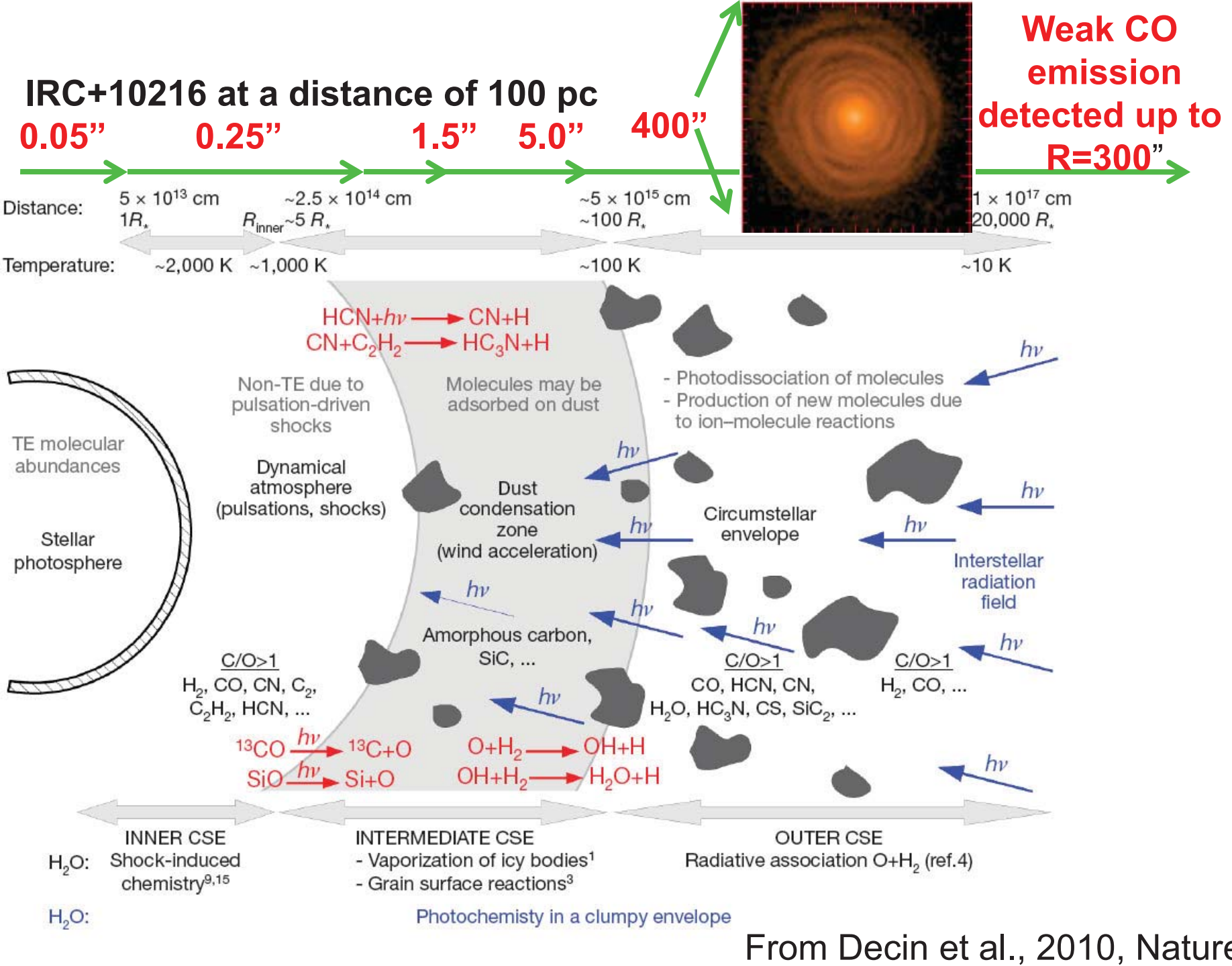

From Decin et al., 2010, Nature

MODELS UNDER THERMAL EQUILIBRIUM

Reaction rates and the path to form molecules are not important. Molecular abundances are determined by their value at thermo-dinamical equilibrium.

That means that two and three body reactions must be much faster that the time scale for dinamic evolution.

Of course, these models will provide reasonable results only for the most dense and warm regions. In the external layers of the envelope molecular abundances will be strongly dependent on the chemical kinetics and on the UV photons entering the envelope.

First studies for cold stars under the hyphotesis of ET :
Russell (1934)
Fujita (1939, 1940, 1941)

These models were able to predict the abundances of the most conspicous diatomic molecules detected in red giant stars (VO, TiO, CN, CH,…). These models also predicted the presence of some Polyatomic molecules that were detected 50 years later.

The models (Fujita) clearly indicated the role of the atomic abundances H:C:N:O in the abundances of diatomic species determined in ET. Russell was even able to apply his models to the Sun and to predict the presence of CO, CN and C_2 for temperatures below 4000 K.

Tsuji 1973 :
Very detailed study of the chemistry under ET in cold stars. He considered 36 elementos and hundreds of molecules

McCabe in 1979 introduces the concept of molecular freezing.

* Molecules are formed in the innermost region of the envelope.

* Refractory species condensate and form dust grains.

* Radiation pression over dust grains and the star pulsation initiate the expansion of the envelope

* When the density and temperature of the gas decrease due to the expansion chemical reactions become very slow. The time scale for dinamic evolution is faster that the formation rate of molecules.

* The molecular abundances in the external layers reflect the abundances produced under ET in the innermost region.

* OK for many species but of very difficult justification for radicals and large carbon-chains.

If A, B y M are neutral species then $k_1 \approx 10^{-11}$ $cm^3 s^{-1}$ and $k_2 \approx 10^{-10}$ $cm^3 s^{-1}$, but k_3 10^{+11} s^{-1}, and

$$dn(AB)/dt \approx 10^{-32}\, n(A)\ n(B)\ \ n(M)\ \ cm^{-3} s^{-1}$$

The best case in the ISM occurs for A=B=M= H

$$H + H + H \Leftrightarrow H_2 + H$$

For hydrides (BH) the optimal case will correspond to A=H, M=H and $B \in (C,N,O)$, i.e., $n(B) \approx 10^{-4}\, n(H)$ and

$$dn(BH)/dt \approx 10^{-36}\, n^3(H)\ cm^{-3}\ s^{-1} \quad B \in (C,N,O)$$

O-rich or C-rich, that is the question !!

O-rich star
[C]/[O] < 1

C-rich star
[C]/[O] > 1

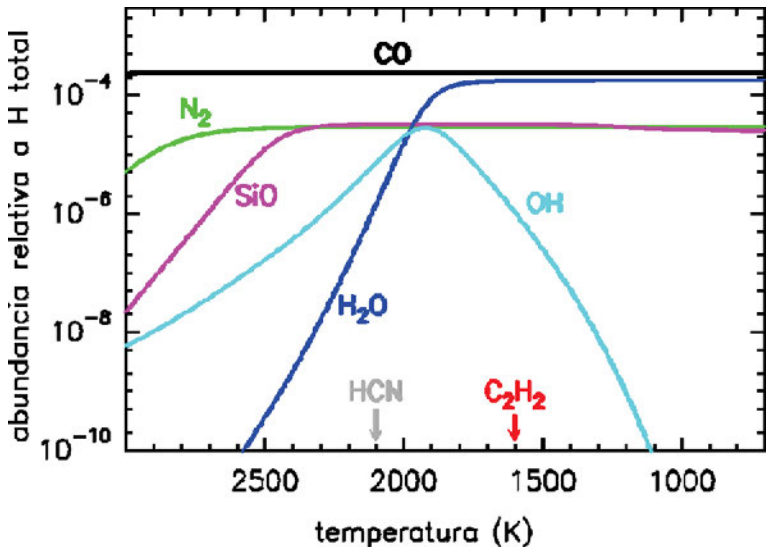

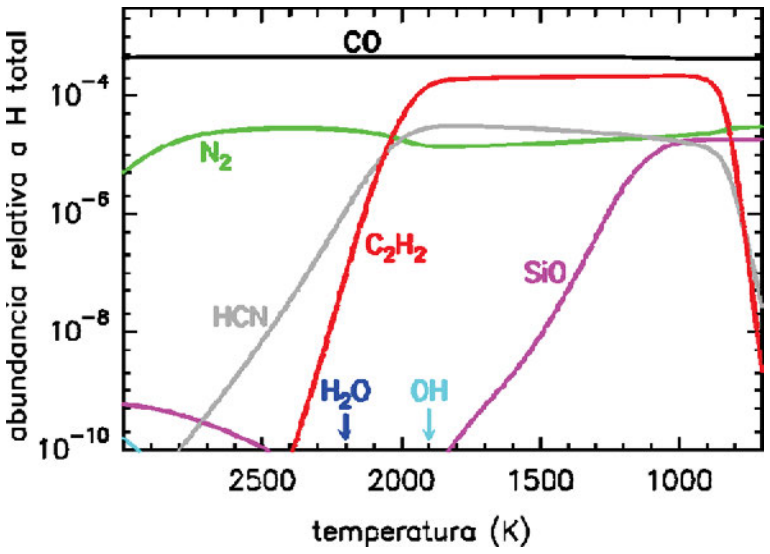

O-bearing molecules:
H_2O, SiO, OH, …

C-bearing molecules:
C_2H_2, HCN, CS, …

C-rich Stars (IRC+10216)

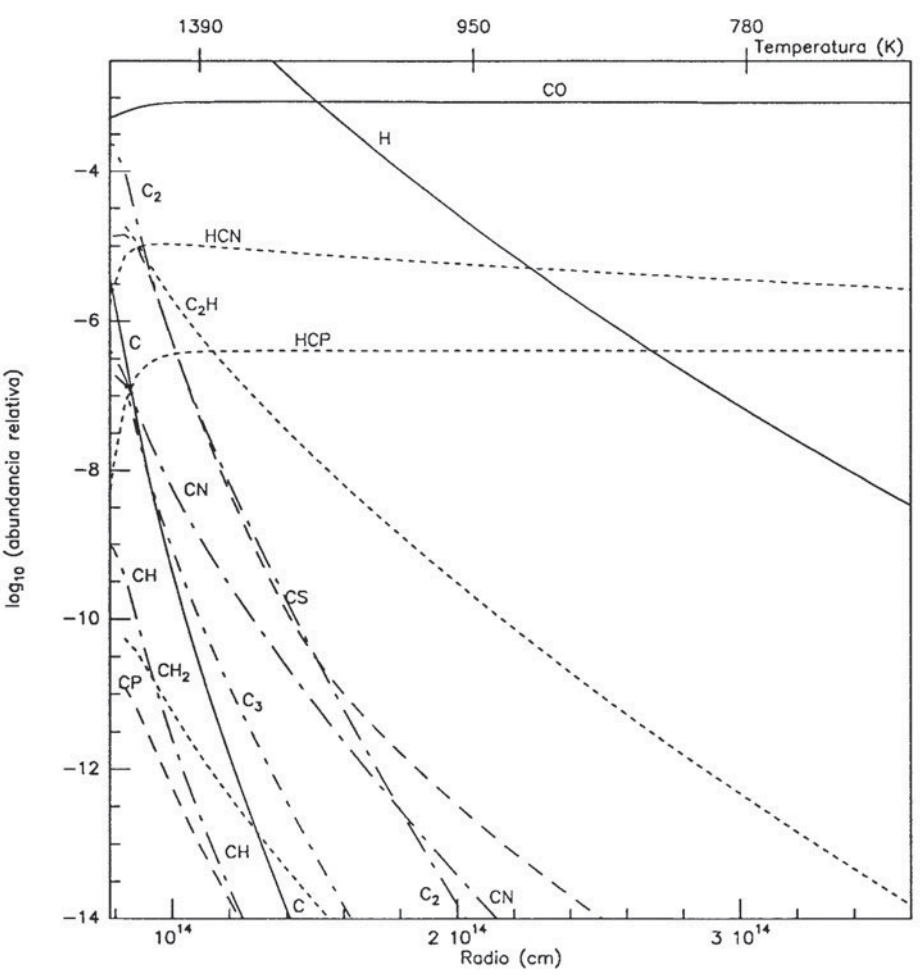

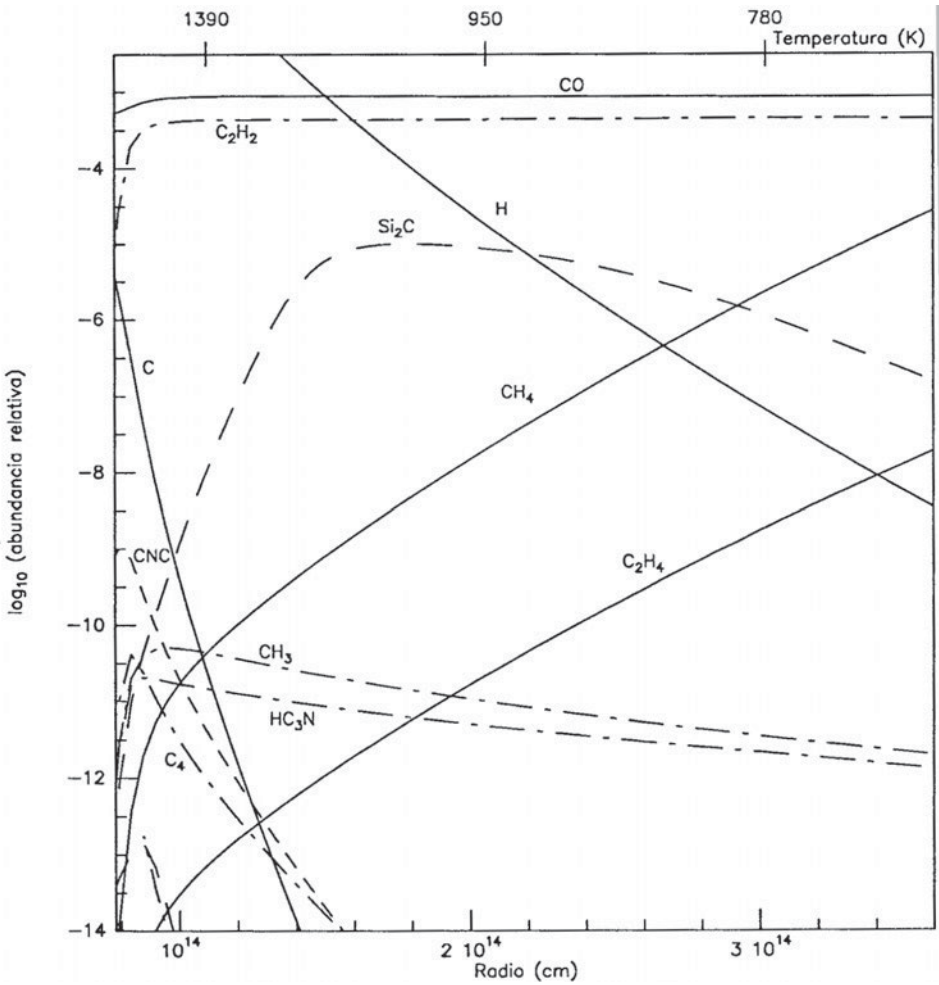

Carbon-bearing Molecules

What happens if we consider big carbon-rich molecules?

C_6H_6

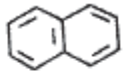

$C_{10}H_8$ (naphthalene)

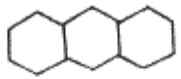

$C_{14}H_{10}$ (anthracene)

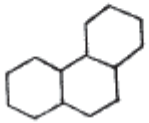

$C_{14}H_{10}$ (phenanthrene)

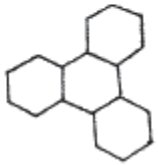

$C_{18}H_{12}$ (triphenylene)

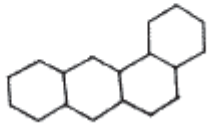

$C_{18}H_{12}$ (benzo(c)phenanthrene)

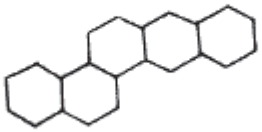

$C_{22}H_{14}$ (benzo(c)chrysene)

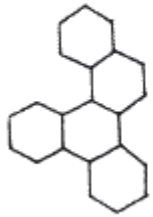

$C_{22}H_{14}$ (benzo(a)triphenylene)

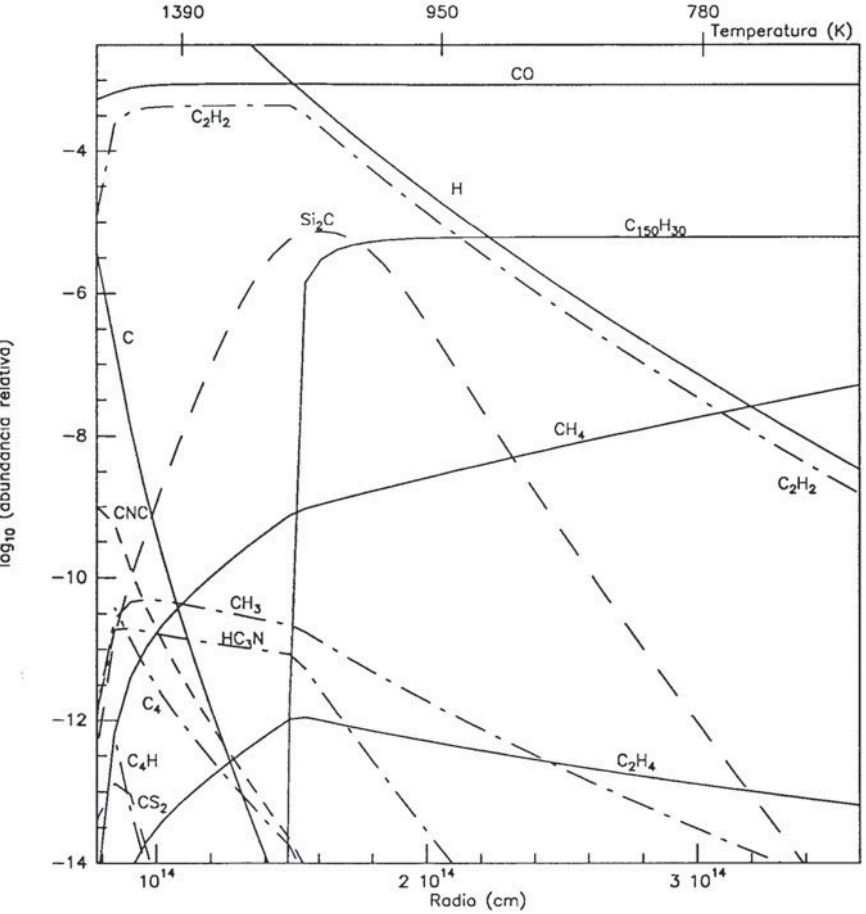

With PAHs

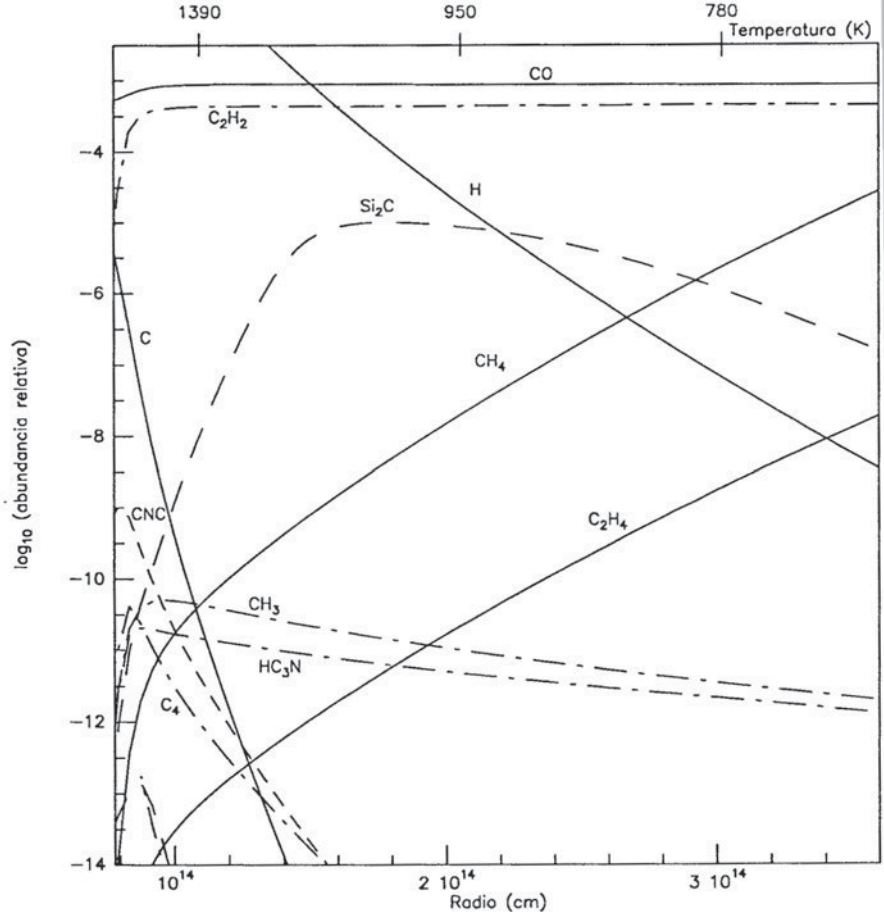

Without PAHs

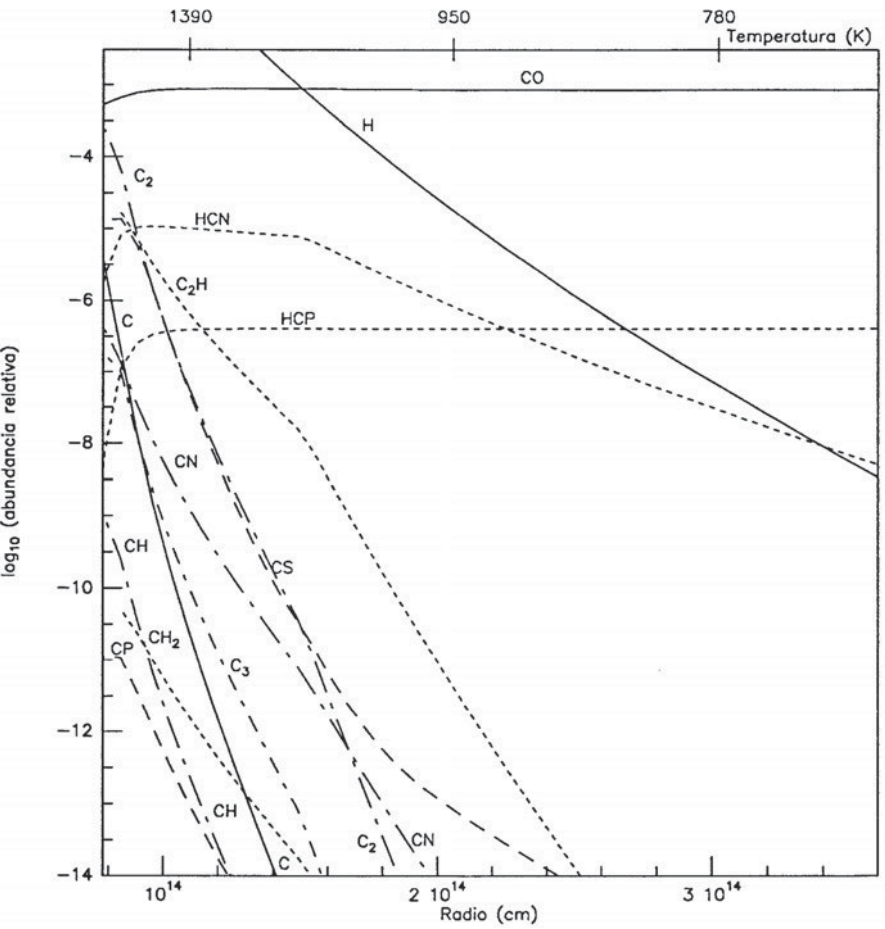

With PAHs

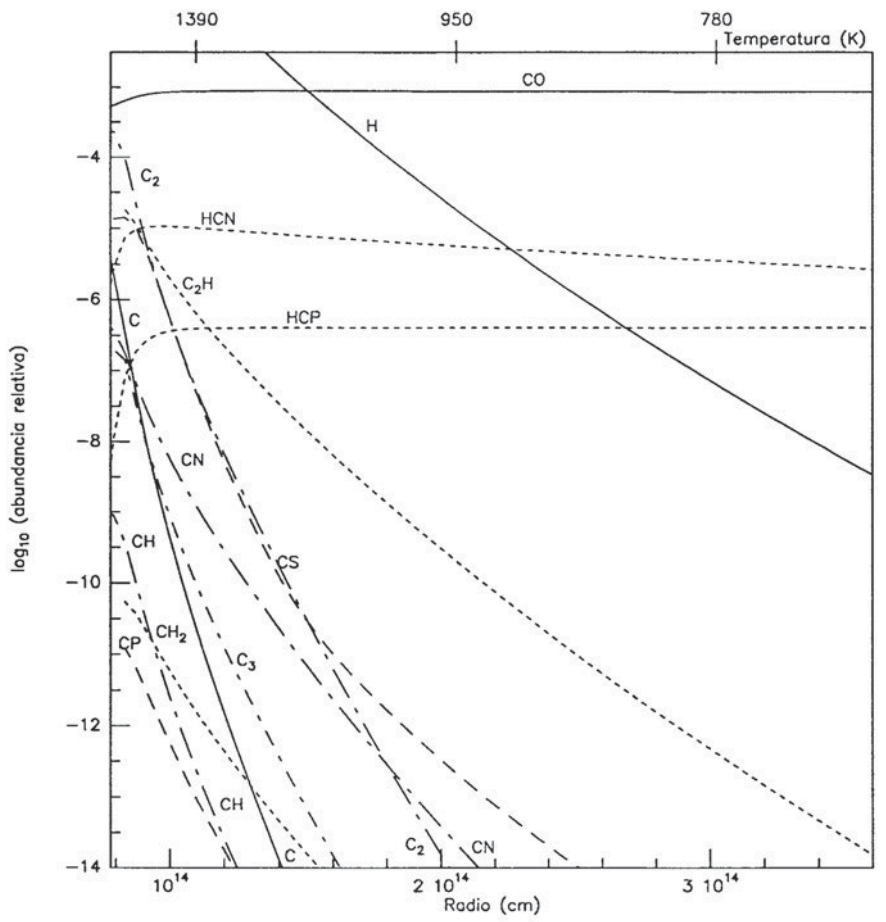

Without PAHs

Molecular abundances in O-rich stars

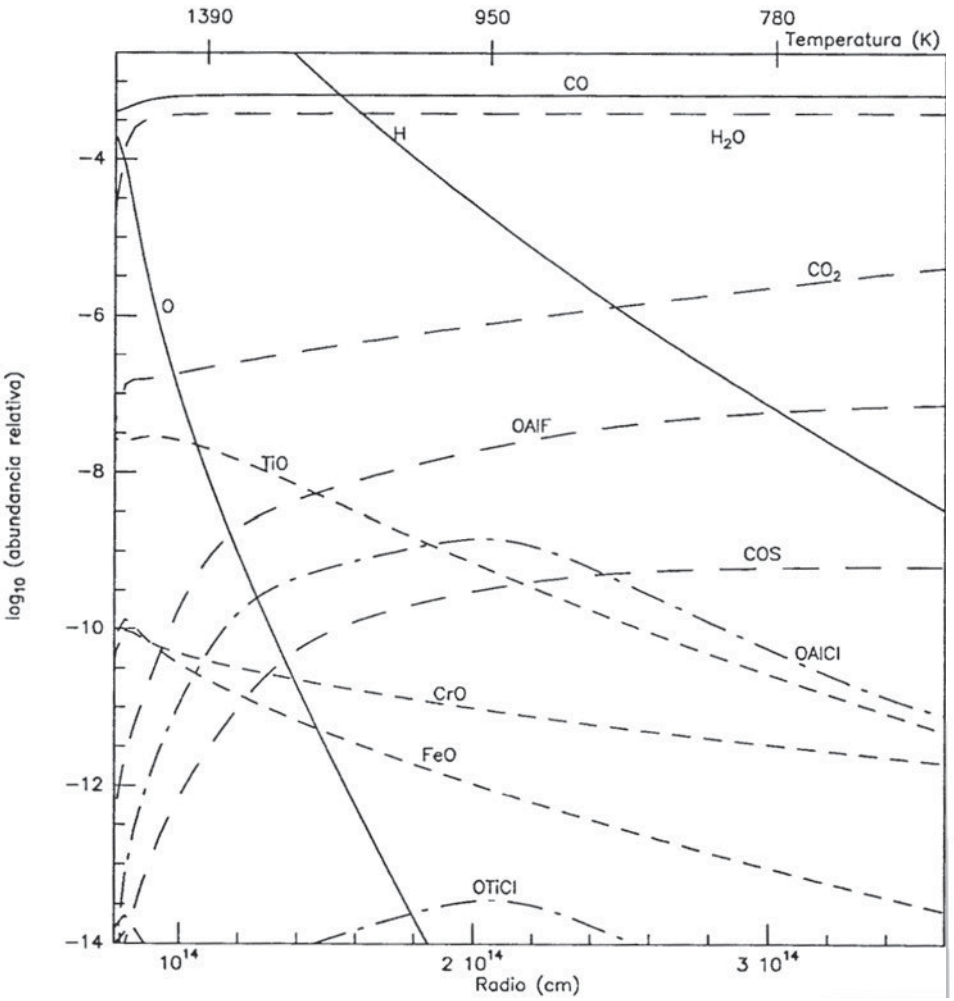

O-rich

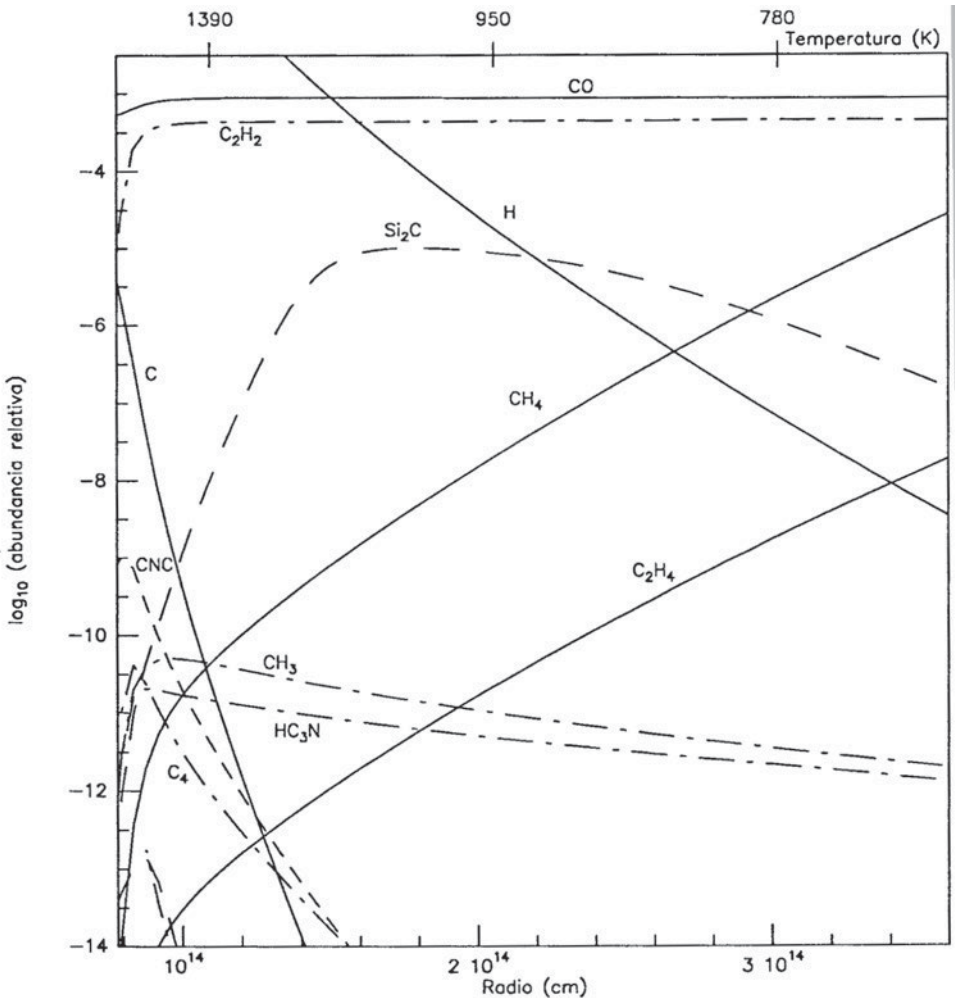

C-rich

O-rich

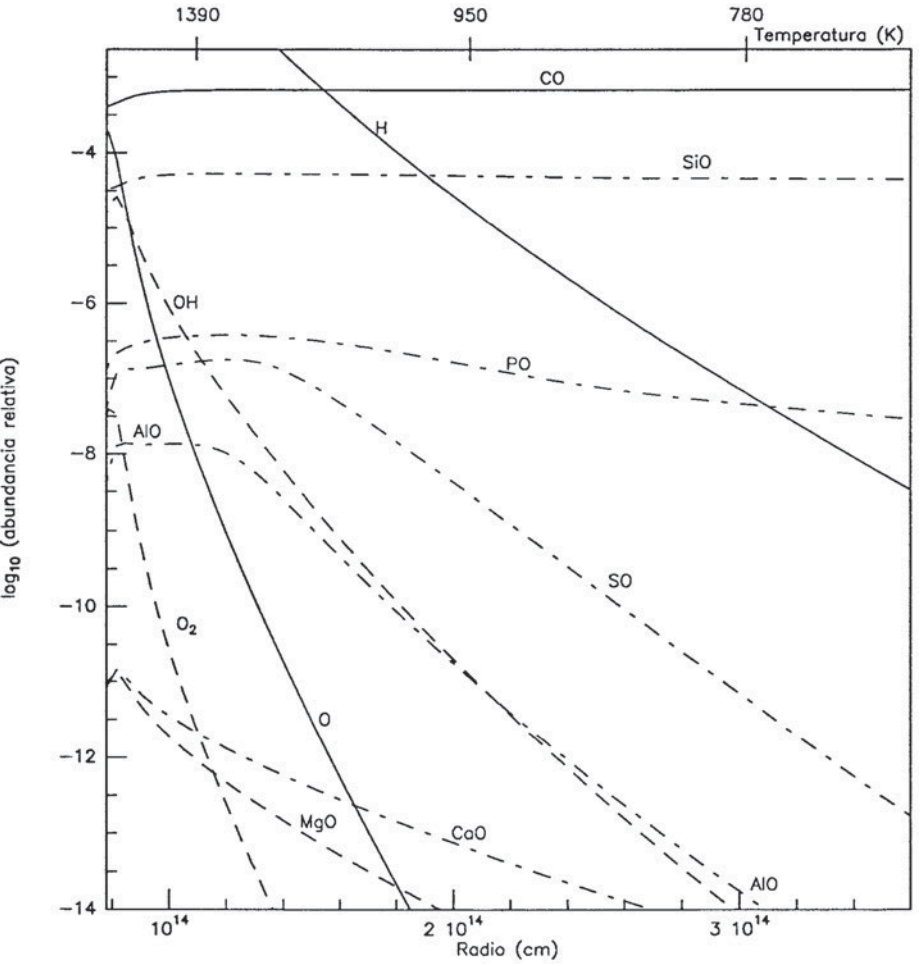
1390
950
780
Temperatura (K)
CO
H
SiO
OH
PO
AlO
SO
O_2
O
MgO
CaO
AlO
log_{10} (abundancia relativa)
−4
−6
−8
−10
−12
−14
10^{14}
$2\ 10^{14}$
$3\ 10^{14}$
Radio (cm)

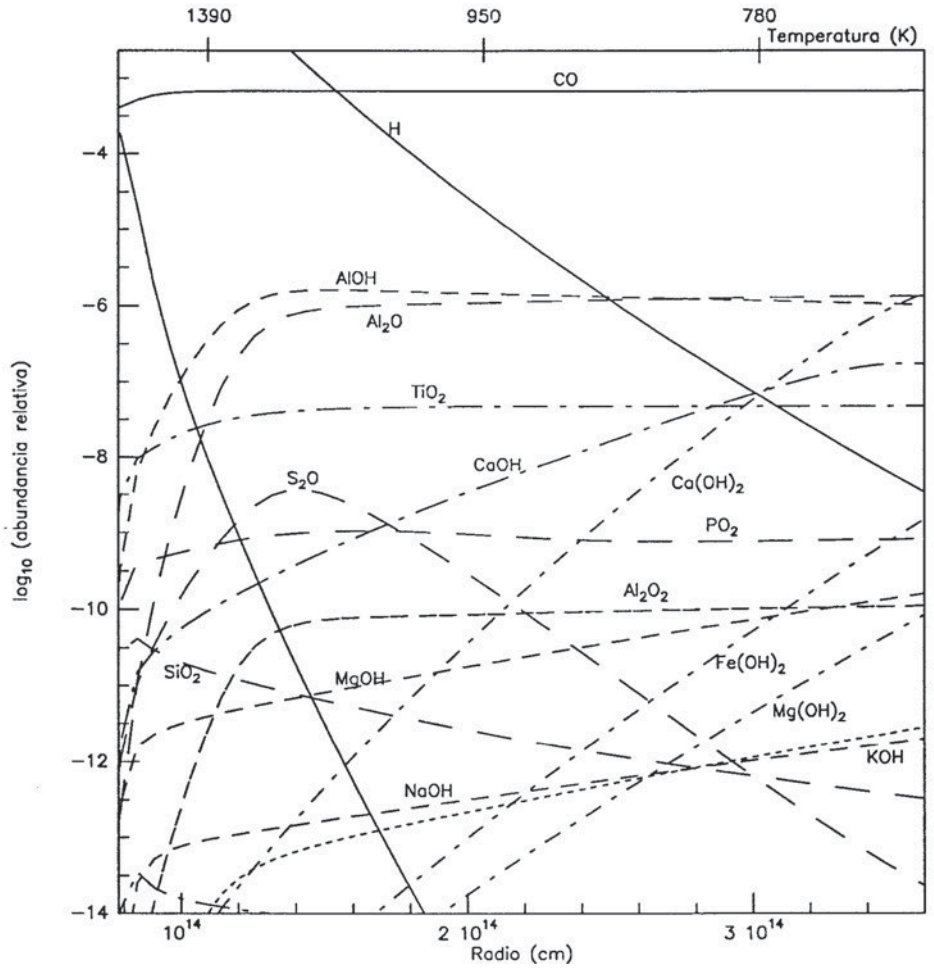
1390
950
780
Temperatura (K)
CO
H
AlOH
Al_2O
TiO_2
S_2O
CaOH
$Ca(OH)_2$
PO_2
Al_2O_2
SiO_2
MgOH
$Fe(OH)_2$
$Mg(OH)_2$
KOH
NaOH
log_{10} (abundancia relativa)
−4
−6
−8
−10
−12
−14
10^{14}
$2\ 10^{14}$
$3\ 10^{14}$
Radio (cm)

METHODS

Astronomical Observations at all frequencies optical, infrared and radio telescopes

Radiative transfer modeling

Chemical modeling

Three different approaches (single dish or interferometric observations):

I) Systematic observation of selected molecular lines in a large sample of objects:

- -Physical conditions derived from each molecule
- -Statistical studies
- -Good estimation of mass loss rates

II) Systematic frequency coverage of a few prototypical objets:

- -Full census of molecular lines. Spectroscopy in space
- -Physical and chemical conditions
- -New molecules. Chemical complexity

IRC+10216, CRL618, VyCMa, IK Tau, OH231

III) Identical to II but with spatial information:

- -In most cases interferometric observations are needed
- -But for a few cases (nearby objects) single dish observations can be used to get a complete line survey at different positions => Physical structure of the envelope.

IRC+10216

Herschel : HIFISTARS & MESS + Some Open Time proposals

The Physical and Chemical Conditions in the dust formation zone in IRC+10216

The first step to understand the chemistry of the whole envelope

Tools: Line Surveys in the Mid and Near Infrared with ISO & Ground Based Telescopes

Cernicharo et al., 1996, A.&A., 315, 201

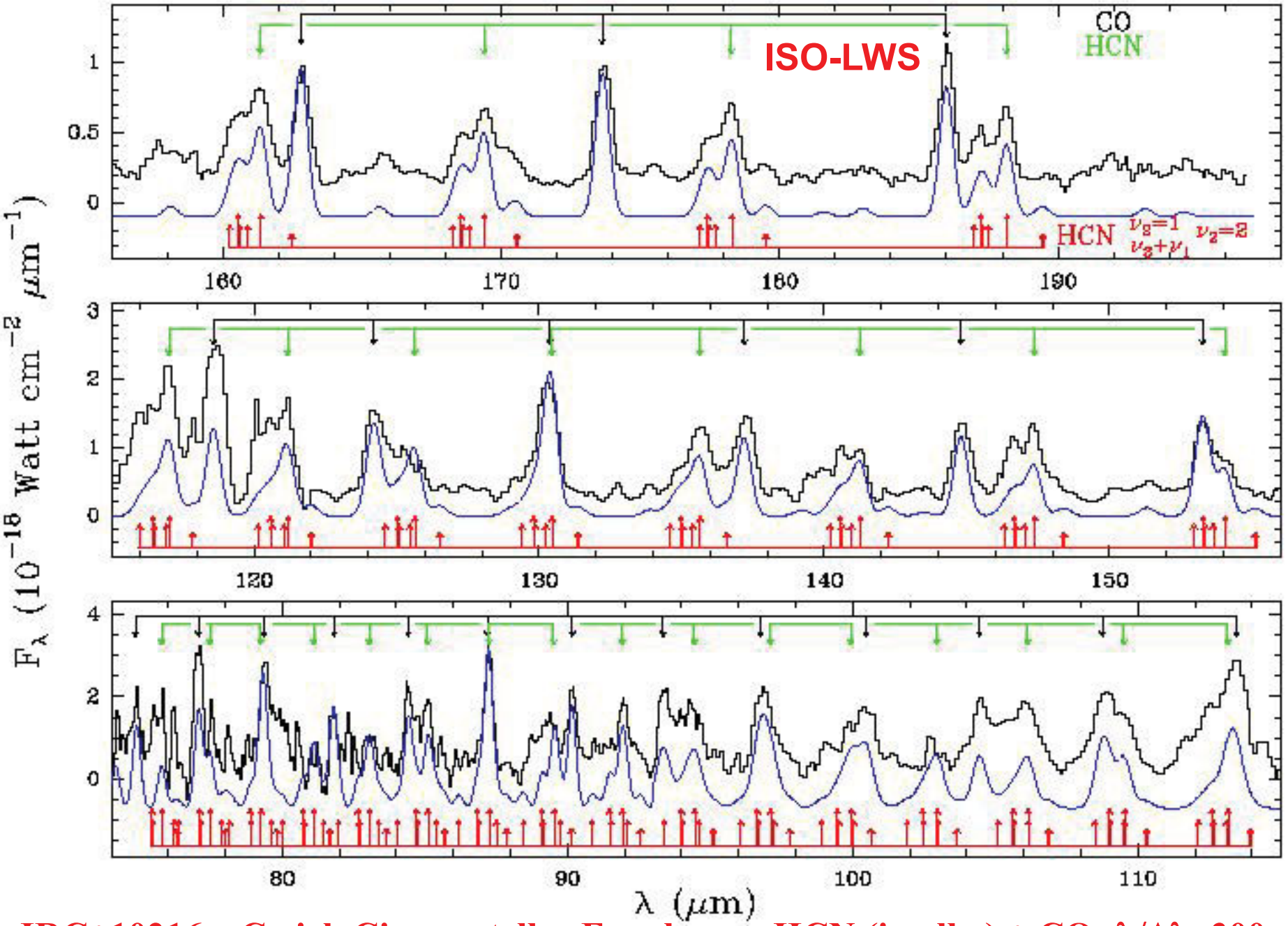

IRC+10216 a C-rich Circumstellar Envolope :: HCN (in all ν) + CO; λ/Δλ~300

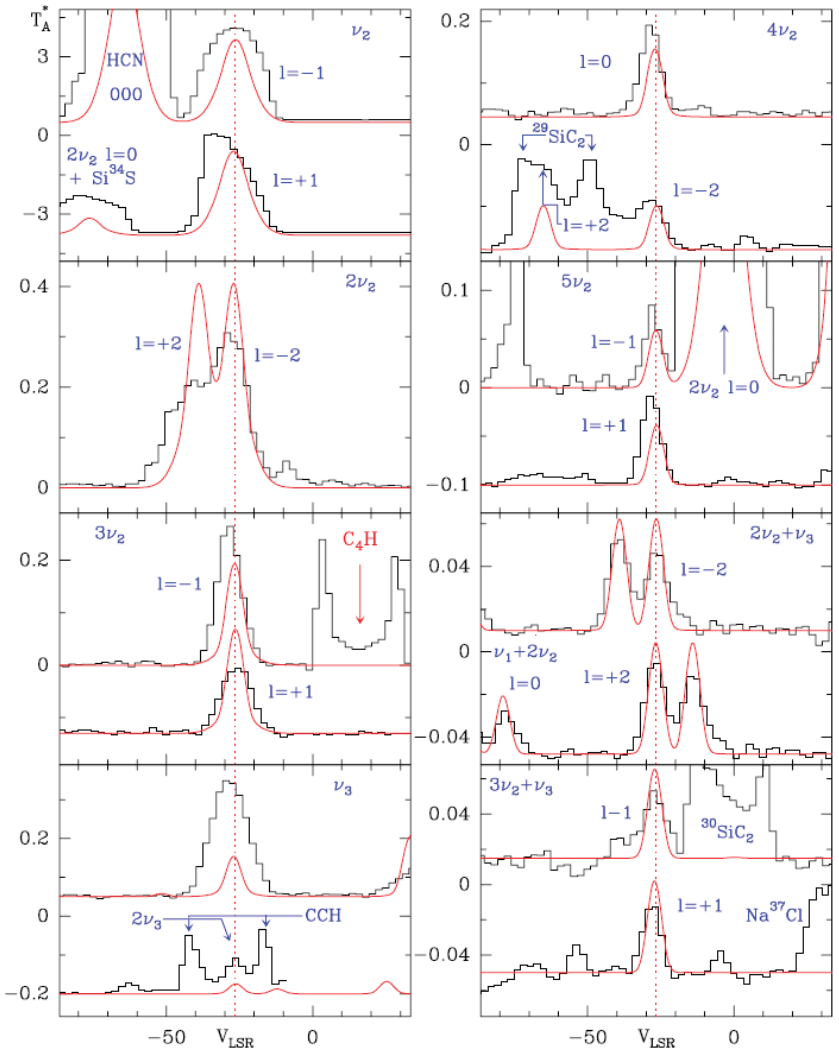

Fig. 1. Selected J = 3–2 lines of HCN in various vibrational states (blue labels). The spectra observed with the IRAM 30-m telescope are indicated by black histograms. The line profiles calculated from our model (see text) are plotted in red. The line parameters are given in Table 1. Intensity scale is antenna temperature. Main beam antenna temperatures can be obtained by dividing the T_A* scale of the 270 GHz data by a factor of 0.4. Velocity resolution is 2.3 km s^{-1}.

A&A 529, L3 (2011)
DOI: 10.1051/0004-6361/201116717

Astronomy & Astrophysics

LETTER TO THE EDITOR

Probing the dust formation region in IRC +10216 with the high vibrational states of hydrogen cyanide⋆,⋆⋆

J. Cernicharo[1], M. Agúndez[2], C. Kahane[3], M. Guélin[4], J. R. Goicoechea[1], N. Marcelino[1], E. De Beck[5], and L. Decin[5]

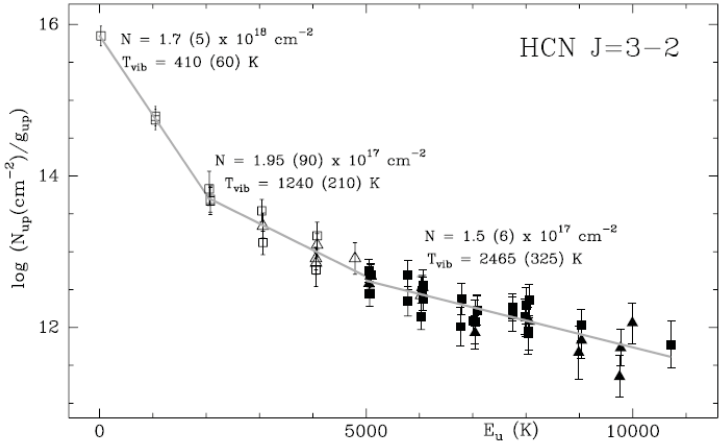

Fig. 2. Vibrational temperature diagram derived from the HCN J = 3–2 lines given in Table 1. Upper level population vs. its energy above the ground state. The data is fitted by 3 line segments corresponding to regions with temperatures T_{vib} ∼ 400 K, 1200 K, and 2400 K, respectively. HCN column densities are averaged over a source size of 1″ diameter. A conservative calibration error of 30% has been applied to all intensities. Values in parentheses correspond to 3σ errors on the derived vibrational temperatures and column densities. Filled triangles correspond to lines with half-power widths $\Delta v < 7$ km s^{-1}, filled squares correspond to lines with $7 < \Delta v < 9$ km s^{-1}, empty triangles correspond to lines with $9 < \Delta v < 12$ km s^{-1}, and empty squares to lines with $\Delta v > 12$ km s^{-1}.

Observations of C_2H_2 and HCN observations with TEXES at the IRTF

PhD of J.Pablo Fonfría (Fonfría et al., 2008, ApJ)

TEXES::Lacy et al., 2002, PASP, 114, 153

720-900 cm^{-1}
11.1-13.9 μm

Spectral resolution 75000
4 km/s

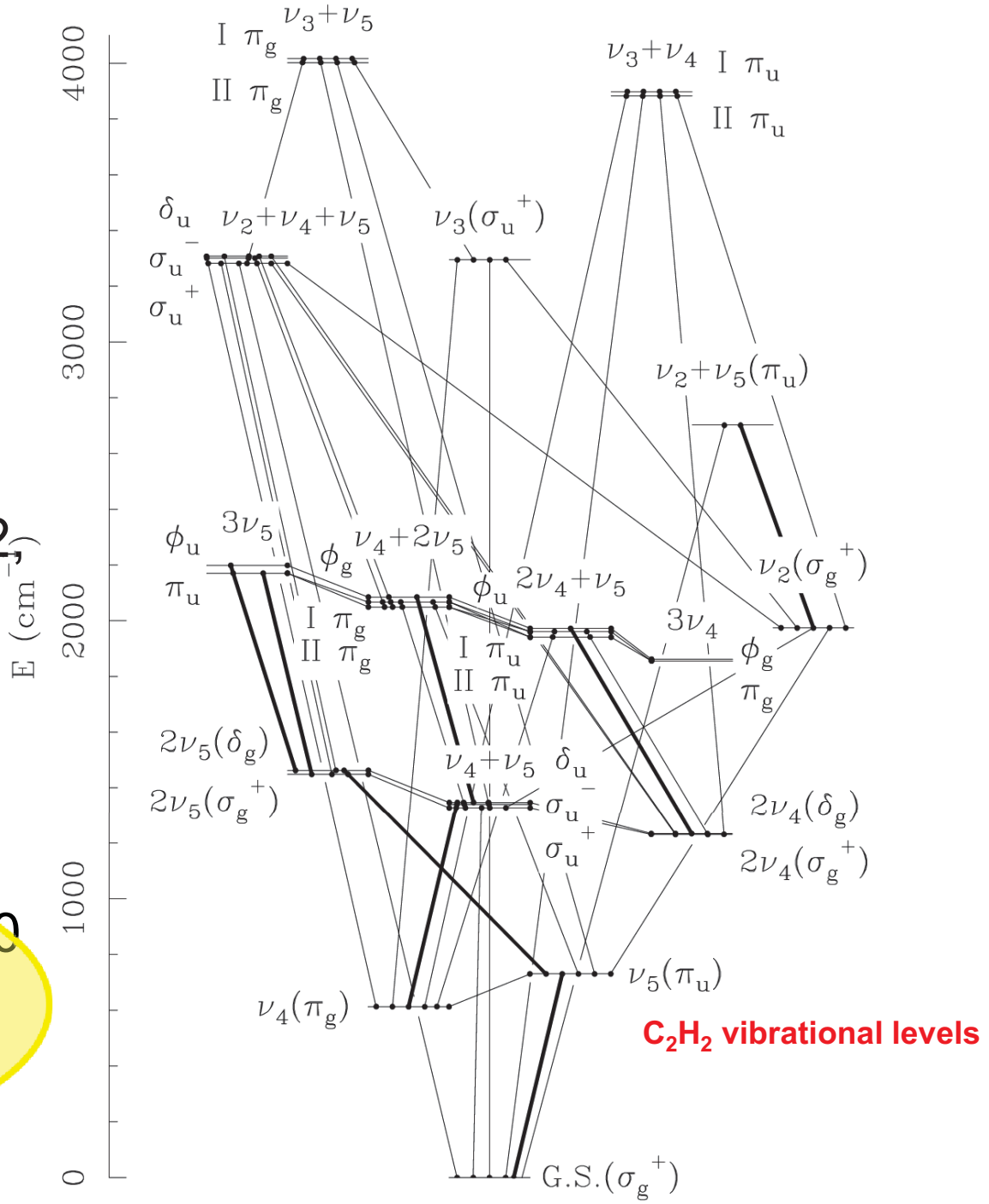

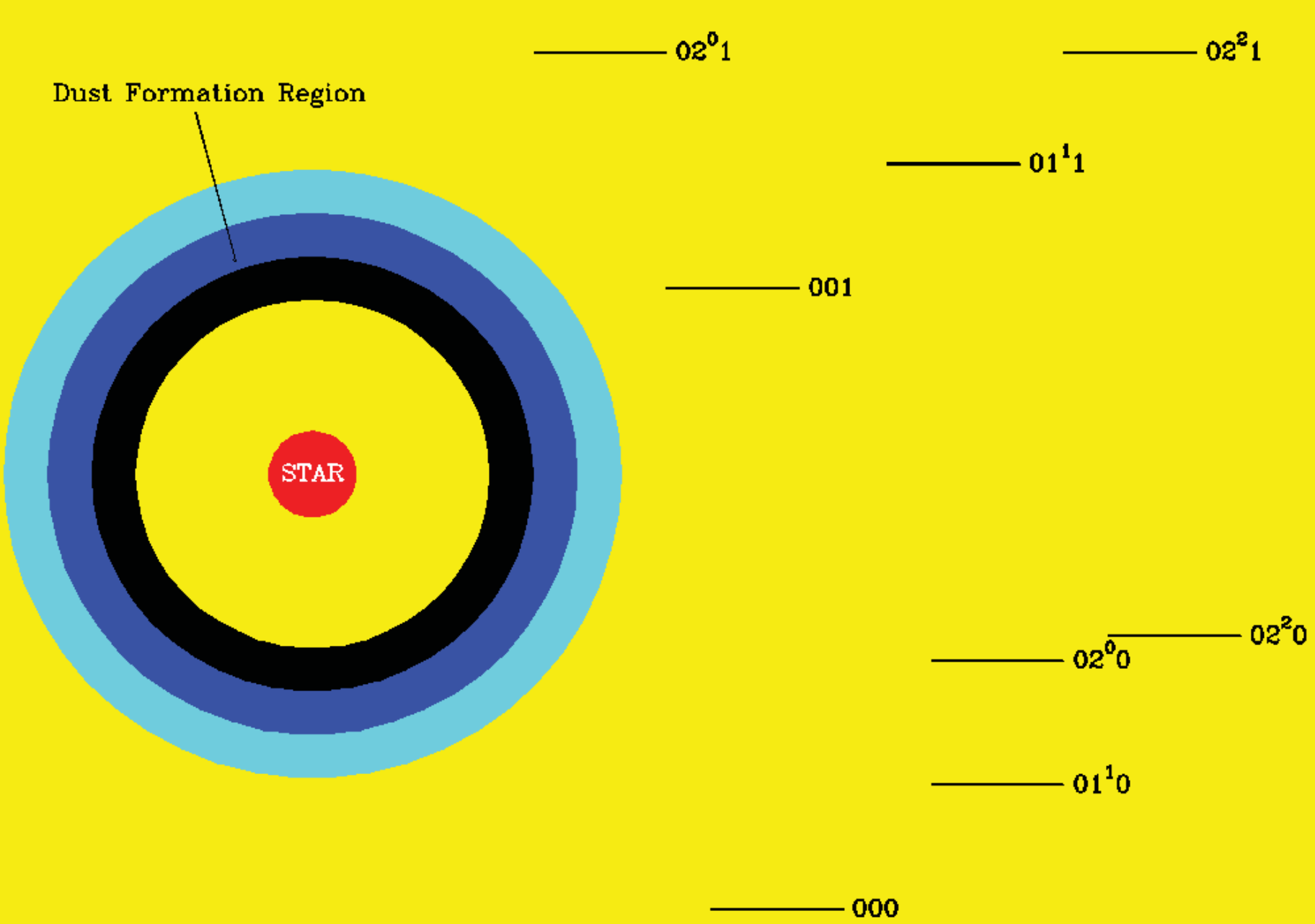
Dust Formation Region
STAR
$02^0 1$
$02^2 1$
$01^1 1$
001
$02^2 0$
$02^0 0$
$01^1 0$
000

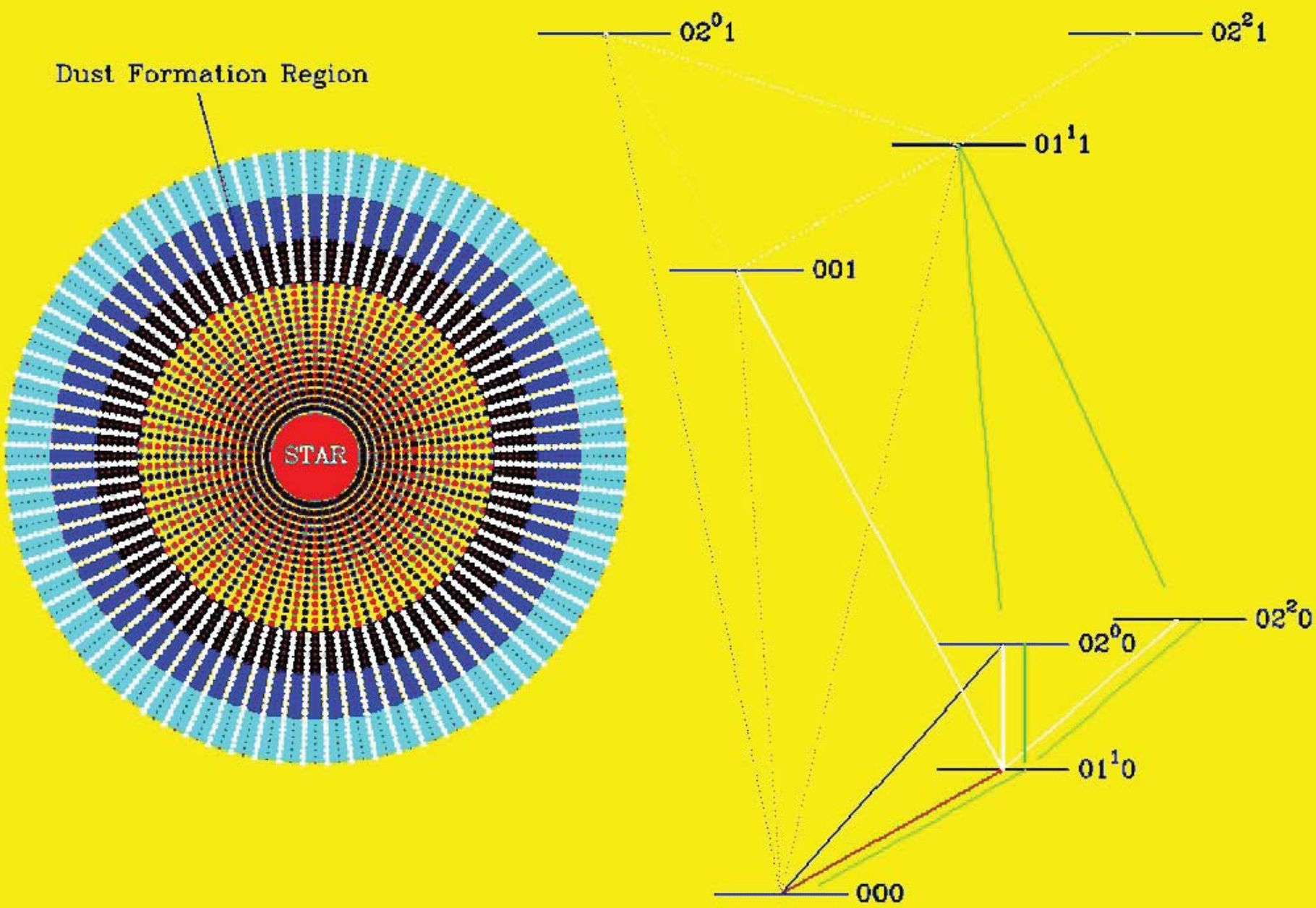
Dust Formation Region
STAR
$02^0 1$
$02^2 1$
$01^1 1$
001
$02^2 0$
$02^0 0$
$01^1 0$
000

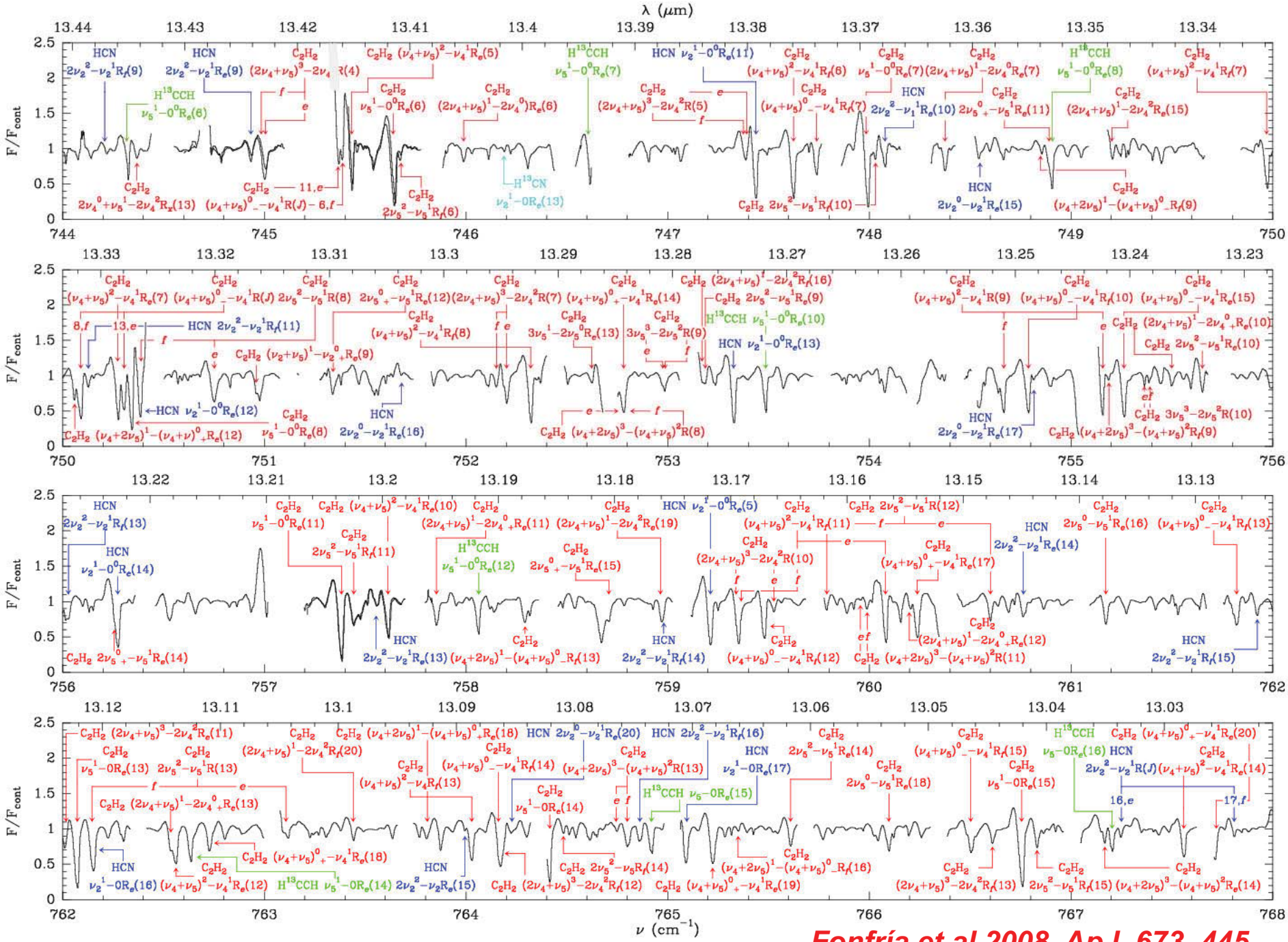

Fonfría et al 2008, ApJ, 673, 445

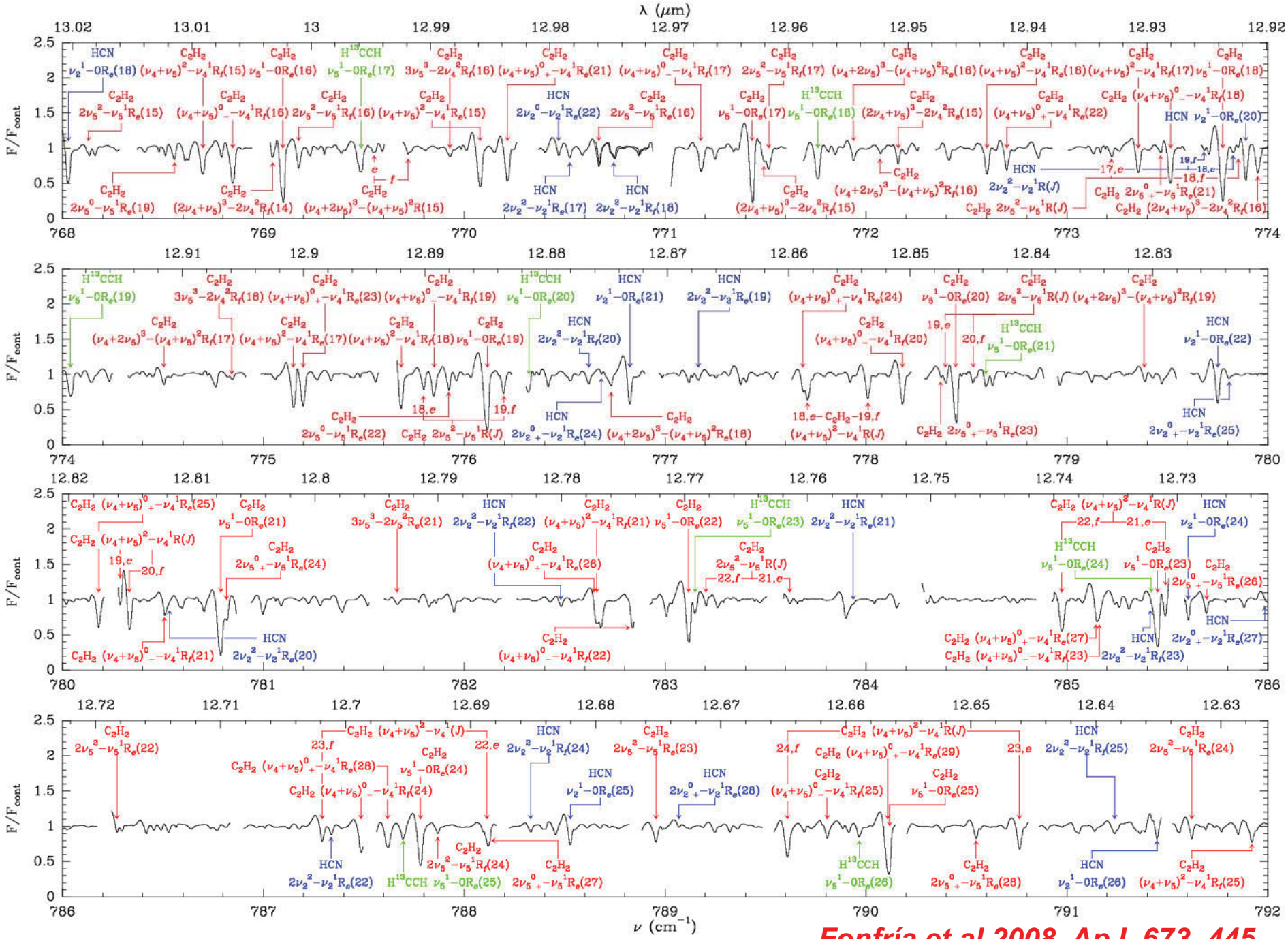

Fonfría et al 2008, ApJ, 673, 445

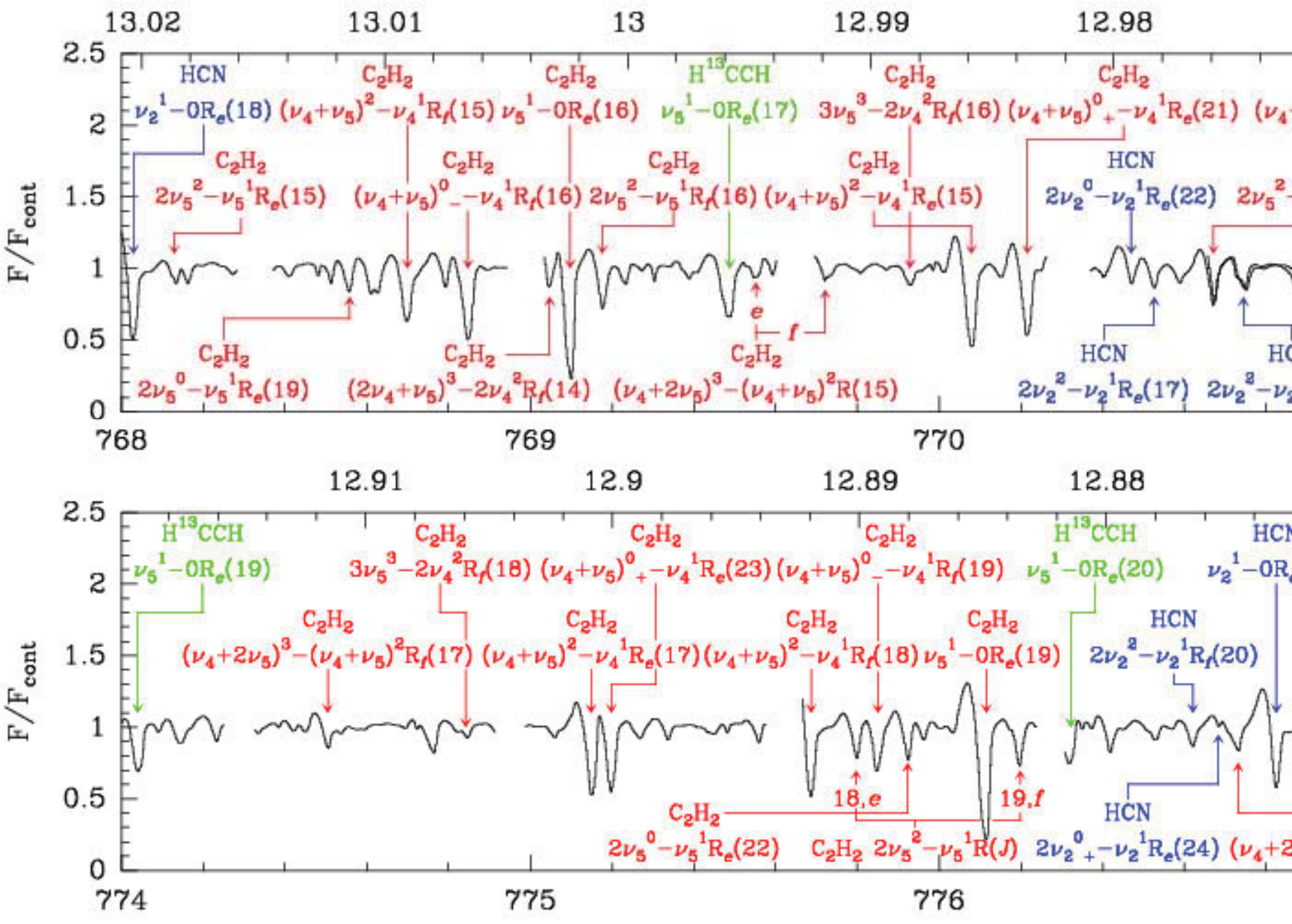
13.02
13.01
13
12.99
12.98
F/F_cont
HCN
ν2^1−0Re(18)
C2H2
(ν4+ν5)^2−ν4^1Rf(15)
C2H2
ν5^1−0Re(16)
H13CCH
ν5^1−0Re(17)
C2H2
3ν5^3−2ν4^2Rf(16)
C2H2
(ν4+ν5)^0+−ν4^1Re(21)
C2H2
2ν5^2−ν5^1Re(15)
C2H2
(ν4+ν5)^0−−ν4^1Rf(16)
C2H2
2ν5^2−ν5^1Rf(16)
C2H2
(ν4+ν5)^2−ν4^1Re(15)
HCN
2ν2^0−ν2^1Re(22)
e
f
C2H2
2ν5^0−ν5^1Re(19)
C2H2
(2ν4+ν5)^3−2ν4^2Rf(14)
C2H2
(ν4+2ν5)^3−(ν4+ν5)^2R(15)
HCN
2ν2^2−ν2^1Re(17)
768
769
770
12.91
12.9
12.89
12.88
F/F_cont
H13CCH
ν5^1−0Re(19)
C2H2
3ν5^3−2ν4^2Rf(18)
C2H2
(ν4+ν5)^0+−ν4^1Re(23)
C2H2
(ν4+ν5)^0−−ν4^1Rf(19)
H13CCH
ν5^1−0Re(20)
HCN
ν2^1−0R
C2H2
(ν4+2ν5)^3−(ν4+ν5)^2Rf(17)
C2H2
(ν4+ν5)^2−ν4^1Re(17)
C2H2
(ν4+ν5)^2−ν4^1Rf(18)
C2H2
ν5^1−0Re(19)
HCN
2ν2^2−ν2^1Rf(20)
18,e
19,f
C2H2
2ν5^0−ν5^1Re(22)
C2H2
2ν5^2−ν5^1R(J)
HCN
2ν2^0+−ν2^1Re(24)
774
775
776

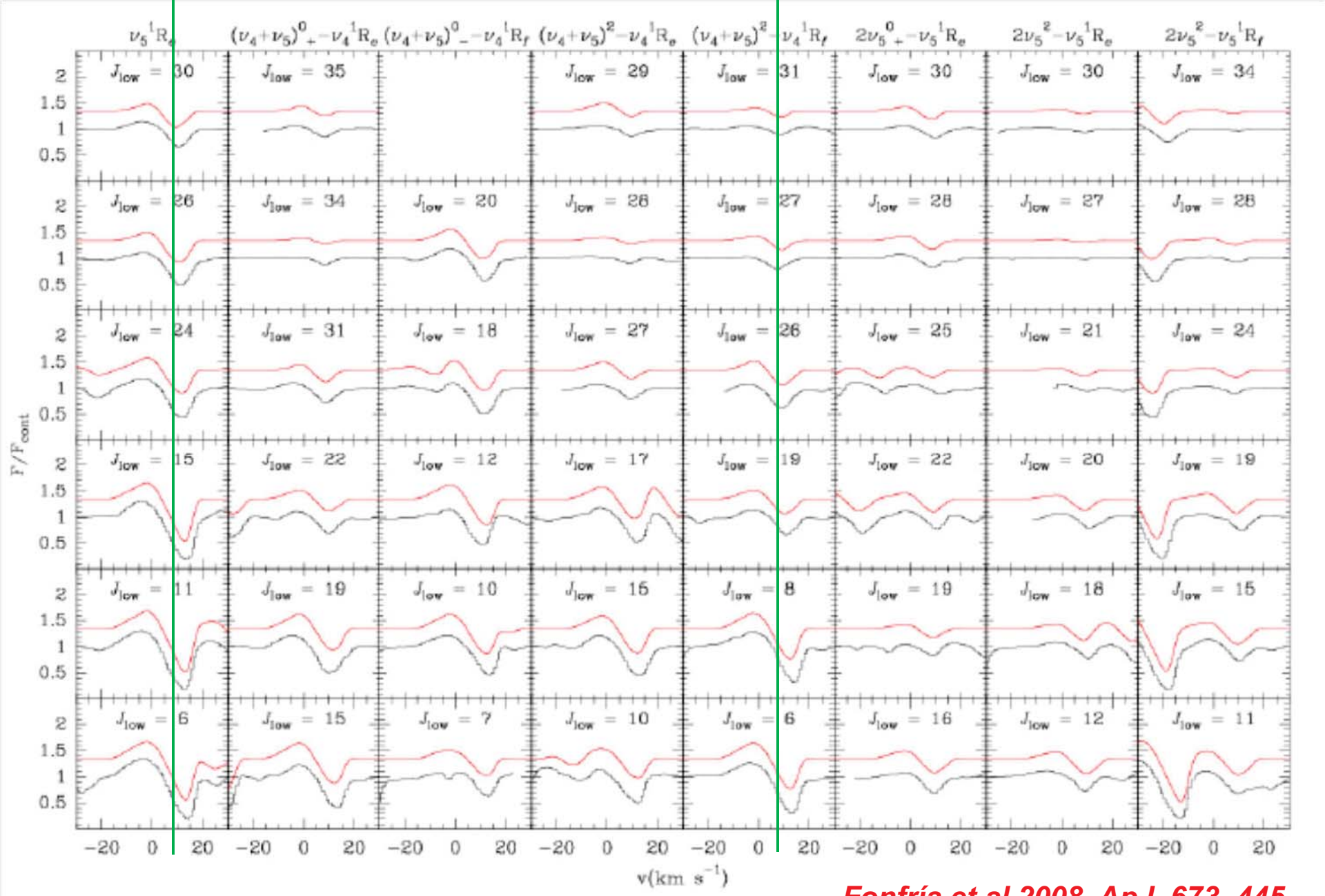

Fonfría et al 2008, ApJ, 673, 445

DATA

MODEL C_2H_2 + HCN + ISOTOPES

Fonfría et al 2008, ApJ, 673, 445

RESULTS

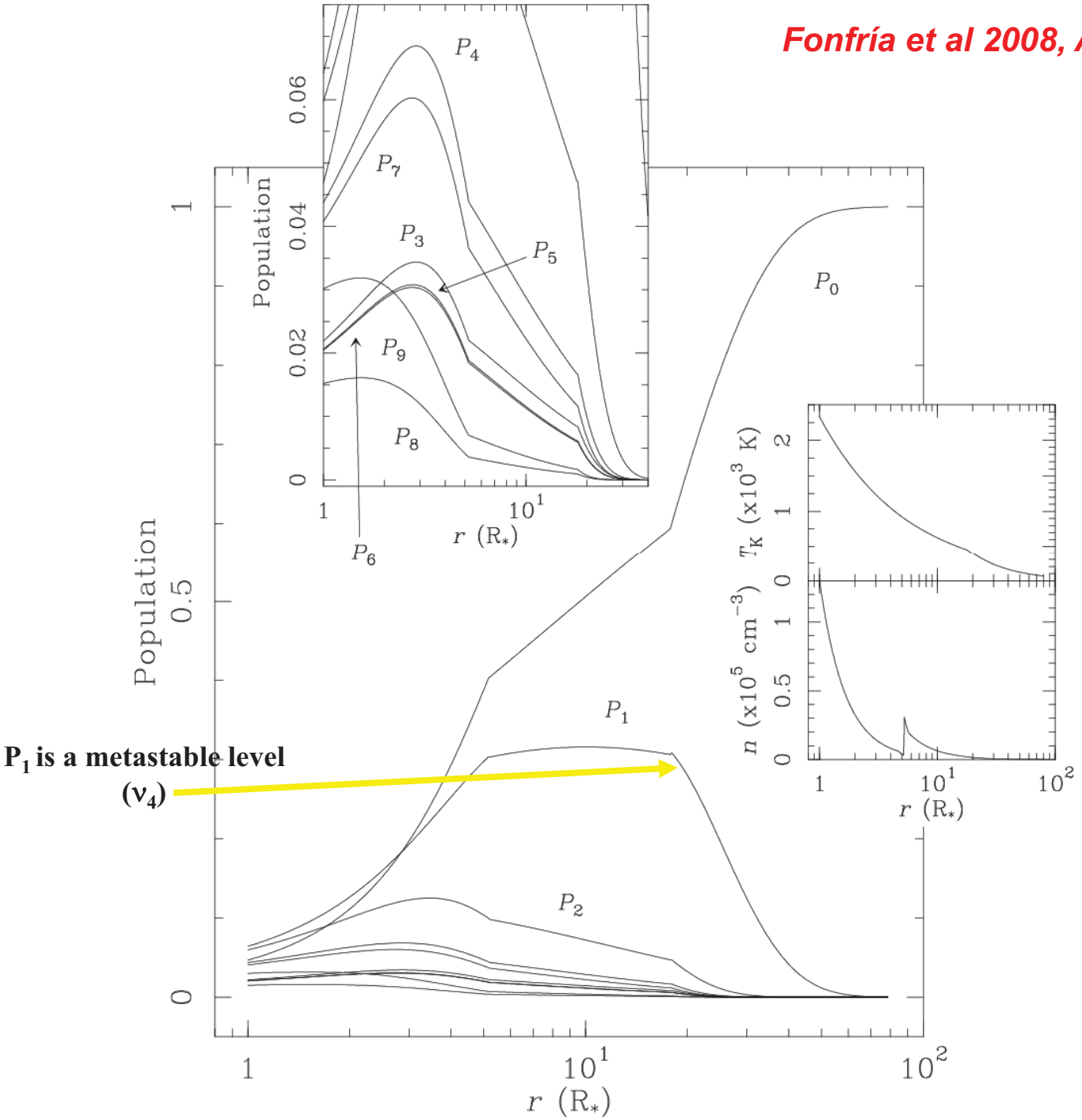

P_1 is a metastable level (ν_4)

$x(C_2H_2)$

Z I 7.5 10^{-6}

Z II 8.0 10^{-5}

ZIII 8.0 10^{-5}

x(HCN)

Z I 2.5 10^{-5}

Z II 5.0 10^{-5}

ZIII 5.0 10^{-5}

$^{12}C/^{13}C=41$

Z I 1- 5 R_*

Z II 5-20 R_*

ZIII > 20 R_*

The middle envelope, Herschel data

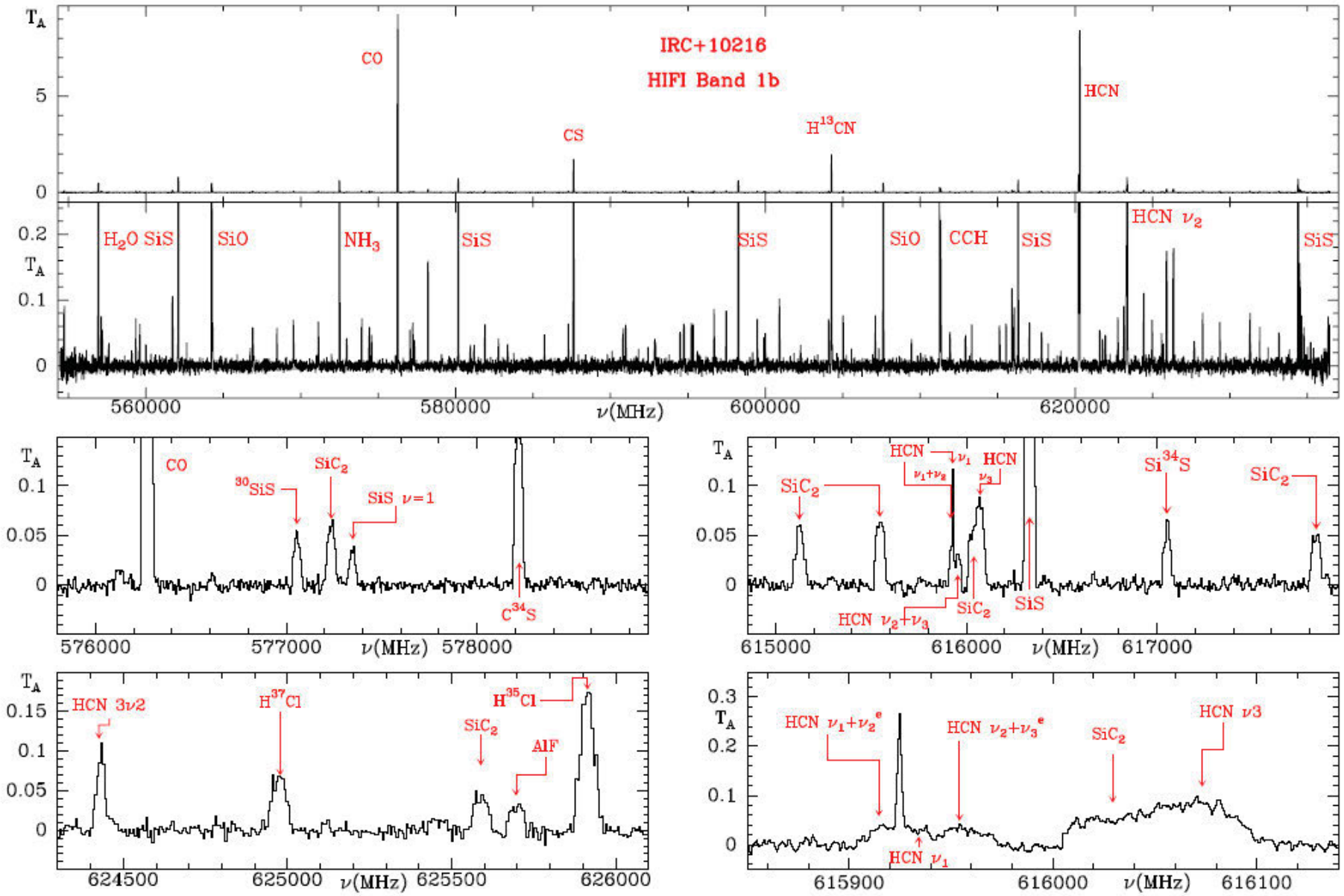

Fig. 1. Spectra of IRC +10216 observed with HIFI band 1b. The two upper panels present the complete spectrum on two different intensity scales. The panels below show different 3 GHz wide ranges of the survey. All data have been smoothed to a spectral resolution of 2.8 km s^{-1} except for the right bottom panel, which shows the spectrum around several vibrational lines of HCN with the nominal WBS resolution (1.1 MHz, ≃0.5 km s^{-1}).

Cernicharo et al., 2010, A&A, HIFI special issue;
HCl has been detected with PACS/SPIRE (Cernicharo et al., 2010, A&A, 518, L136)

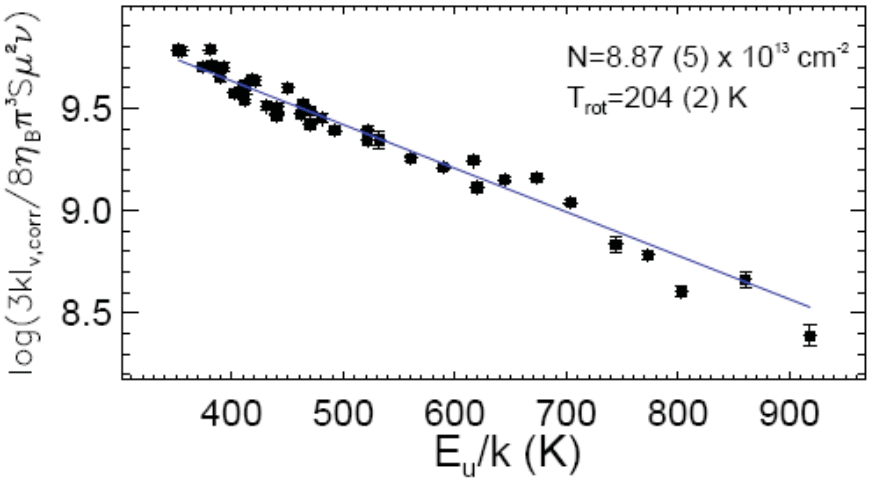

Fig. 2. Rotational diagram for the observed SiC_2 lines. The rotational temperature is 204 K and the beam averaged column density of SiC_2 is 8.9×10^{13} cm^{-2}.

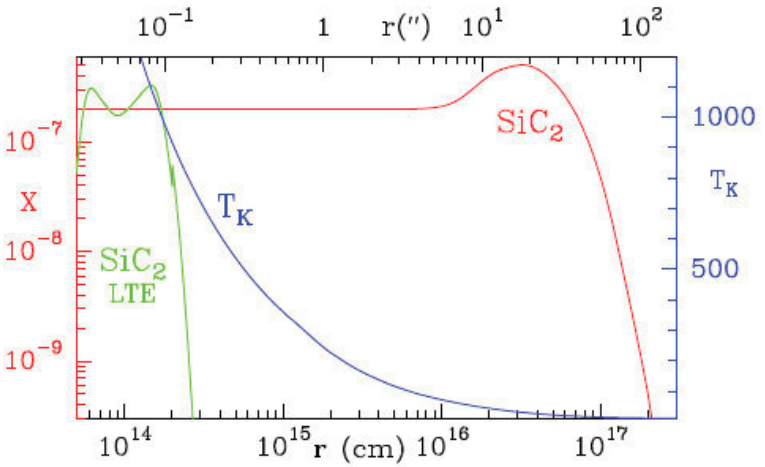

Fig. 3. Abundance of SiC_2, X, derived from the chemical model described in the text (red line) and in thermodynamical equilibrium (green line). The blue line shows the kinetic temperature, T_K, of the gas. The axis shows the distance to the star in cm (bottom) and the angular distance (top) as seen from the Earth (d=120pc).

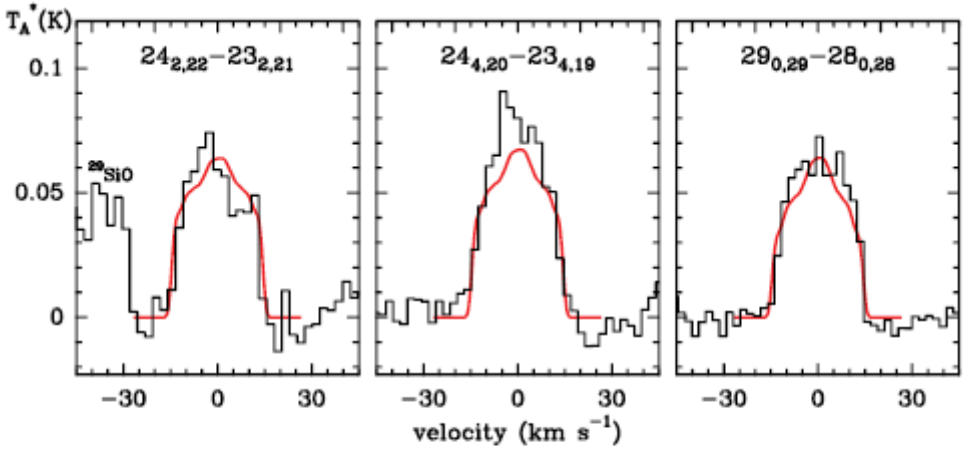

Fig. 4. Comparison between the line profiles of three rotational transitions of SiC_2 as observed with HIFI (black histograms) and as calculated with the radiative transfer model (red lines) using the abundance profile shown in red in Fig. 3.

Cernicharo et al. 2010, HIFI special issue

SiC_2 abundance enhanced in the external layer through

Si + CCH

and

Si + C_2H_2

The radio data (30m IRAM, SMA, PdBI, …)

Chemical Modelling of the envelope

PhD of Marcelino Agúndez

Physical and chemical properties of the dust formation zone

C_2H_2 & HCN in the inner shell

PhD of J.Pablo Fonfría

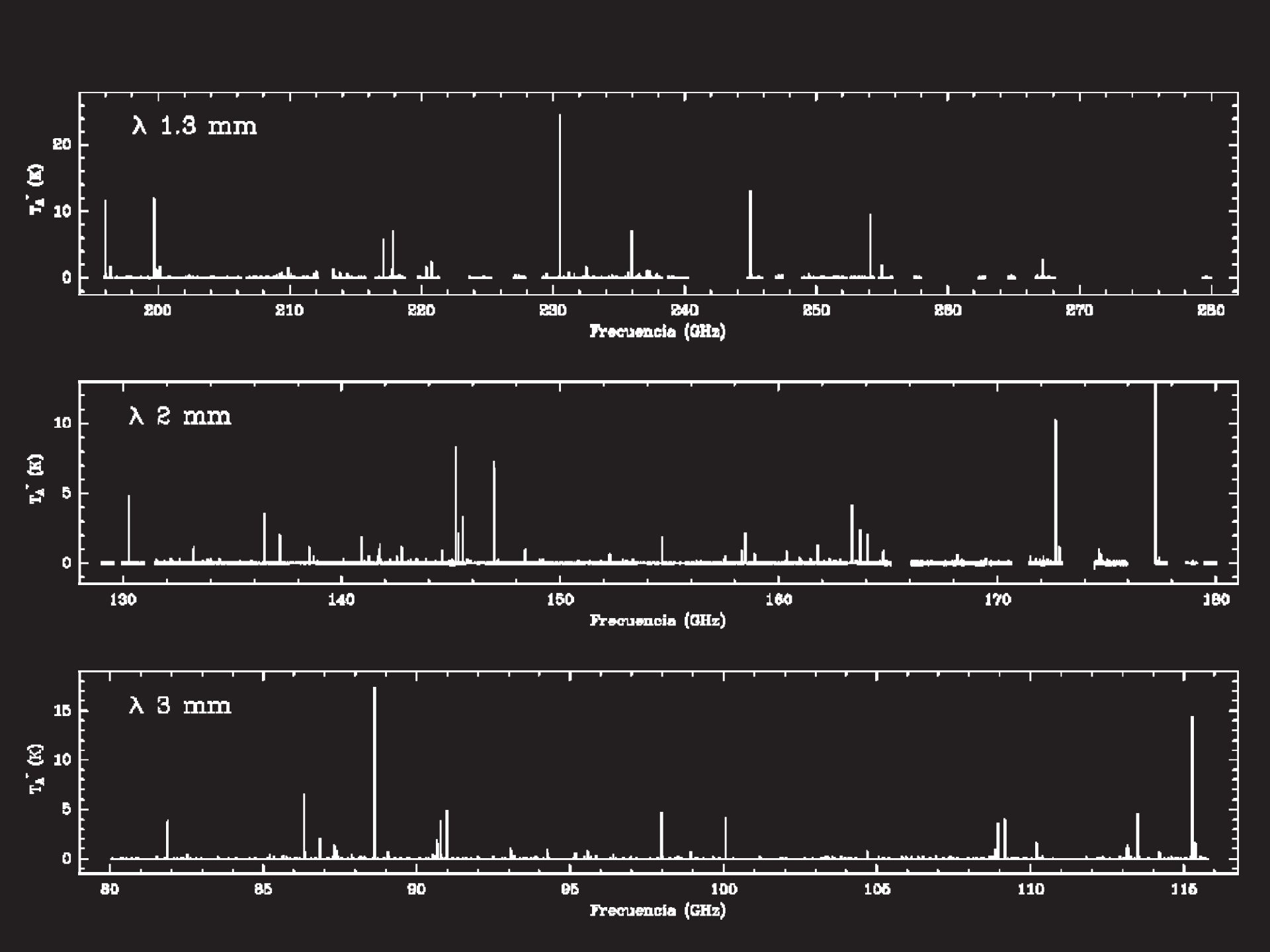
λ 1.3 mm
T_A^* (K)
0
10
20
200
210
220
230
240
250
260
270
280
Frecuencia (GHz)
λ 2 mm
T_A^* (K)
0
5
10
130
140
150
160
170
180
Frecuencia (GHz)
λ 3 mm
T_A^* (K)
0
5
10
15
80
85
90
95
100
105
110
115
Frecuencia (GHz)

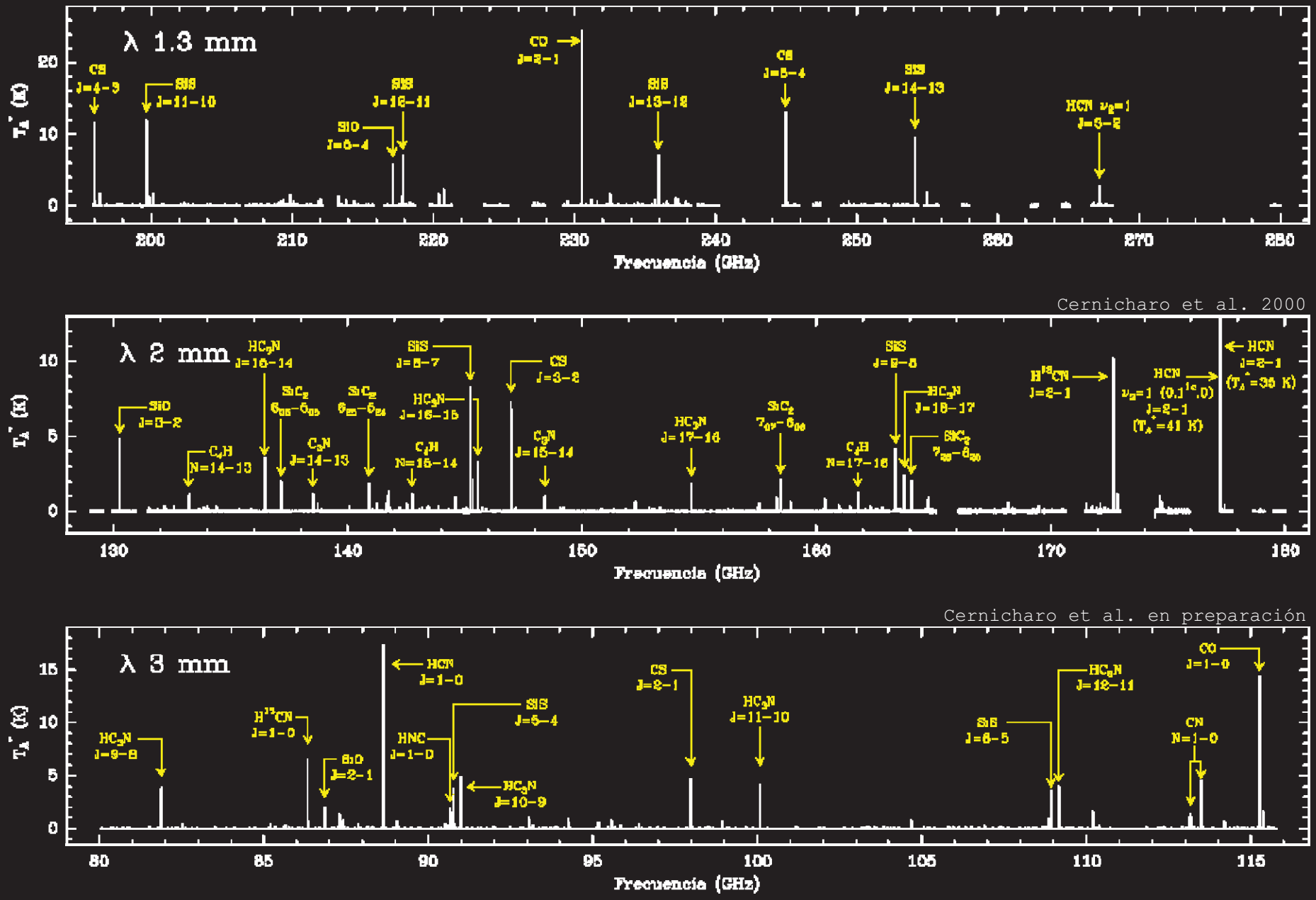
λ 1.3 mm
CS J=4-3
SiS J=11-10
SiO J=6-4
SiS J=12-11
CO J=2-1
SiS J=13-12
CS J=5-4
SiS J=14-13
HCN ν2=1 J=3-2
T_A* (K)
Frecuencia (GHz)
Cernicharo et al. 2000
λ 2 mm
SiO J=5-4
HC3N J=16-14
C4H N=14-13
SiC2 6m-5m
C3N J=14-13
SiC2 6m-5m
SiS J=8-7
HC3N J=16-15
C4H N=15-14
CS J=3-2
C3N J=15-14
HC3N J=17-16
SiC2 7m-6m
C4H N=17-16
SiS J=9-8
HC3N J=18-17
SiC2 7m-6m
H13CN J=2-1
HCN ν2=1 (0,1lc,0) J=2-1 (TA*=41 K)
HCN J=2-1 (TA*=36 K)
T_A* (K)
Frecuencia (GHz)
Cernicharo et al. en preparación
λ 3 mm
HC3N J=9-8
H13CN J=1-0
SiO J=2-1
HCN J=1-0
HNC J=1-0
SiS J=5-4
HC3N J=10-9
CS J=2-1
HC3N J=11-10
SiS J=6-5
HC3N J=12-11
CO J=1-0
CN N=1-0
T_A* (K)
Frecuencia (GHz)

Line survey at λ@3 mm carried out with the IRAM 30-m radio Telescope:

- 80.05-115.75 GHz
- 1339 emission lines (~37 lines/GHz)
- 886 assigned to rotational transitions of 60 molecules (different isotopoloques and vibrationally excited states)
- 453 unassigned lines (only 31 with T_A^* > 10 mK)
- high sensitivity: rms(T_A^*) < 1 mK for most frequencies

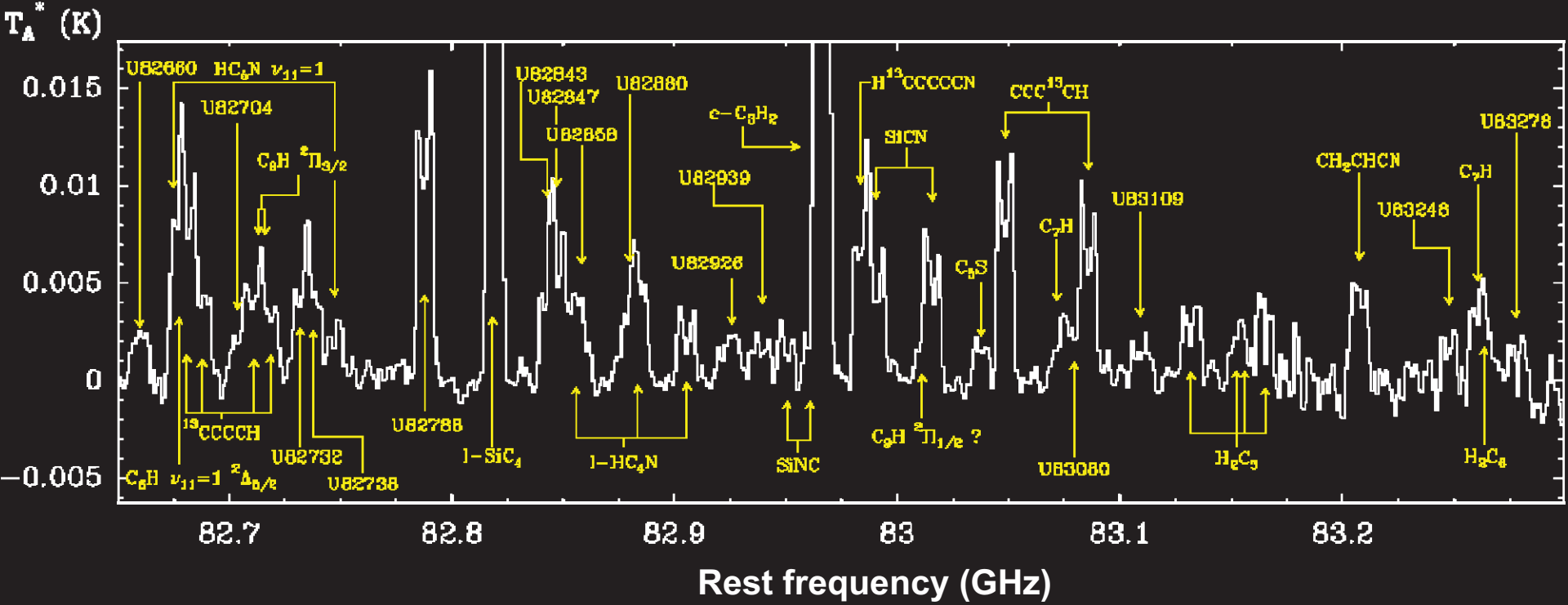

LVG multishell models

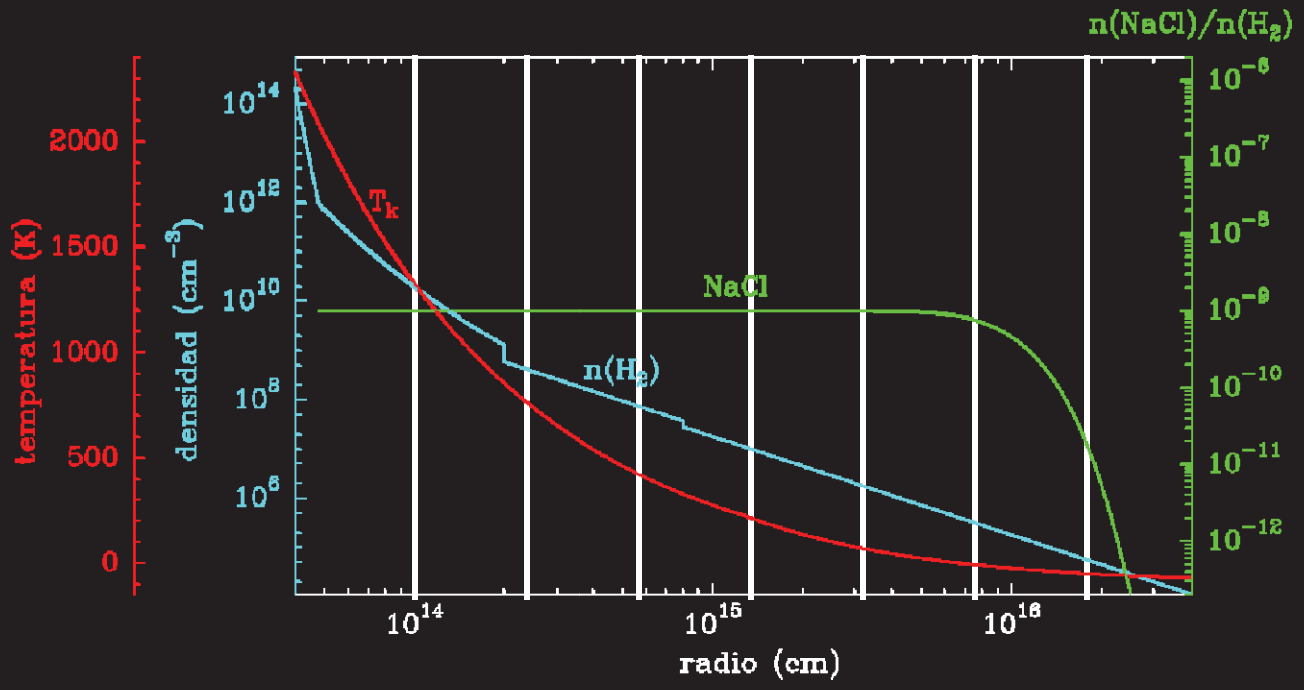

Results

NaCl

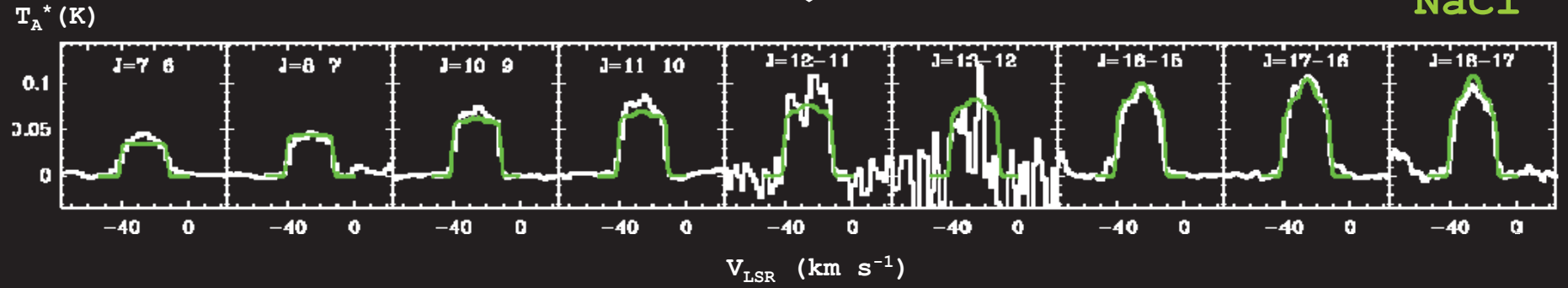

10^{-3}	CO	1(-3)													
10^{-4}			C_2H_2	8(-5)											
					HCN	2(-5)									
10^{-5}			CH_4	3.5(-6)											
			C_2H	3(-6)	NH_3	2(-6)									
			C_4H	2.5(-6)	CN	1.7(-6)									
			C_2	1(-6)	HC_3N	1.4(-6)			SiC_2	1.2(-6)					
10^{-6}			C_3	1(-6)					SiS	1(-6)					
					C_3N	4(-7)	CS	5(-7)							
									SiH_4	2.2(-7)					
					HC_5N	2(-7)			SiO	1.2(-7)					
10^{-7}	H_2O	1(-7)	C_5	1(-7)	HNC	1(-7)									
			$l\text{-}C_3H$	5(-8)											
	OH	4(-8)	C_6H	4(-8)					SiC	4(-8)					
			C_5H	3(-8)	CH_3CN	3(-8)	C_2S	3(-8)						AlCl	3.5(-8)
			$c\text{-}C_3H_2$	3(-8)											
			CH_3C_2H	3(-8)											
			$c\text{-}C_3H$	2(-8)	HC_7N	2(-8)					HCP	2.5(-8)			
			C_2H_4	2(-8)										NaCN	
	H_2CO	1.3(-8)	H_2C_4	1.4(-8)			C_3S	1.2(-8)							
10^{-8}											CP	1(-8)			
			C_8H	8(-9)	HC_9N	8(-9)	H_2CS	7(-9)	SiN	8(-9)	PH_3	8(-9)	MgNC	8(-9)	
					CH_2CN	7(-9)							AlF	7.5(-9)	
					HC_2N	6(-9)									
					C_5N	4(-9)									
			C_7H	3(-9)	HCCNC	4(-9)									
			H_2C_6	3(-9)	C_2H_3CN	4(-9)	H_2S	4(-9)	$c\text{-}SiC_3$	4(-9)					
			C_6H^-	3(-9)	C_5N^-	2.3(-9)			SiC_4	3(-9)					
	C_3O	2(-9)	C_8H^-	1.5(-9)	HC_4N	2(-9)			SiCN	2(-9)					
			H_2C_3	1.5(-9)	C_3N^-	1.1(-9)	C_5S	1.2(-9)	SiNC	1.1(-9)	PN	1(-9)	NaCl	1(-9)	
10^{-9}											C_2P	1(-9)	AlNC	1(-9)	
	HCO^+	7(-10)			HNCCC	5(-10)							MgCN	5(-10)	
			C_4H^-	3(-10)									KCl	2.5(-10)	
10^{-10}															

RESULTS: THE OUTER ENVELOPE --- Chemical kinetic models

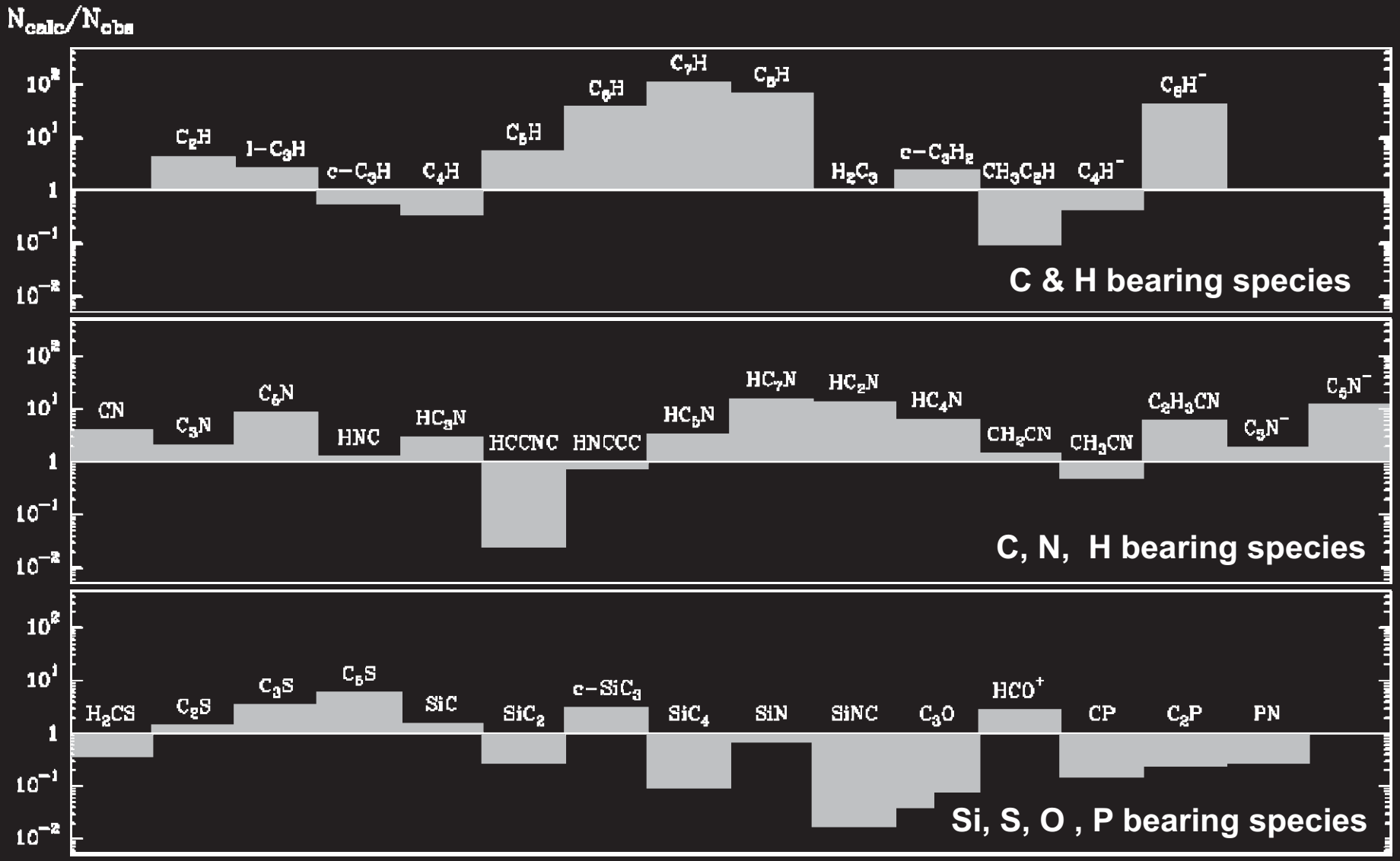

RESULTS: THE OUTER ENVELOPE --- Chemical kinetic models

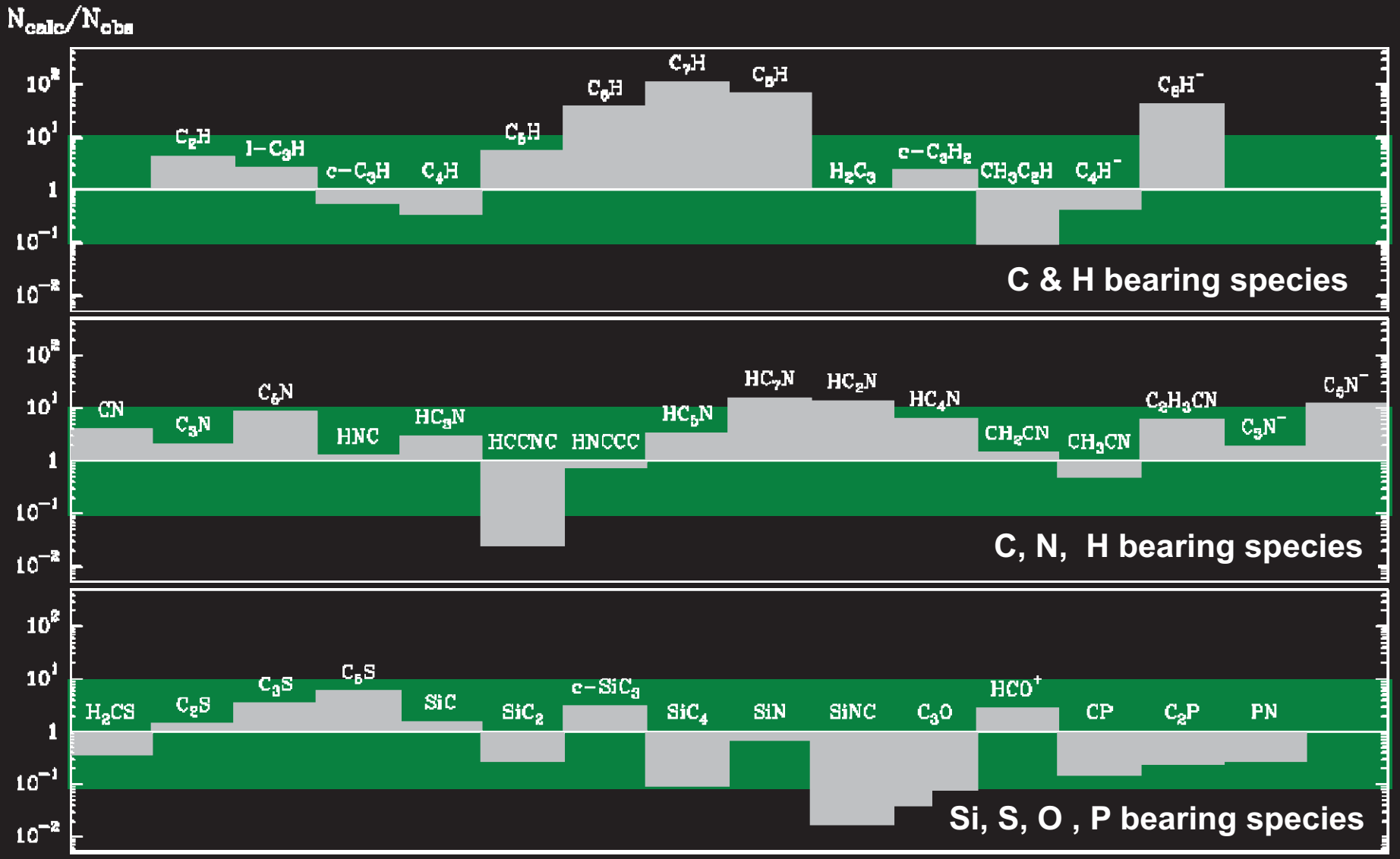

HOW EXOTIC THE CHEMISTRY OF C-rich Evolved Stars can be ?

Nature Vol. 289 19 February 1981

Can negative molecular ions be detected in dense interstellar clouds?

Eric Herbst

Department of Physics, Duke University, Durham,
North Carolina 27706

The recent laboratory measurement[1–3] of rapid radiative electron attachment processes

$$A + e \rightarrow A^- h\nu$$

where A is a molecular species has renewed speculation on whether negative molecular ions can be synthesized efficiently in dense interstellar clouds. We argue here that for certain interstellar species A, the abundance ratio $[A^-]/[A]$ may be as high as 0.01–0.1 in commonly assumed physical conditions. If this abundance ratio were correct, negative molecular ions might be detectable in dense interstellar clouds if their microwave spectral frequencies had been determined in the laboratory. It will be shown, however, that this is currently an unlikely prospect.

ANIONS

2006 C_6H^- en IRC +10216 y TMC-1 (McCarthy et al.)

2007 C_4H^- en IRC +10216 (Cernicharo et al.)

2007 C_8H^- en IRC +10216 y TMC-1 (Remijan et al.; Brünken et al.)

2008 C_3N^- en IRC +10216 (Thaddeus et al.)

2008 C_5N^- en IRC +10216 (Cernicharo et al.)

2010 CN- en IRC +10216 (Agúndez et al.)

C_6H^- en L1527 (Sakai et al. 2007)
C_4H^- en L1527 (Agúndez et al. 2008)
C_6H^- en L1544 y L1521F (Gupta et al. 2009)

IRC +10216
Is the only source where all anions have been observed
C_4H^-, C_6H^-, C_8H^-, C_3N^-, C_5N^-, and CN^-

RESULTA: SPECIFIC RESULTS : ANIONS

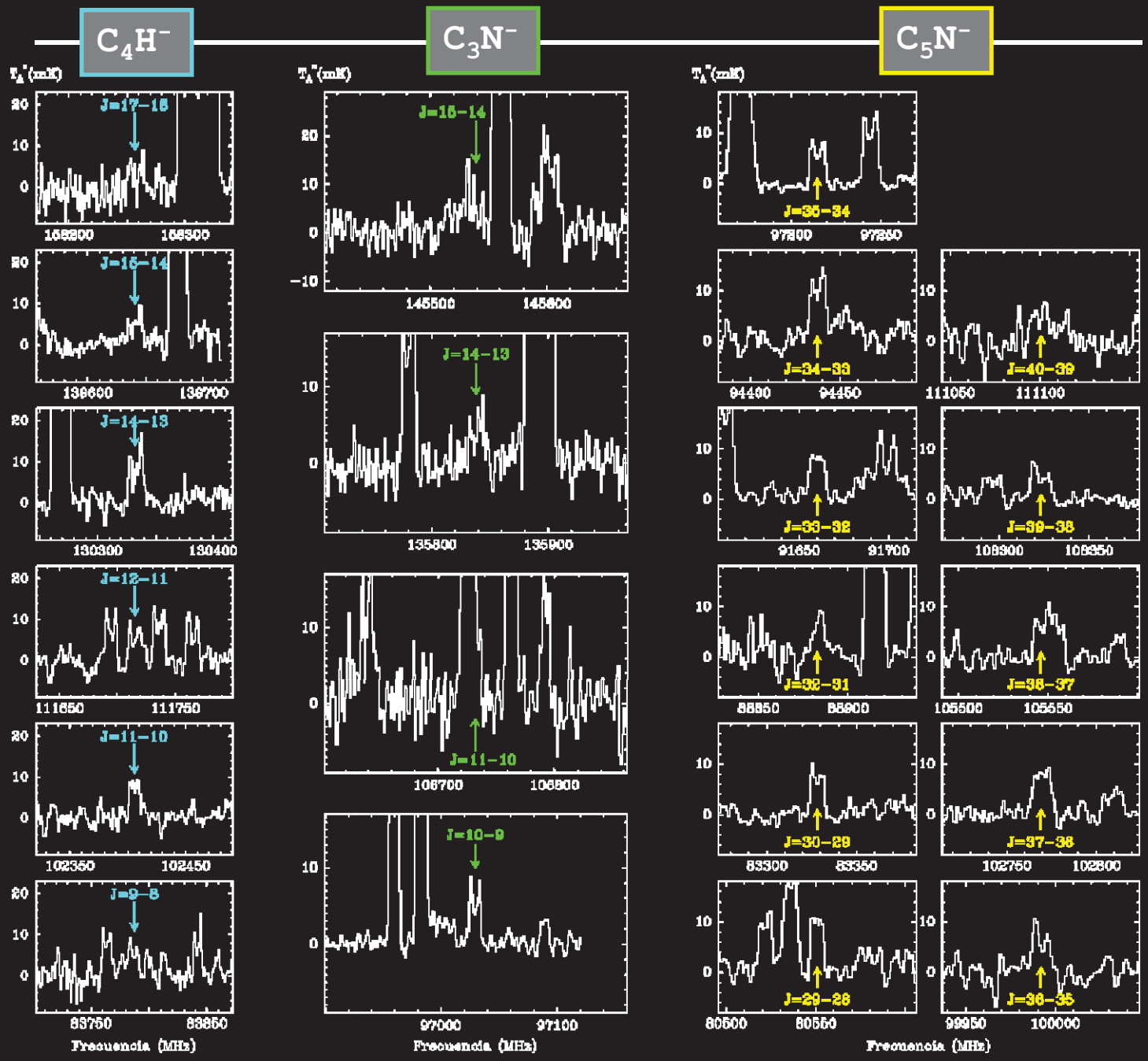

The origin of water in C-rich objects

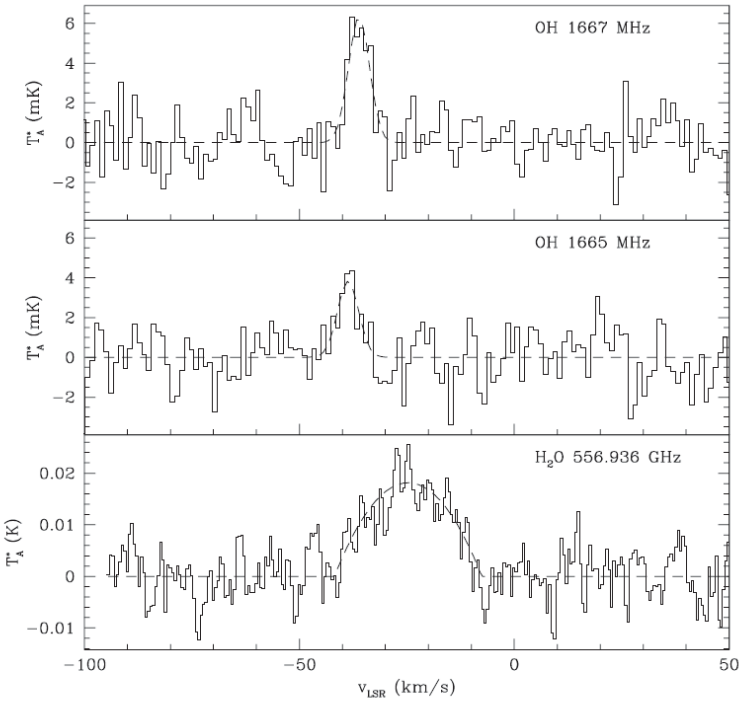

FIG. 1.—Spectra of IRC +10216 at a rest frequency of 556.936 GHz (Melnick et al. 2001) and 1665 and 1667 MHz. For the 556.936 GHz line, the dashed line is a fitted parabola, as expected for an optically thick expanding spherical shell. The dashed lines in the 1665 and 1667 MHz spectra are fitted Gaussians. Parameters for all fits are listed in Table 1.

Melnick 2001, Ford & Neufeld 2001, Ford et al., 2003 (SWAS results)

H_2O, OH and abundant NH_3 in a C-rich star (IRC+10216)

Derived water abundance in these papers has to be reduced by a factor ≈10 due to efficient IR pumping of the rotational levels (Agúndez & Cernicharo 2006)

Hasegawa 2006 (ODIN results)

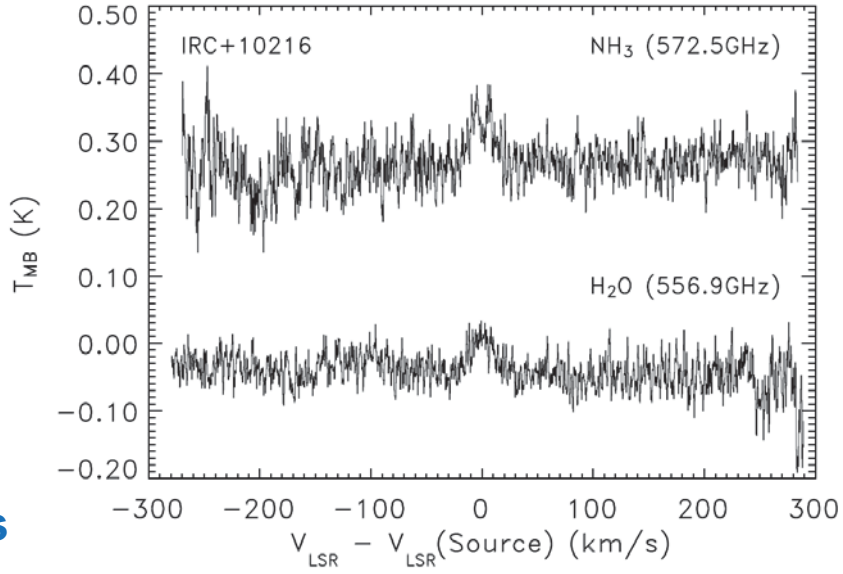

FIG. 1.—NH_3 ($J_K = 1_0 \rightarrow 0_0$) (*top*) and H_2O ($J_{K^-,K^+} = 1_{10} \rightarrow 1_{01}$) (*bottom*) spectra obtained with *Odin* in IRC +10216. The baselines have not been removed the spectra. The frequency resolution is 0.62 MHz in this figure. The NH_3 spectrum has been offset by 0.35 K.

HIFISTARS results
H_2O in all stars, C/O>1, ≈1 & <1
-see also MESS results-

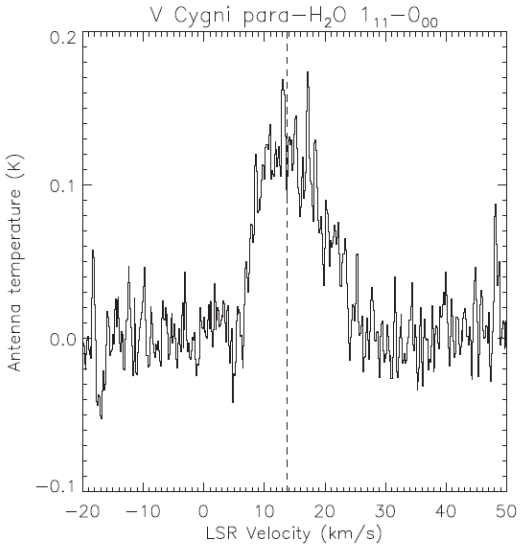

Fig. 1. Continuum-subtracted spectrum of para-H_2O $1_{11} - 0_{00}$ obtained toward V Cygni. The vertical dashed line indicates the LSR velocity of the source, as determined by BW01 from observations of the CO $J = 2 - 1$ line.

Neufeld et al., 2010

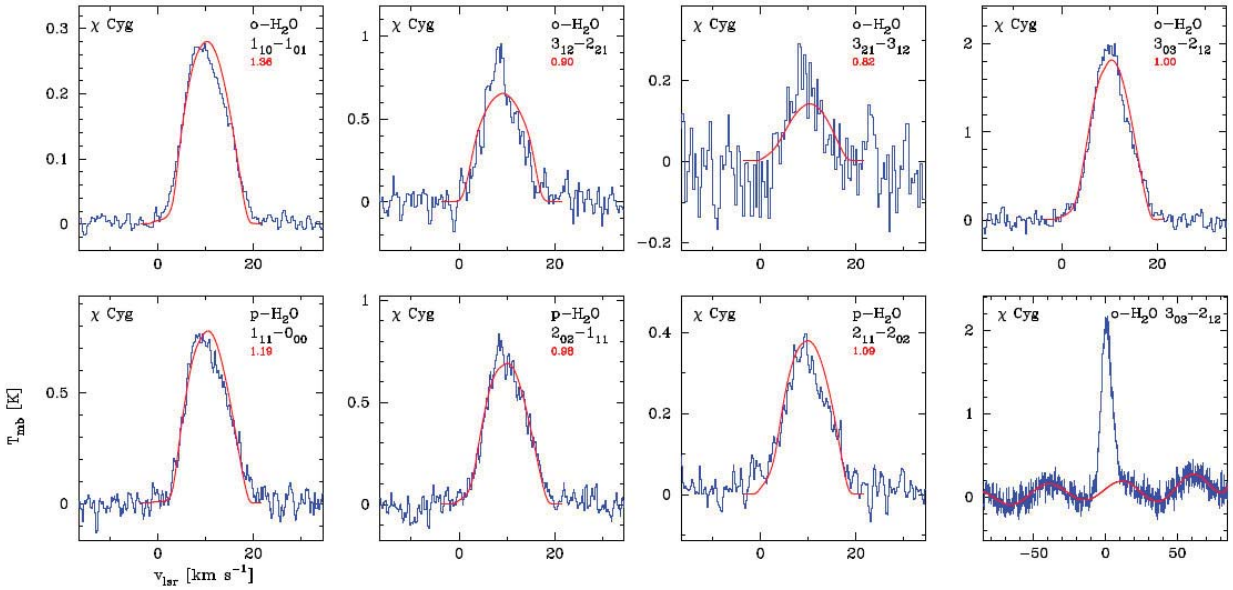

Justtanont et al., 2010

Fig. 3. The model fits (smooth lines) to the HIFI ortho- and para-H_2O lines (histogram). The scaling factor (used to scale the model result to fit the observed integrated intensity) is given for each line, showing the goodness of the fit. The pipeline-reduced data of the $3_{03} - 2_{12}$ line are plotted along with the fitted baseline at the bottom right. This line is affected by standing waves within HIFI.

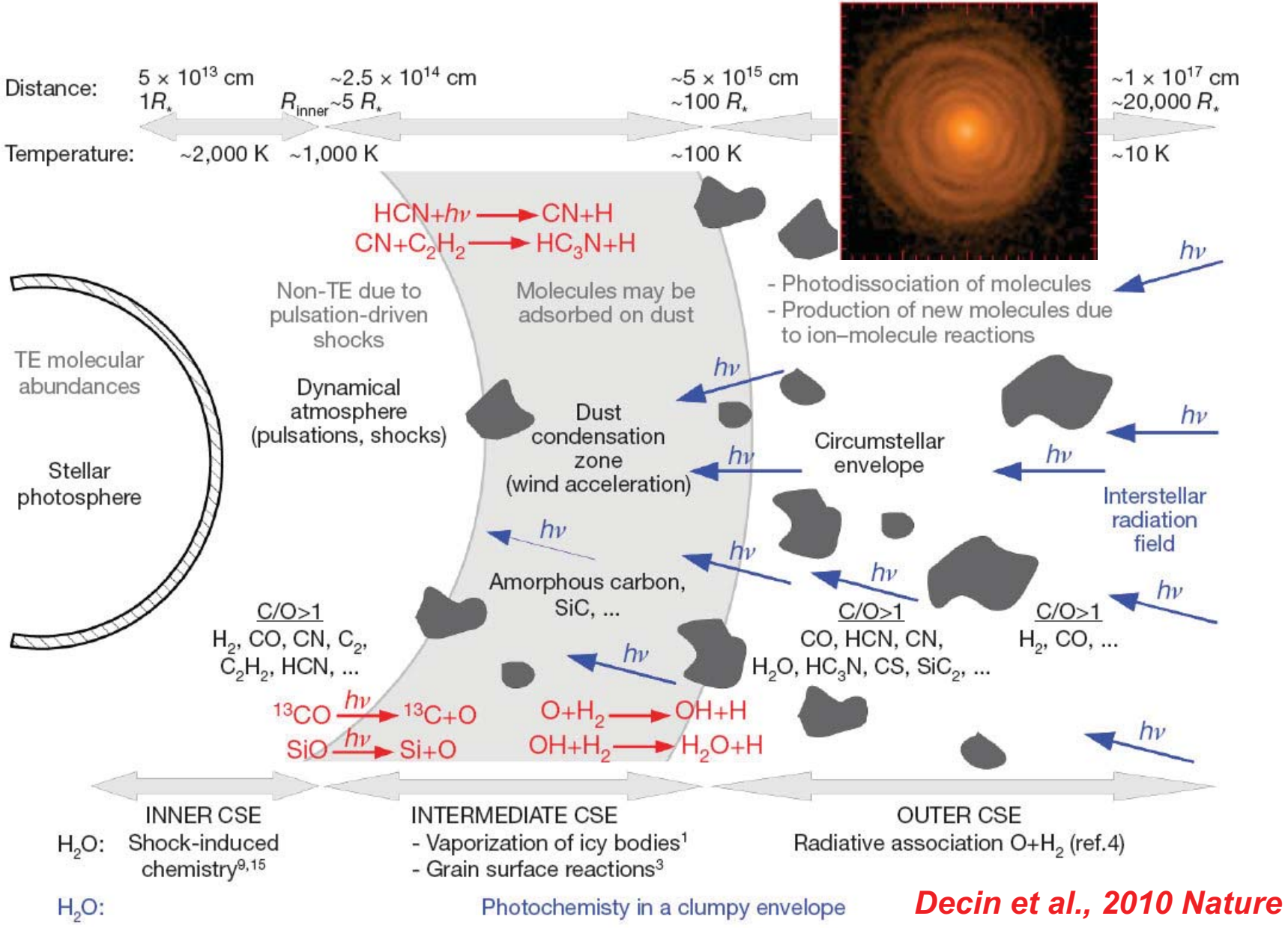

Decin et al., 2010 Nature

Oxygen atoms available from the photodissociation of ^{13}CO and SiO

Agúndez & Cernicharo 2006

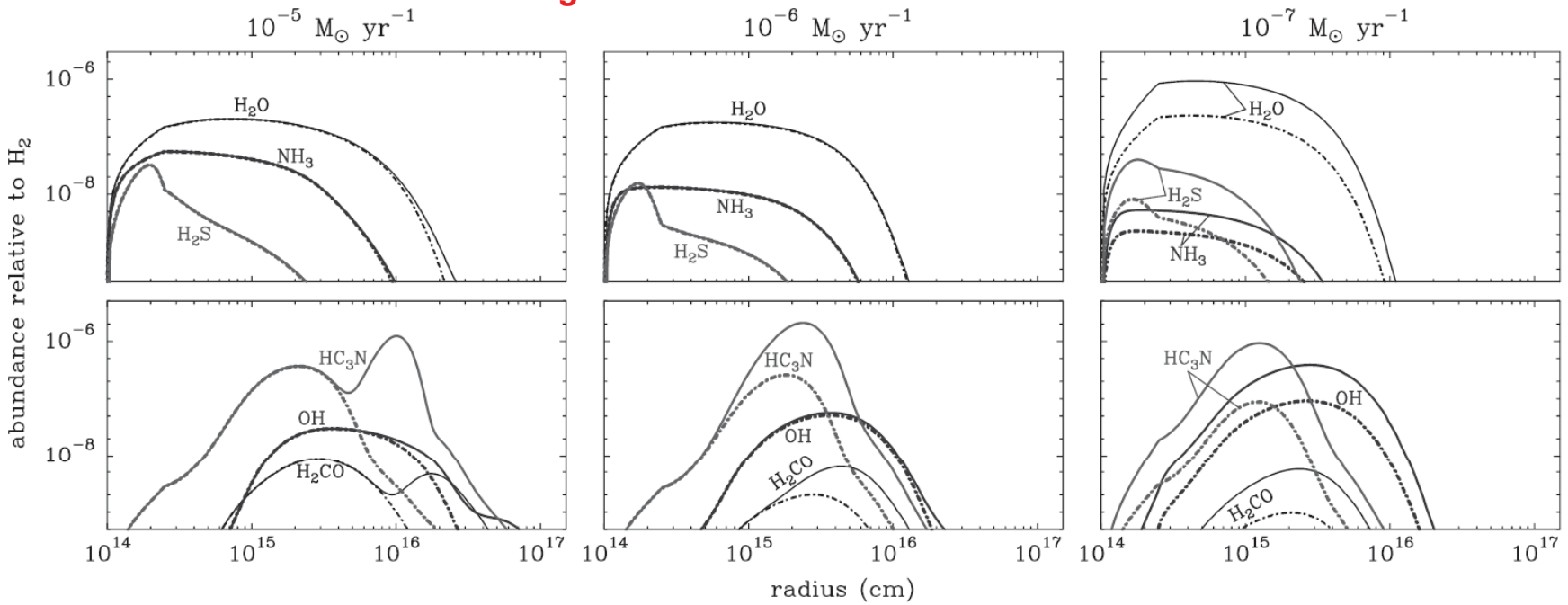

Fig. 2.— Calculated abundance of several molecules as a function of radius for carbon-rich CSEs with mass loss rates of 10^{-5}, 10^{-6}, and 10^{-7} $M_\odot$ yr^{-1}. Dashed-dotted lines correspond to the abundance of the minor UV exposed component and continuous lines to the abundance weighted-averaged over the minor and major components.

Detailed chemical modeling of clumpy envelopes : H_2O, OH and H_2CO could be abundant in C-rich AGBs. HC_3N abundance enhanced in the inner envelope.

Agúndez, Cernicharo & Guélin 2010, ApJ, in press

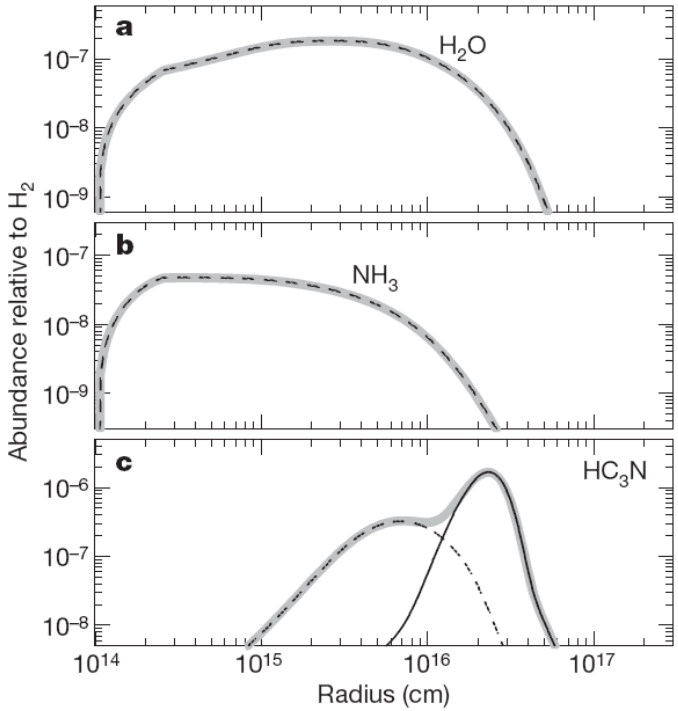

Figure 3 | Fractional abundances in the clumpy circumstellar environme of IRC +10216. The chemical model simulates a clumpy envelope structu where a fraction of the interstellar UV photons is able to penetrate deep i the envelope (Supplementary Information). **a**–**c**, Predictions for the radi distribution of the fractional abundances relative to H_2 of H_2O (**a**), NH_3 (**b**) and HC_3N (**c**) for a model with a minor UV-illuminated component superposed on a major UV-shielded component. The minor component shown in this figure contains 10% of the total circumstellar mass ($f_M = 0.$ which is illuminated by interstellar UV photons through a cone where mat fills 70% of the solid angle of arrival of interstellar light ($f_\Omega = 0.3$). Dashe black lines correspond to the minor UV-illuminated component, continuc black lines to the major UV-shielded component, and thick grey lines to weighted average abundance over the two components. The weighted aver abundance is computed as $\bar{X}_i(r) = (1-f_M)X_i^{\text{major}}(r) + (f_M)X_i^{\text{minor}}(r)$, whe $X_i^{\text{major}}(r)$ and $X_i^{\text{minor}}(r)$ are the abundance of the species i in the major U shielded and minor UV-illuminated component, respectively, as a function of radius r. Note that for H_2O and NH_3 the contribution from the major UV-shielded component is negligible, and the dashed and thick grey line coincide.

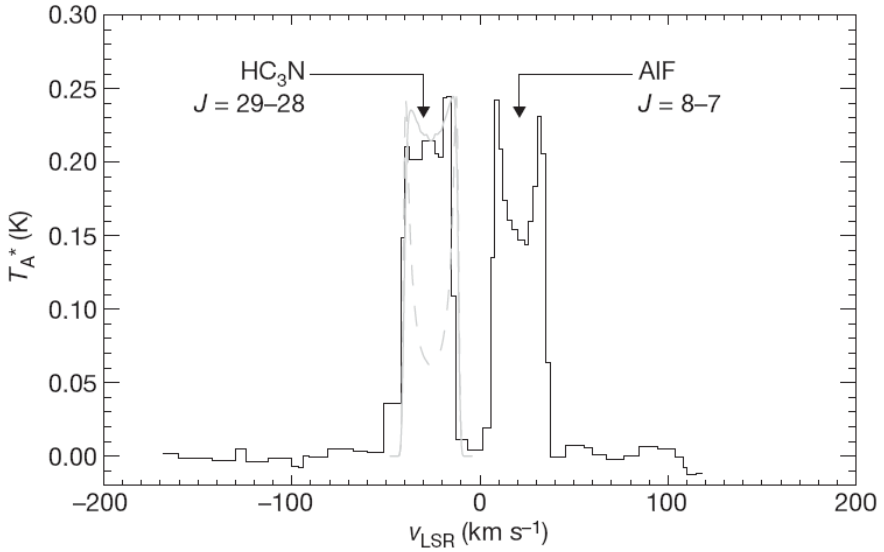

Figure 4 | HC_3N as observed in the envelope of IRC +10216. The HC_3N $J = 29-28$, $J = 33-32$ and $J = 37-36$ lines have been observed with the IRAM telescope. All three HC_3N lines show a clear flat-topped profile. Only the HC_3N $J = 29-28$ line is shown in this figure, and its line profile is compared to that of the AlF $J = 8-7$ line (black line). Both lines were observed with the same telescope, the same beam and the same pointing, and have been calibrated in the same way. Whereas the AlF line profile is 'U'-shaped, the HC_3N line is flat topped, clearly indicating that HC_3N arises from gas extending to inner radii. The grey lines show two model predictions: the dashed grey line corresponds to a model prediction only taking the major UV-shielded component into account, the full grey line shows the theoretical line profile for a model including both the major UV-shielded component and the minor UV-illuminated component. The spectrum is plotted in terms of intensity (T_A^* in K) versus v_{LSR} (in km s^{-1}).

The predicted H2O abundance profile fits well the PACS/SPIRE data

Decin et al., 2010, Nature

CONCLUSIONS

(a) COMPOSITION OF THE CSE of IRC +10216

(1a) IRC +10216 is one of the riches sources in molecules in the sky with 76 species (50% of the total number of known molecules in space).

(2a) Only a few O-bearing species (H_2O, CO, SiO, CCCO, OH, H_2CO)

(3a) Chemistry is dominated by unsaturated carbon chain molecules (H/C<1)

(4ª) Only a few species saturated (CH_4, NH_3, SiH_4 PH_3)

(5a) Only ~5 % of S, Si, P are in form of molecules in the gas phase.

(6a) Metal bearing species. HCl & HF recently detected with Herschel

(7a) Silicon Dicarbide is the most abundant (polar) SiC-bearing molecule. SiC is a photodissociation product of SiC_2.

(b) ORIGIN OF THE MOLECULES

(1b) Molecules formed in the inner shell (observed abundances in agreement with thermodynamical chemical equilibrium)

(2b) Molecules formed in the external envelope (carbon chain radicals, Metal isocyanides):Chemical models explain most abundances but fail for the longest ones probably due to the lack of reactions between C_n C_nH C_nH_n and their anions Photodestruction rates are in most cases crude estimates.

(3b) PAHs are not significantly formed in the gas phase in the inner layers of IRC

Our understanding of molecular complexity is limited by the lack of laboratory data and limited completness of chemical networks.

(3b) H_2O, H_2CO and OH explained by the clumpy structure of the envelope. HC_3N abundance enhanced in the inner envelope

THE FINAL PRODUCT

- New Molecules
- Abundances for all species
- Isotopic abundances (nuclear evolution)
- Clear differentation of the different layers of the CSE
- Chemistry of exotic species (anions)
- A detailed study of missing reactions in present chemical networks

Millimeterwave survey of the Protoplanetary Nebula CRL 618 and complete model

Juan R. Pardo and José Cernicharo / CSIC (Madrid)

Outline

- C-rich Post-AGB objects as efficient factories of complex molecules.
- The PPN vs AGB phase.
- Characteristics of CRL 618.
  - Previous mm data.
  - ISO data.
- 80-275 GHz survey of CRL 618
  - Observational features.
  - Analysis and model. Physical conditions. Chemical abundances.
- Future research.

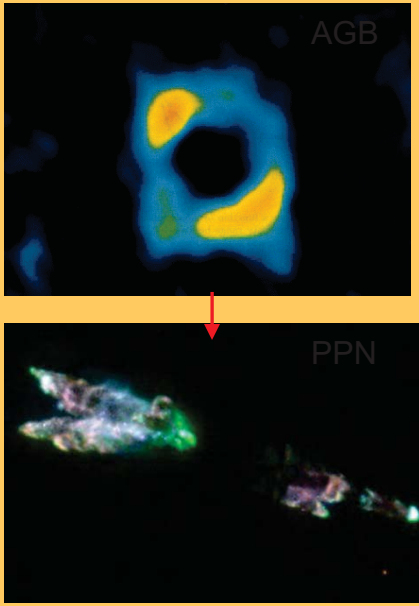

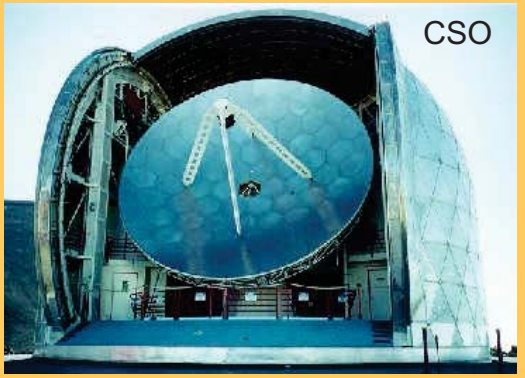

THE POST-AGB PHASE IS INTERESTING FOR THE FORMATION OF COMPLEX MOLECULES IN SPACE, SPECIALLLY IN C-RICH OBJECTS

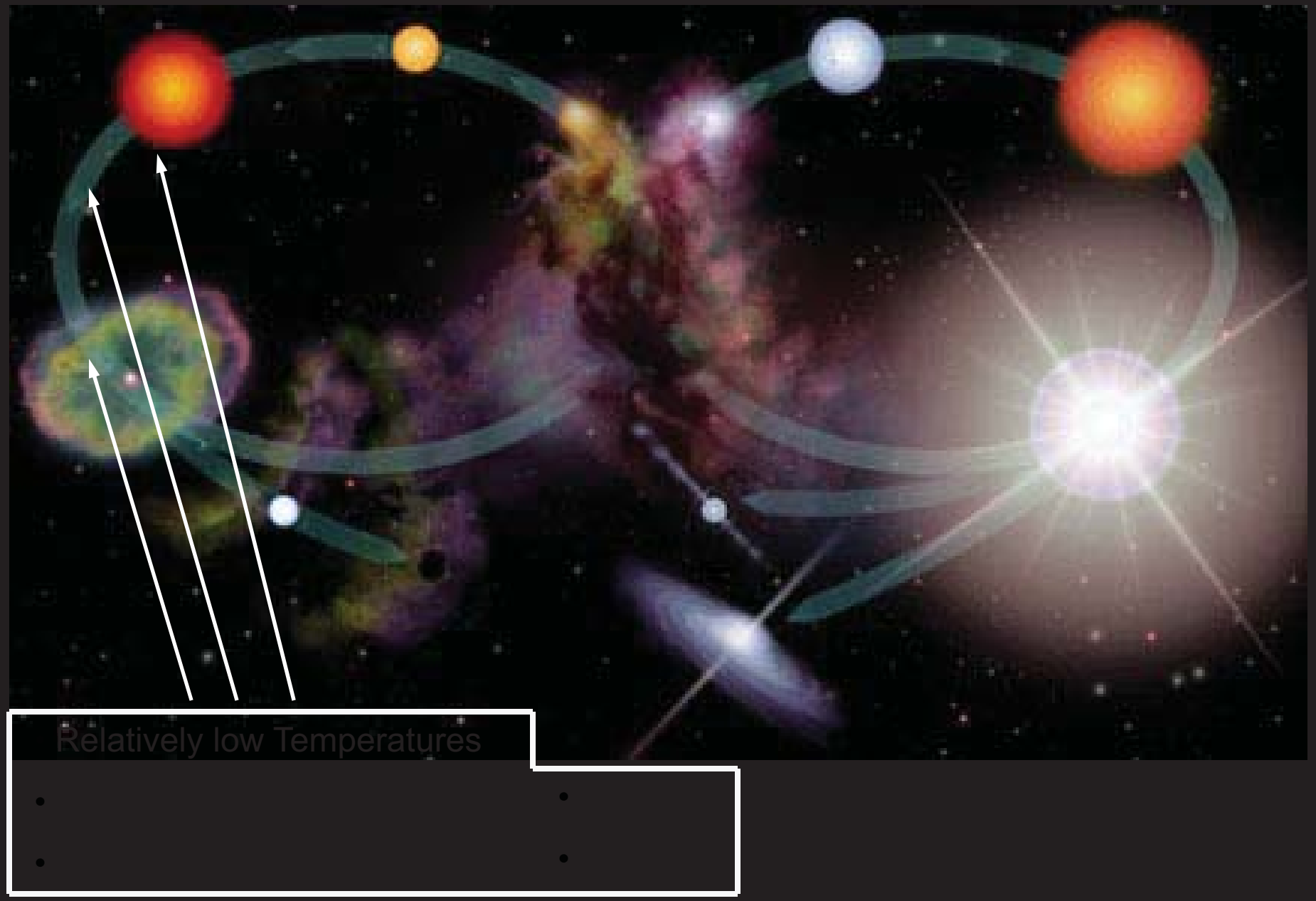

POST-AGB OBJECTS ATRACTED GREAT ATTENTION FROM THE MOLECULAR CHEMISTRY POINT OF VIEW WITH THE DISCOVERY OF C_6H_6 IN CRL 618

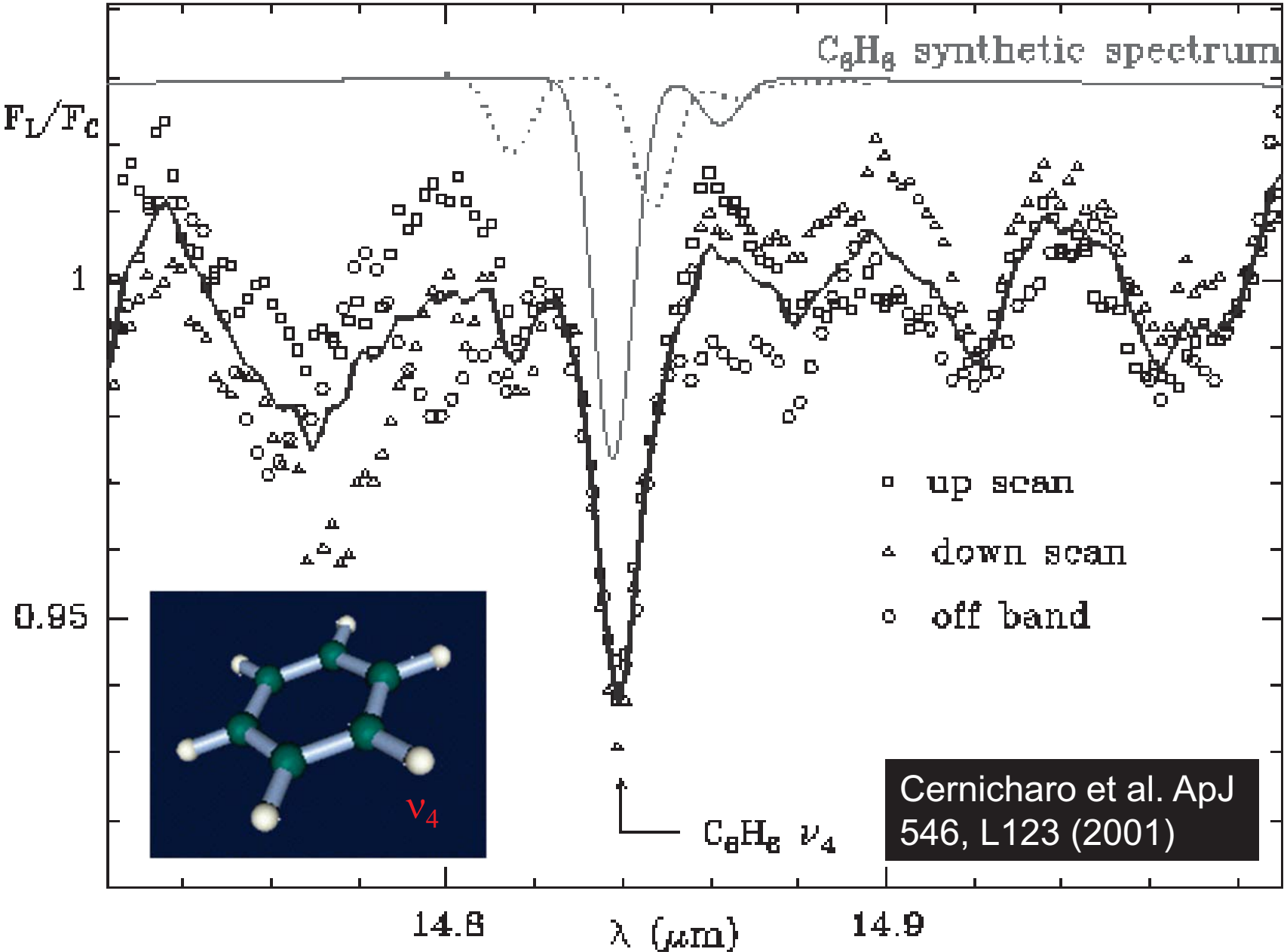

Cernicharo et al. ApJ 546, L123 (2001)

Research Program: Chemical evolution in the Post-AGB Phase

Methodology

- Line surveys at mm, submm and FIR wavelengths of a sample of objects representing the AGB to PN evolution phase: IRC10216, CRL2688, CRL618, NGC7027.
- Develop the most complete line catalogs.
- Develop radiative transfer models: LTE, LVG, 2D, 3D...
- Develop chemical models.
- Include dynamics and morphology in the models.
- Coordinate efforts with the rest of the community (Herschel GT and OT proposals).

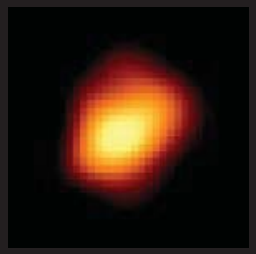
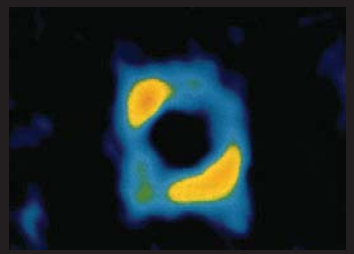
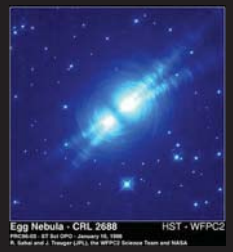


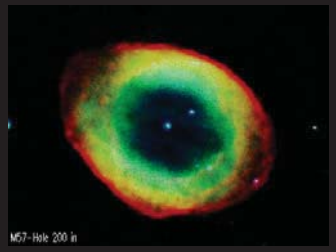

AGB → PN

Instruments: IRAM-30m, CSO & ISO (ALMA & Herschel in the future)

Molecular complexity: AGB vs PPN

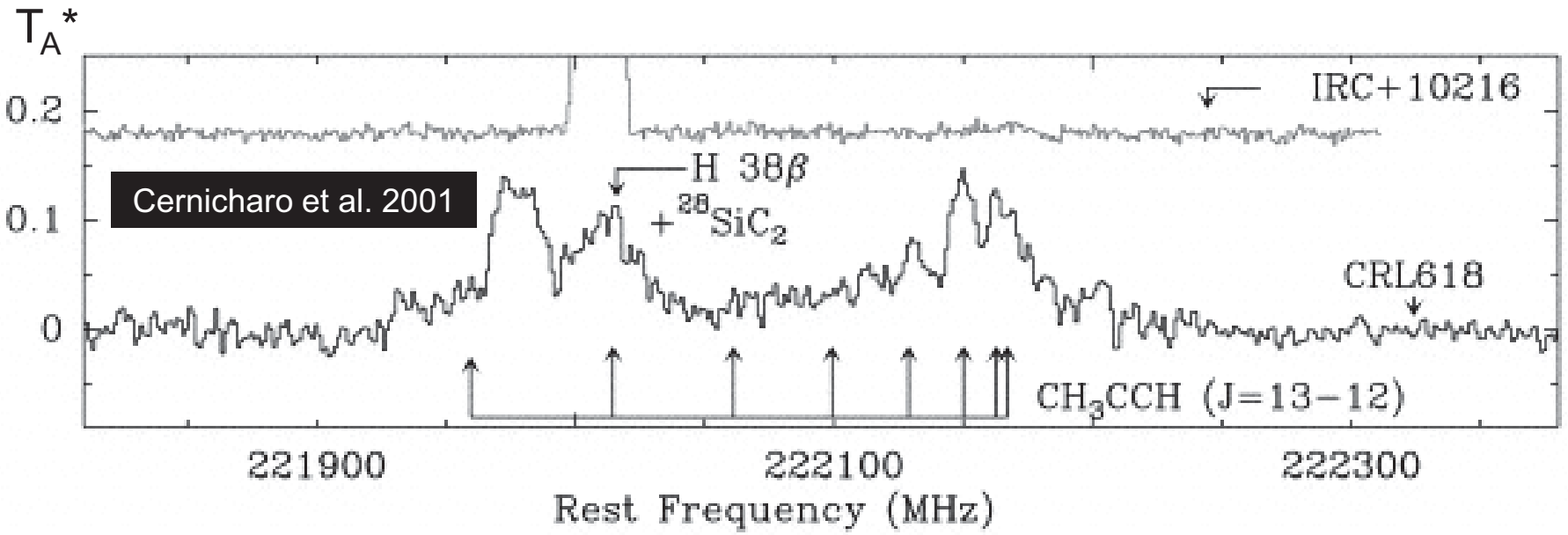

Complete line surveys of CRL 618 have being carried out

Short description of CRL 618

- It is the best example of a protoplanetary nebula with a dense envelope.
- Central star is of B0 type surrounded by an ultracompact HII region.
- Its distance is only 1.7 kpc.
- It displays a high velocity wind (200 kms^{-1}).
- It is experiencing a very fast evolution (PPNe ~1000 years).
  - The mm continuum flux is variable.
  - There is a large chemical richness being created thanks to the presence of shocks, dust and intense UV radiation.

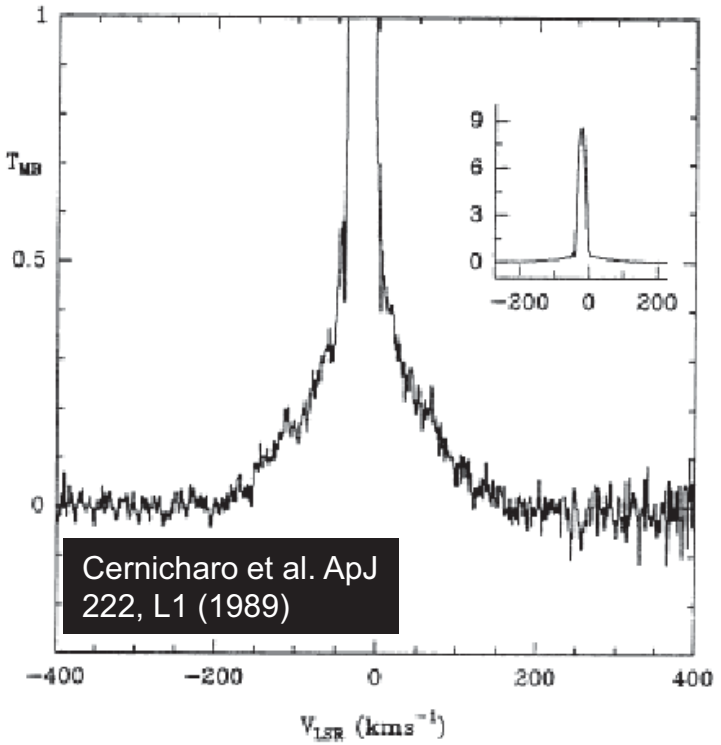

HIGH VELOCITY WIND: originally seen in CO but also visible in some other abundant molecular species.

The IRAM 30m millimeterwave survey of CRL 618

- Observations conducted between 1994 and 2002.
- Image sideband rejection always > 12 db.
- 8 receivers (82-116, 130-184, 201-258 y 240-276 GHz)
- Pointing and focus always on CRL 618.
- Wobbler switching (60") / Spectrometers: $\Delta\upsilon$~ 1 MHz.
- System temperatures in the range 100 and 800 K.

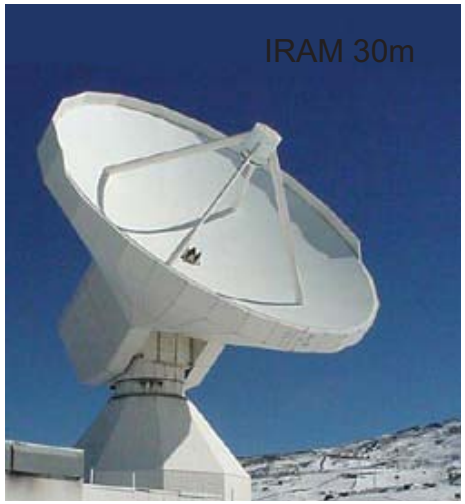

Complementary Observations:

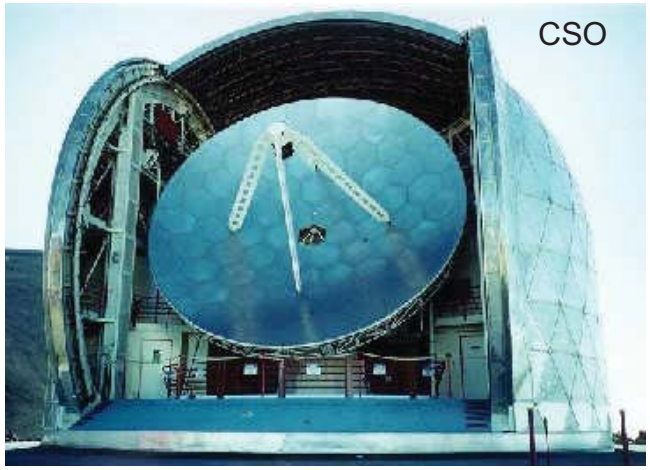

Results: continuum flux

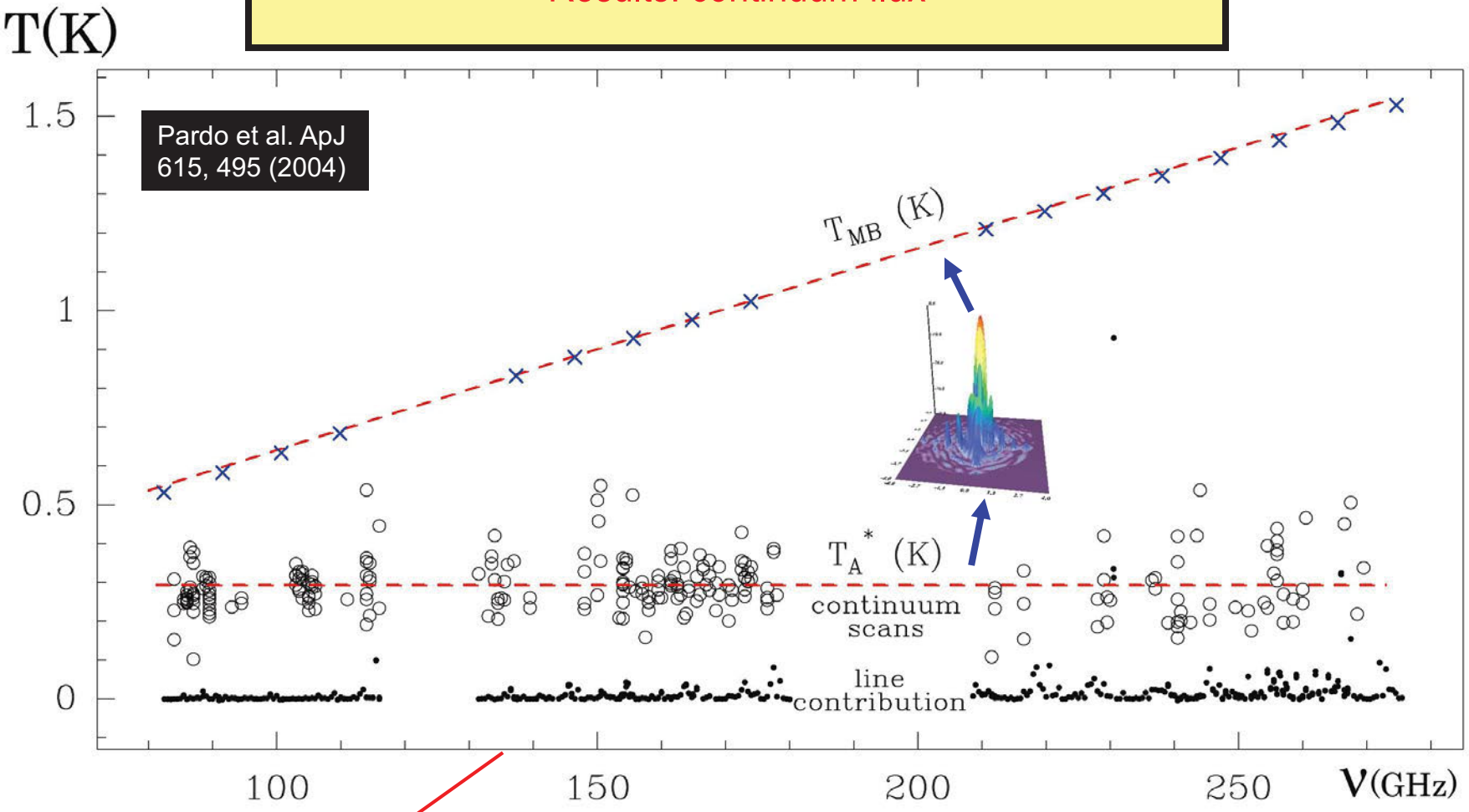

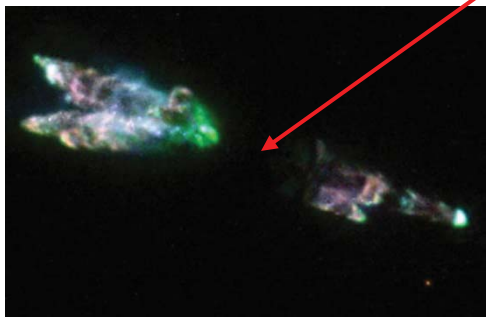

This data have been obtained from the pointing scans on CRL 618 itself. Variability may be hidden in the dispersion of the data points.

Analysis of the continuum flux

- There is evidence of variability.
- The average over 8 years provides T_A^* following a horizontal line in the 80-276 GHz frequency range.
- The flux increases from 1.75 Jy at 90 GHz to 3.4 Jy at 240 GHz.
- The observed flux is well reproduced considering a central source as follows:
  - A size in the range 0.22" - 0.27"
  - An effective temperature at 200 GHz between 3900 - 6400 K.
  - An spectral index ~ -1.15, -1.12.
- The emission mechanisms seem to be:
  - Free-free emission.
  - Dust.

Results: Spectral Lines

λ ~ 3 mm

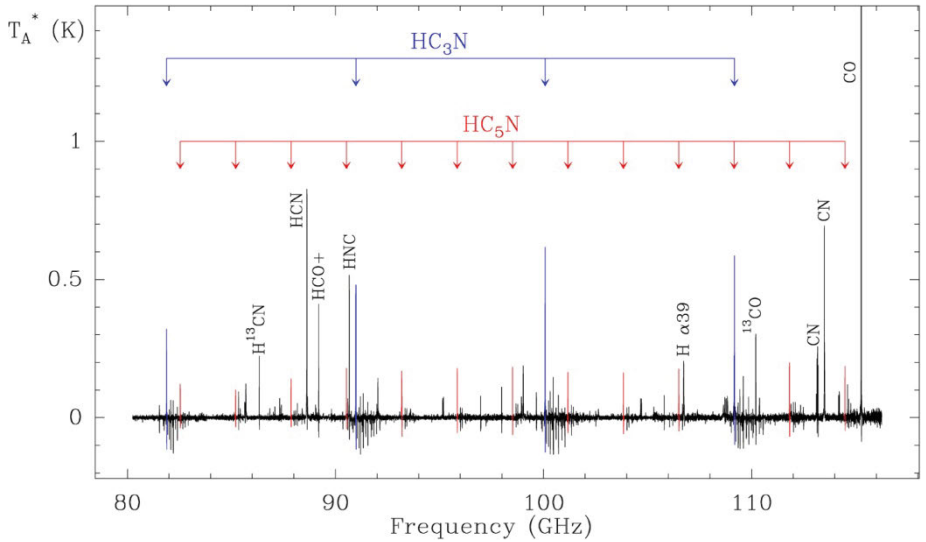

λ ~ 2 mm

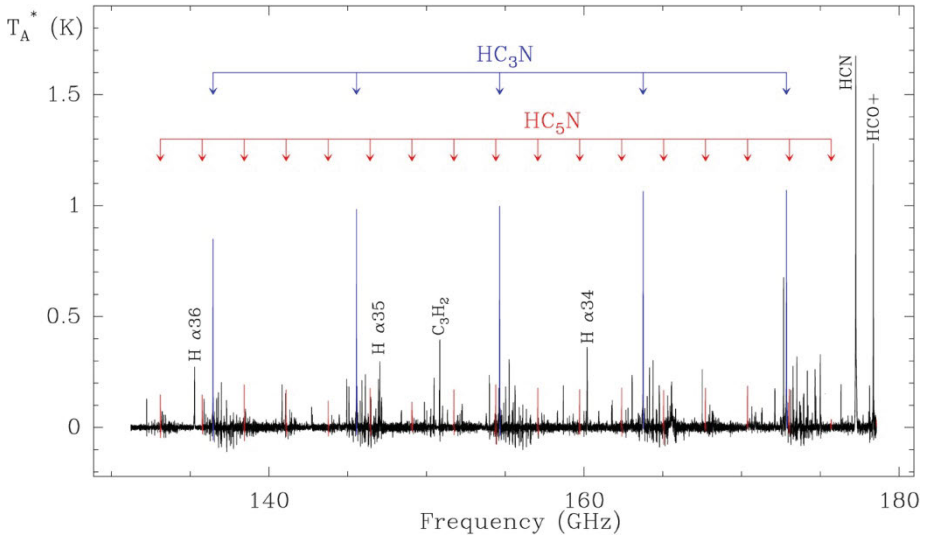

λ ~ 1.3 mm

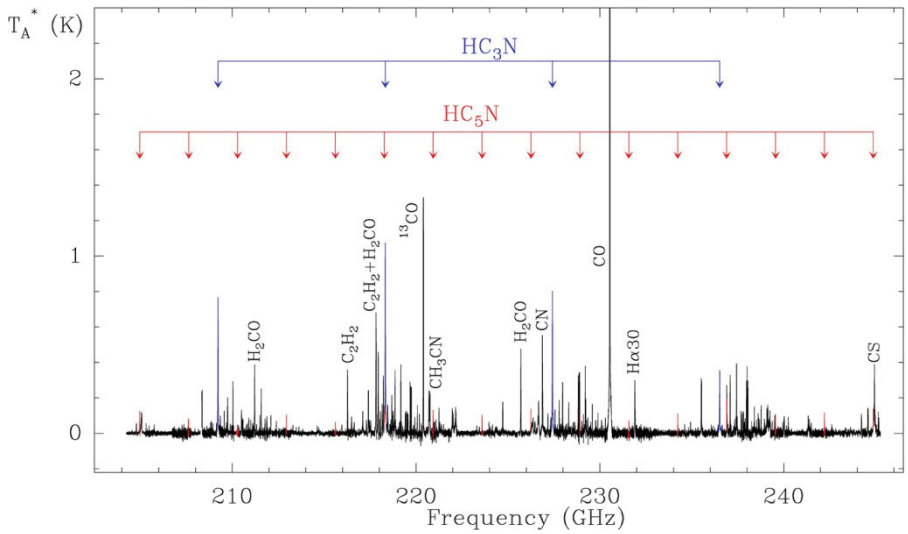

λ ~ 1.0 mm

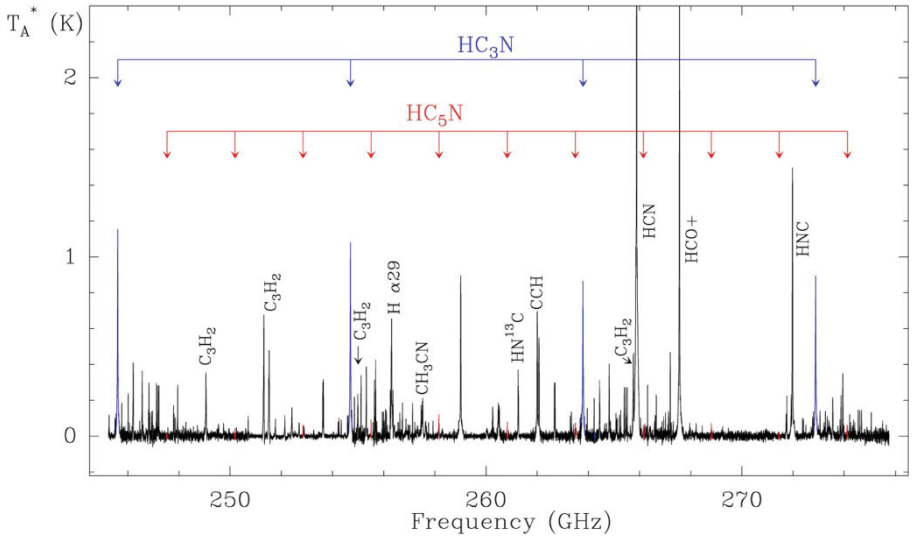

General characteristics of the mm-wave lines in CRL 618

- We have detected more than 3100 lines of more than 20 molecular species + recombination lines of H and He.
- The spectrum is dominated by HC_3N and HC_5N, with ~ 85% of the total number of features detected.
- In general the absorption part of the P-Cygni profiles is less deep as frequency increases.
- The lines of some species do not display absorption.
- Abundant molecules, such as CO, HCN, HCO^+, display lines with wide wings, corresponding to a high velocity outflow.

The large number of transitions for each molecular species available in the survey should allow to probe the object with a lot of detail even if the angular resolution is limited.

MORFOLOGY - PHYSICAL CONDITIONS - CHEMICAL ABUNDANCES - DYNAMICS

HC_3N Spectroscopy

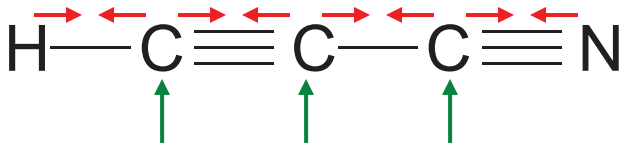

- 3 bending modes de (doubly degenerated) y 4 stretching modes.
- Bending modes : (ν_7,ν_6,ν_5): Energies up to 663 cm^{-1}
- Stretching modes: ν_4 at 881 cm^{-1}, the others above 2000 cm^{-1} (non detected).
- 14 different vibrationally excited states detected, with energies up to 1100 cm^{-1}.
- The line profiles in CRL618 show: high velocity wind, slowly expanding envelope, cold circumstellar shell. Most lines have P-Cygni profiles, specially at low frequencies..

Observational characteristics of CRL618

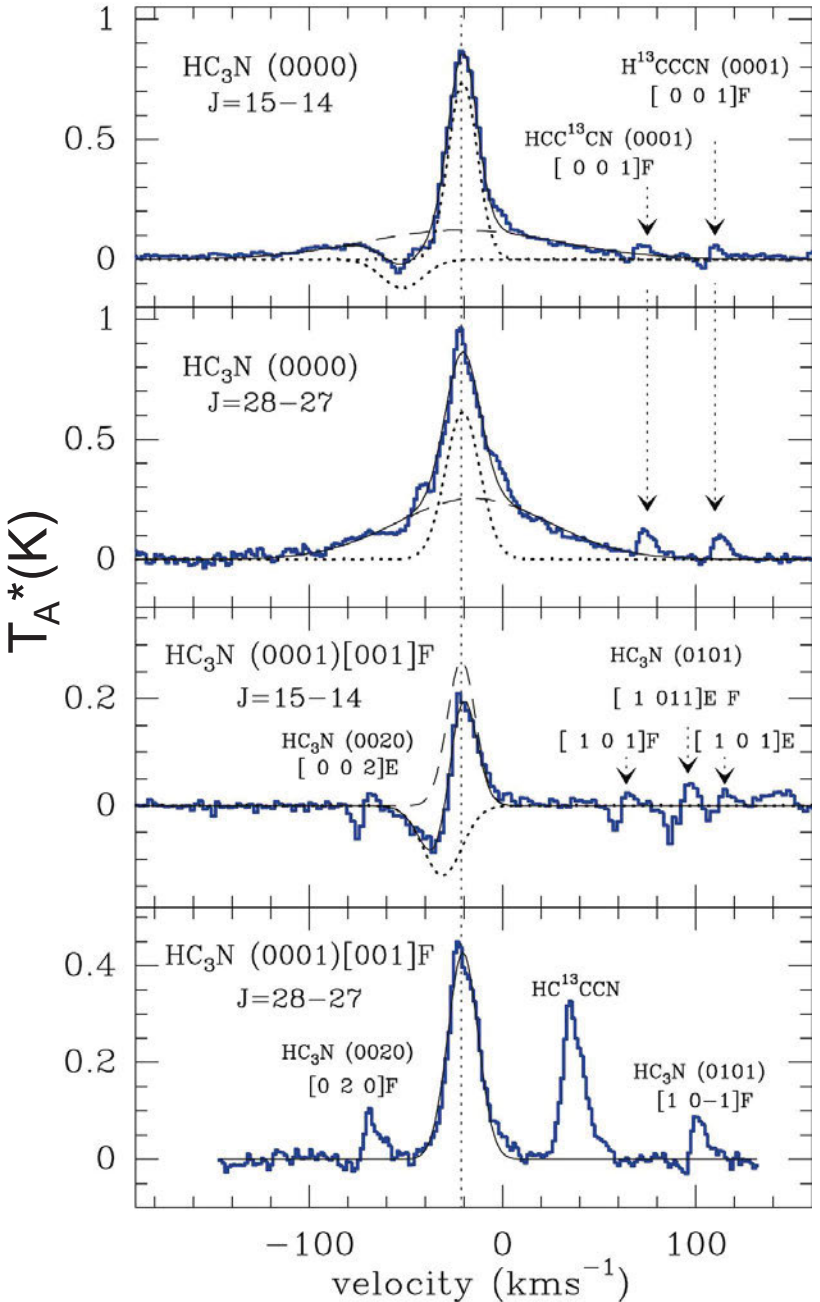

Probing CRL 618 step by step

Region of formation of P-Cygni profiles (innermost envelope)

Tool: HC_3N lines in vibrationally excited states

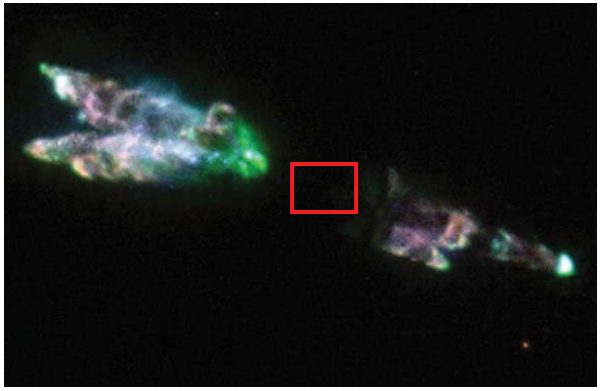

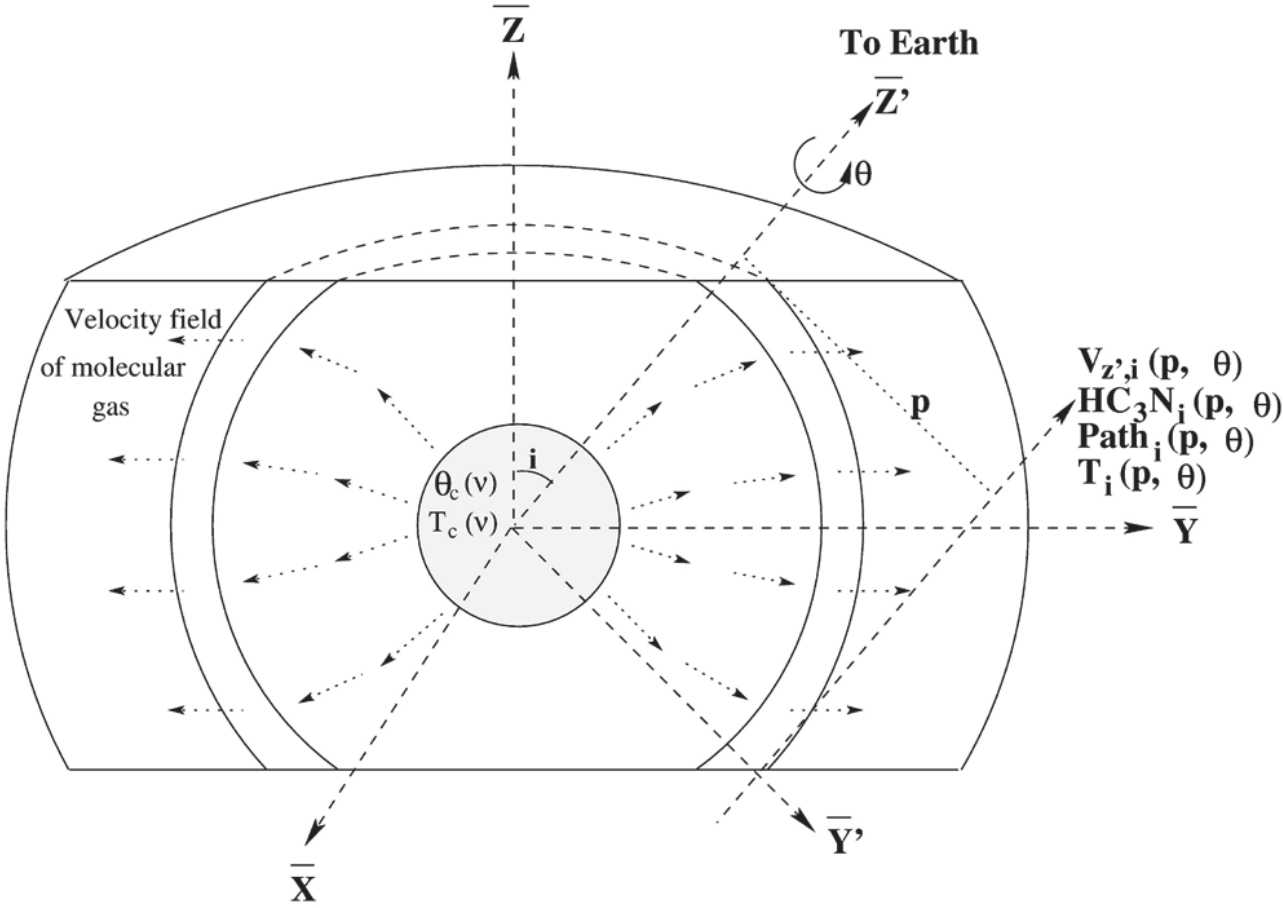

Help: Previous studies, interferometric maps

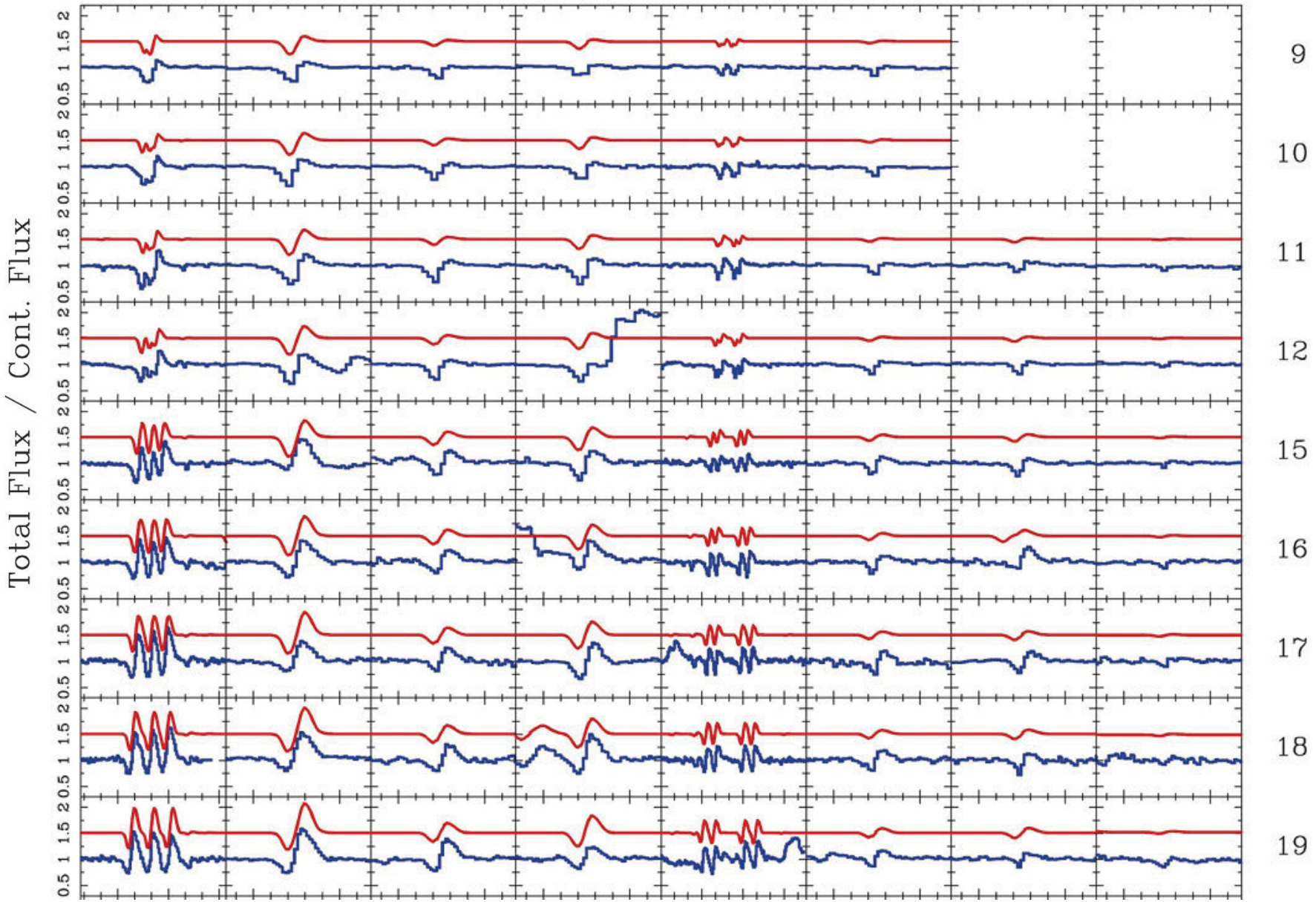

Pardo et al. ApJ 615, 495 (2004)

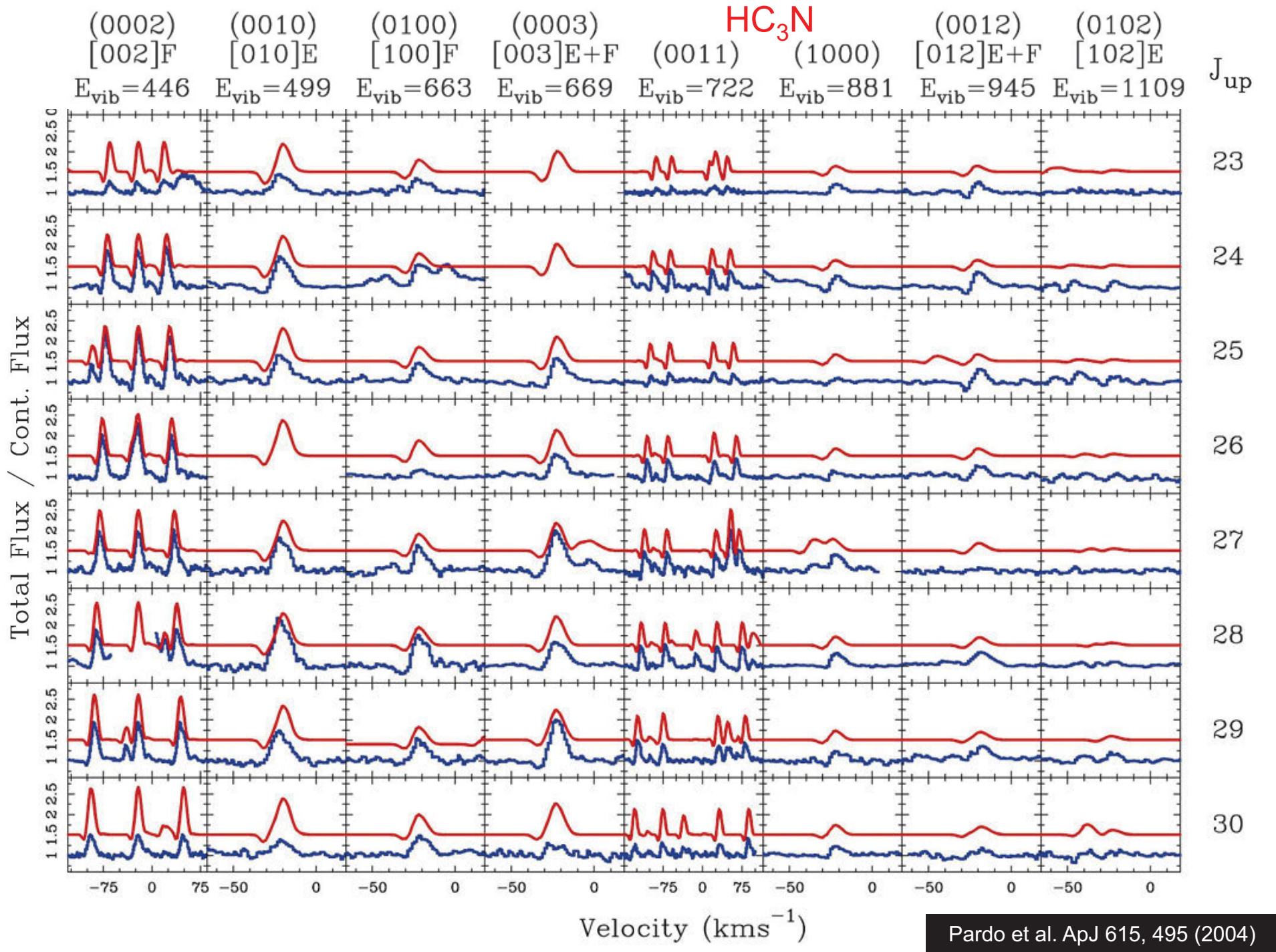
HC3N
(0002) [002]F Evib=446
(0010) [010]E Evib=499
(0100) [100]F Evib=663
(0003) [003]E+F Evib=669
(0011) Evib=722
(1000) Evib=881
(0012) [012]E+F Evib=945
(0102) [102]E Evib=1109
Jup
23
24
25
26
27
28
29
30
Total Flux / Cont. Flux
Velocity (kms−1)
Pardo et al. ApJ 615, 495 (2004)

TEMPERATURE AND HC_3N COLUMN DENSITY IN THE INNER SLOWLY EXPANDING ENVELOPE OF CRL 618 FROM χ^2 FITTING OF LINES IN VIBRATIONALLY EXCITED STATES OF HC_3N

$$\chi = \frac{1}{Nl} \sum_i \sqrt{\frac{\sum_j |Yd - Ym|^2}{Nch}}$$

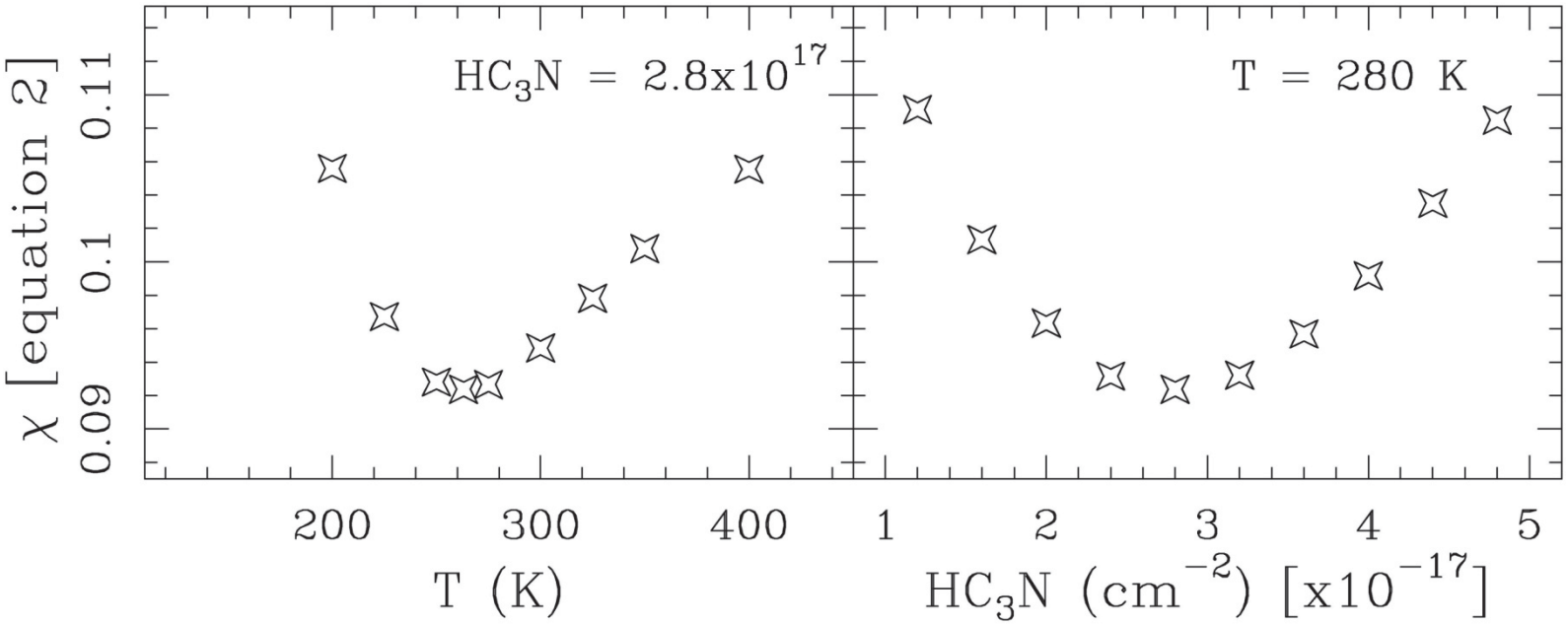

Inclination			40 deg
SEE		CCS	
parameter	value	parameter	value
Diameter	1.5”	Internal size	3.0”
Truncation	0.7	External size	4.5”
T_{rot}	263 K	α_T (see Fig. 1)	30 deg
v_r at 0.27”	5.0 kms^{-1}	$T^{CCS}_{rot,HC_{5,7}N}$	50-70 K
v_r at 1.5”	12.0 kms^{-1}	$T^{CCS}_{rot,other}$	∼30 K
v_{xy} at 0.27”	0.0 kms^{-1}	[HC_3N] at 3.0”	0.8 cm^{-3}
v_{xy} at 1.5”	6.0 kms^{-1}	[HC_3N] exponent	-1.0
v_{turb} at 0.27”	3.5 kms^{-1}	v_{CCS} at 3.0”	22 kms^{-1}
v_{turb} at 1.5”	3.5 kms^{-1}	$v_{turb,CCS}$ at 3.0”	12 kms^{-1}
[HC_3N] at 0.27”	154 cm^{-3}	v_{CCS} at 4.5”	8 kms^{-1}
[HC_3N] exponent	-1.8	$v_{turb,CCS}$ at 4.5”	5 kms^{-1}

Notes - Angles in arcseconds refer to diameters.[HC_3N] exponents give the power law of density with respect to angular distance.
v_r: radial velocity. v_{xy}: azimuthal velocity. v_{turb}: Turbulence velocity.

Probing CRL 618 step by step: Cold Circumstellar Shell

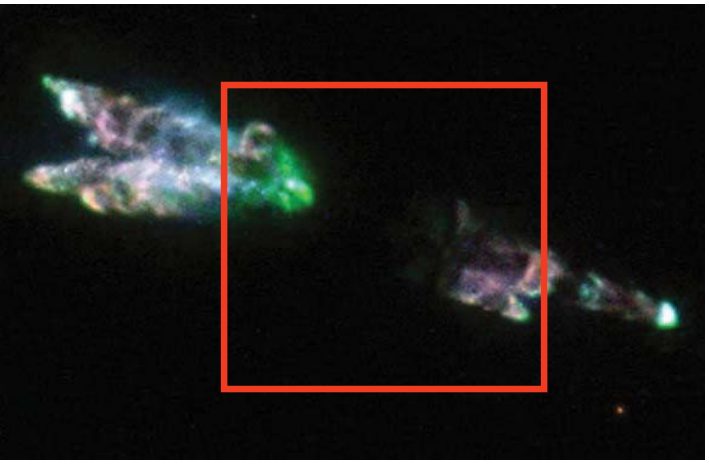

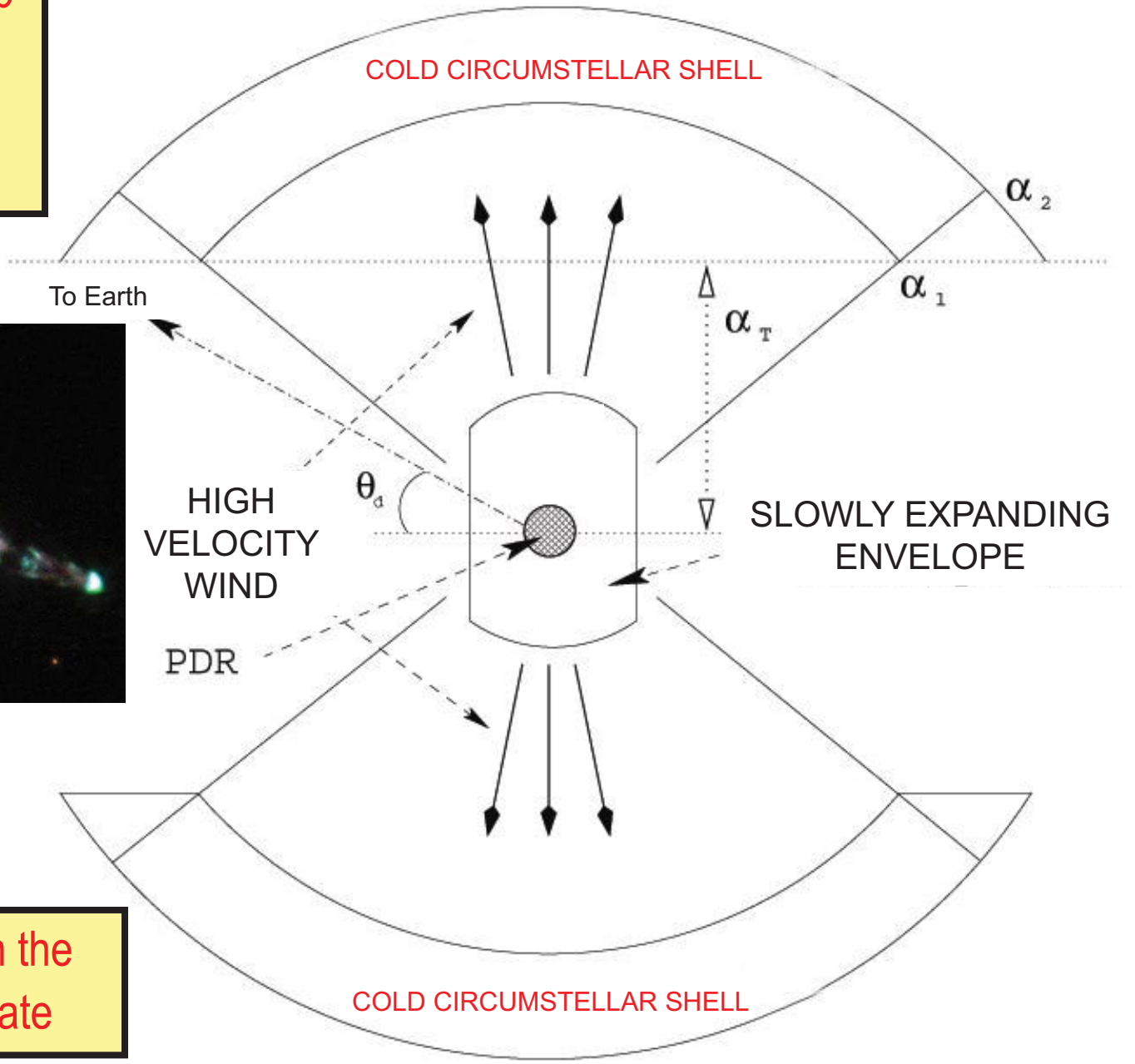

Tool: HC_3N & HC_5N in the ground vibrational state

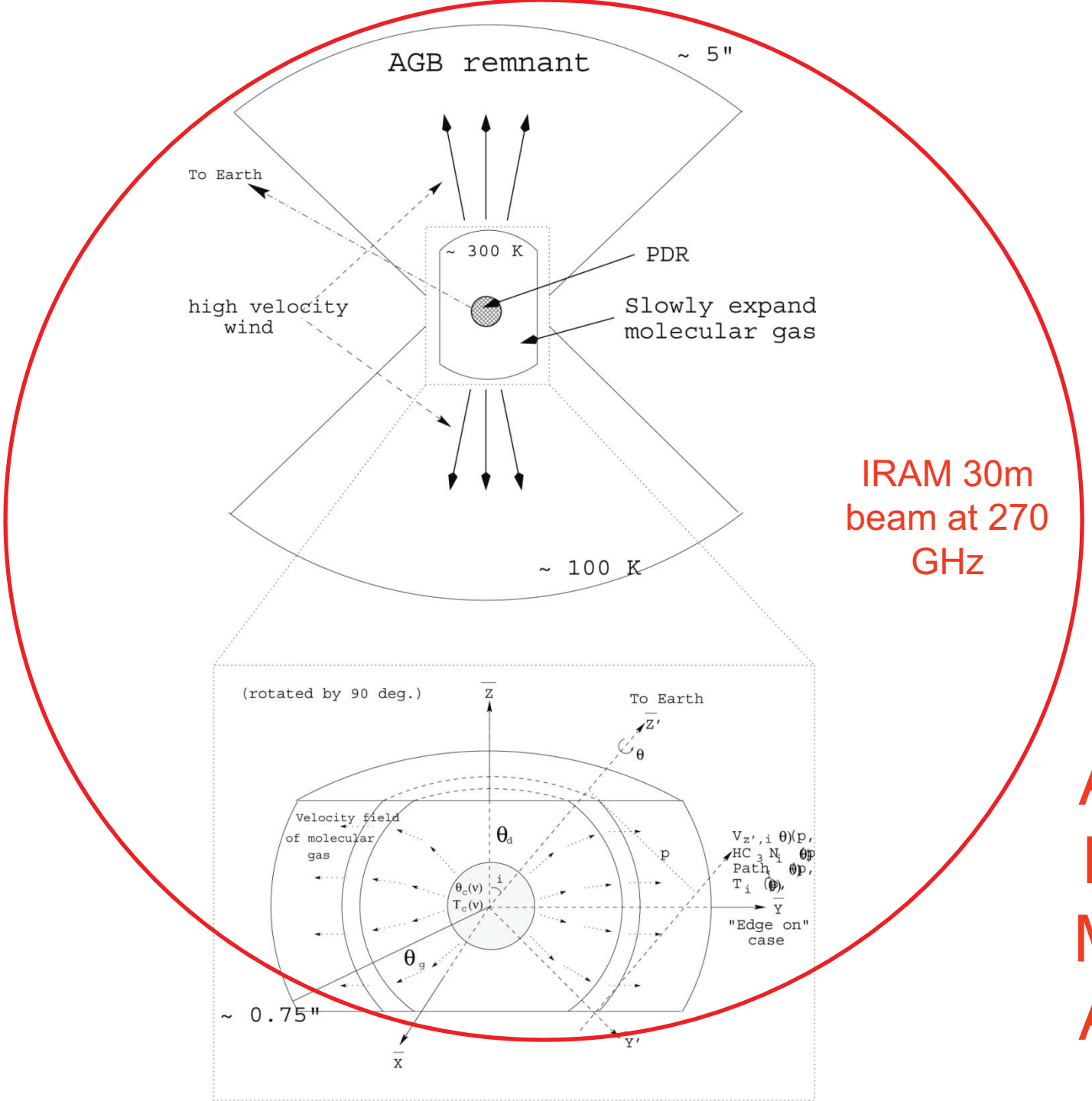
AGB remnant
~ 5"
To Earth
~ 300 K
PDR
high velocity wind
Slowly expand molecular gas
~ 100 K
IRAM 30m beam at 270 GHz
(rotated by 90 deg.)
Z
To Earth
Z'
θ
Velocity field of molecular gas
θd
p
i
θc(v)
Tc(v)
Y
"Edge on" case
θg
~ 0.75"
X
Y'
ALMA

Pardo et al. ApJ
628, 275 (2005)

HC_3N,
ground
vibrational
state

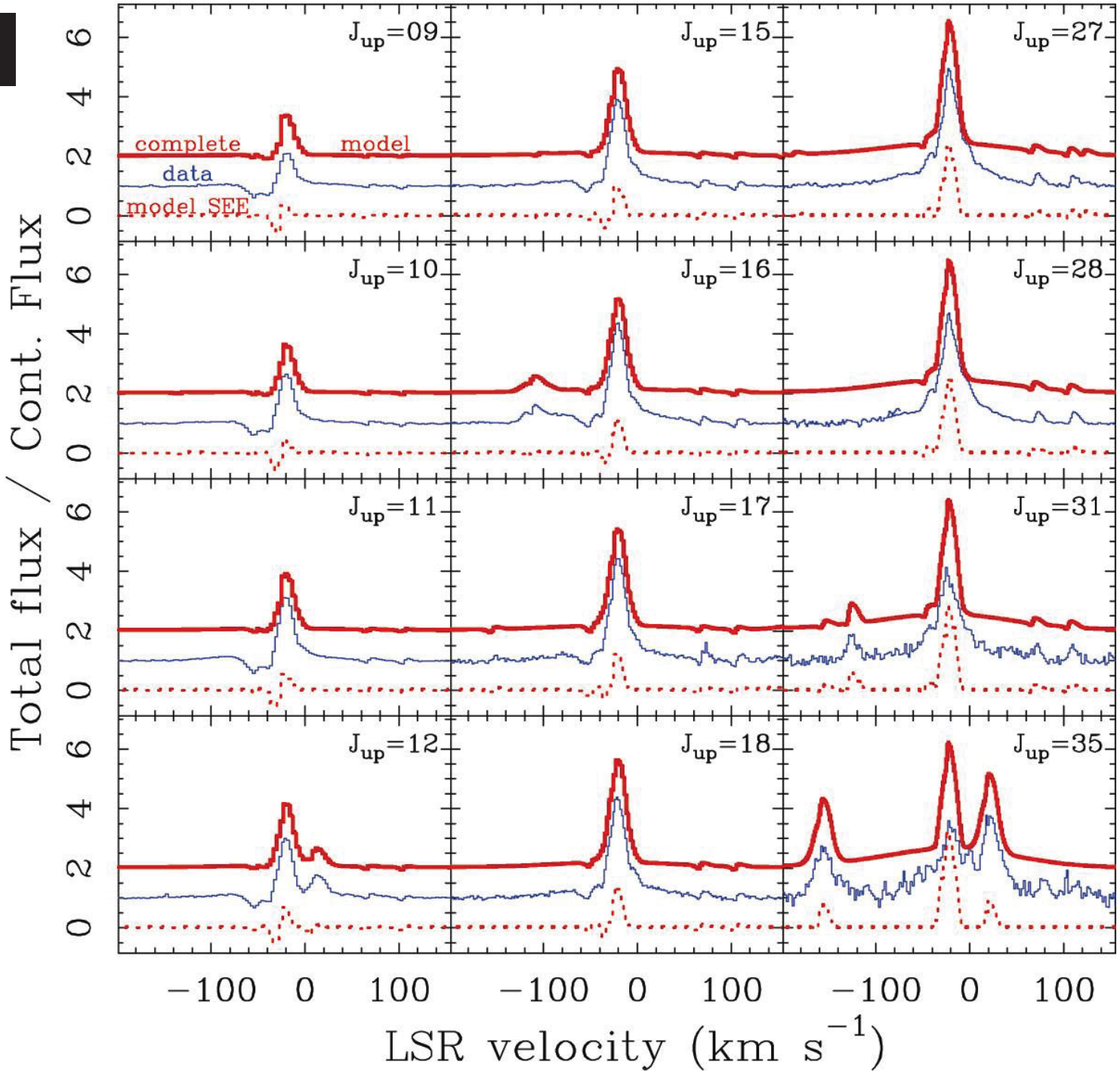

HC_5N, ground vibrational state

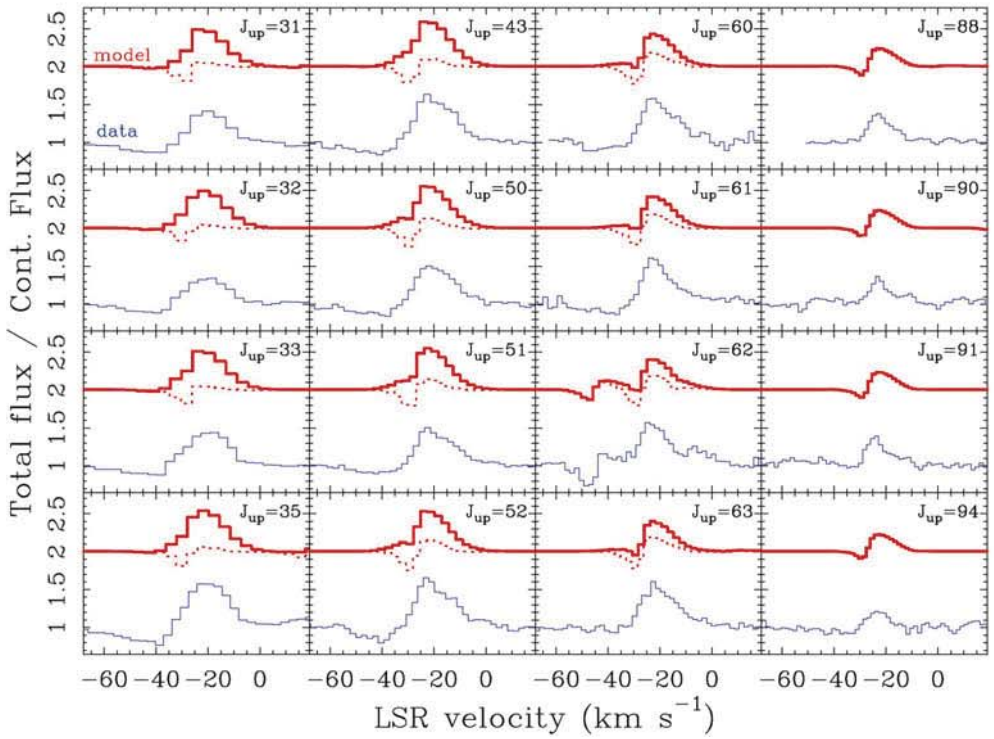

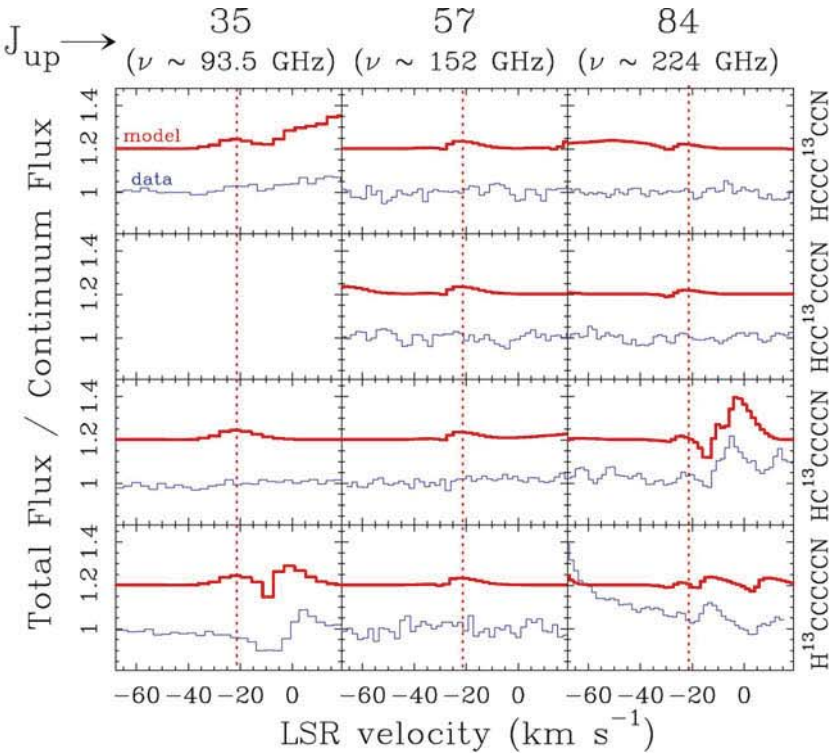

Pardo et al. ApJ
628, 275 (2005)

Inclination			40 deg
SEE		CCS	
parameter	value	parameter	value
Diameter	1.5”	Internal size	3.0”
Truncation	0.7	External size	4.5”
T_{rot}	263 K	α_T (see Fig. 1)	30 deg
v_r at 0.27”	5.0 kms^{-1}	$T^{CCS}_{rot,HC_{5,7}N}$	50-70 K
v_r at 1.5”	12.0 kms^{-1}	$T^{CCS}_{rot,other}$	∼30 K
v_{xy} at 0.27”	0.0 kms^{-1}	[HC_3N] at 3.0”	0.8 cm^{-3}
v_{xy} at 1.5”	6.0 kms^{-1}	[HC_3N] exponent	-1.0
v_{turb} at 0.27”	3.5 kms^{-1}	v_{CCS} at 3.0”	22 kms^{-1}
v_{turb} at 1.5”	3.5 kms^{-1}	$v_{turb,CCS}$ at 3.0”	12 kms^{-1}
[HC_3N] at 0.27”	154 cm^{-3}	v_{CCS} at 4.5”	8 kms^{-1}
[HC_3N] exponent	-1.8	$v_{turb,CCS}$ at 4.5”	5 kms^{-1}

Notes.- Angles in arcseconds refer to diameters.[HC_3N] exponents give the power law of density with respect to angular distance. v_r: radial velocity. v_{xy}: azimuthal velocity. v_{turb}: Turbulence velocity.

Probing CRL618 step by step High Velocity Wind

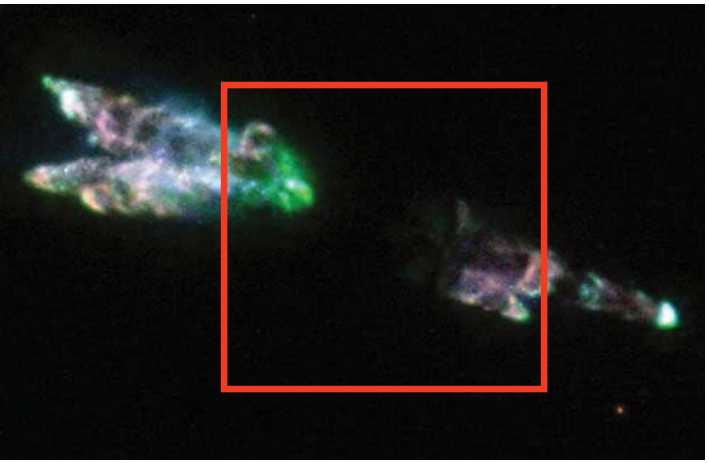

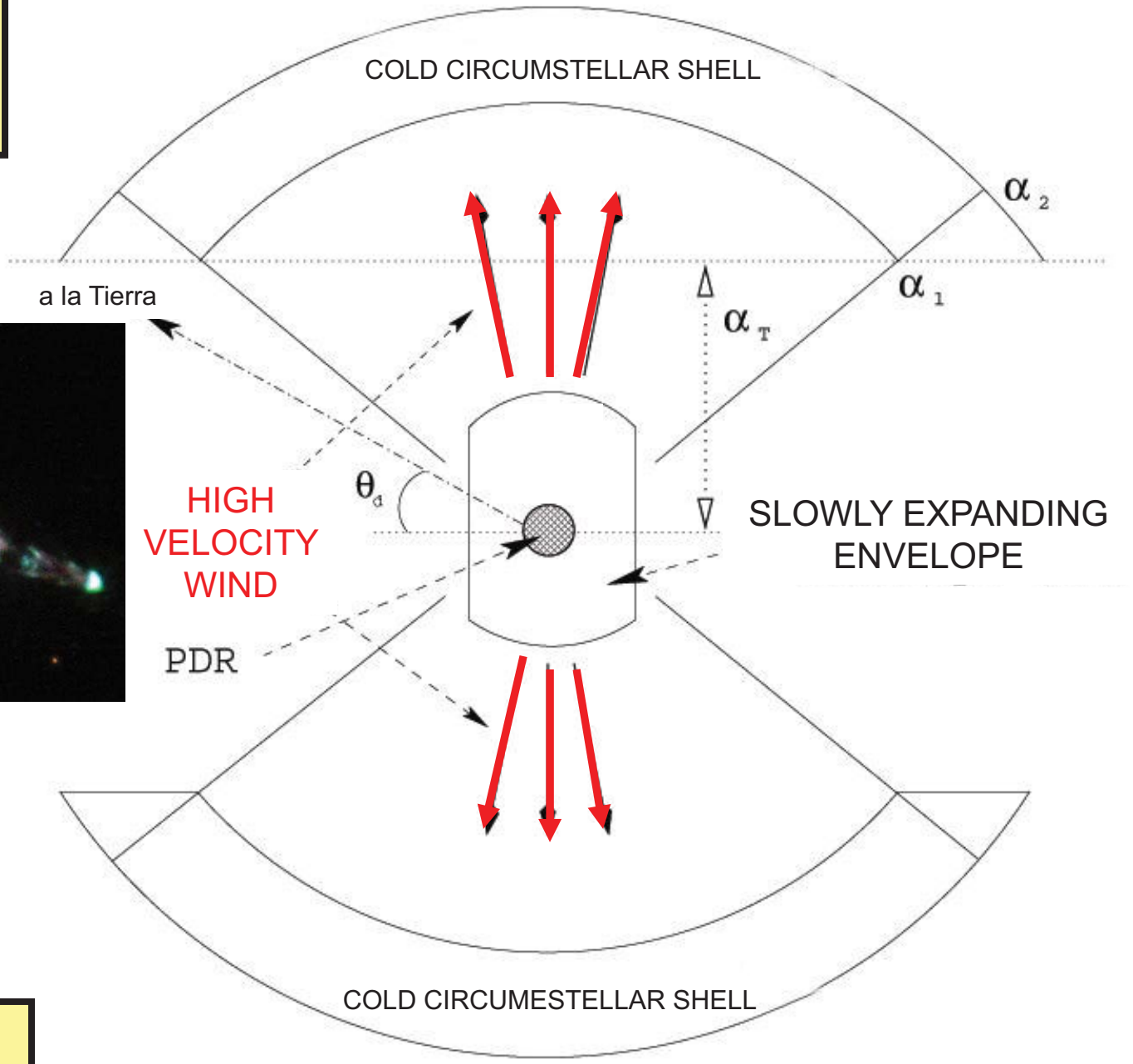

Tool: CO,HCN, HCO^+

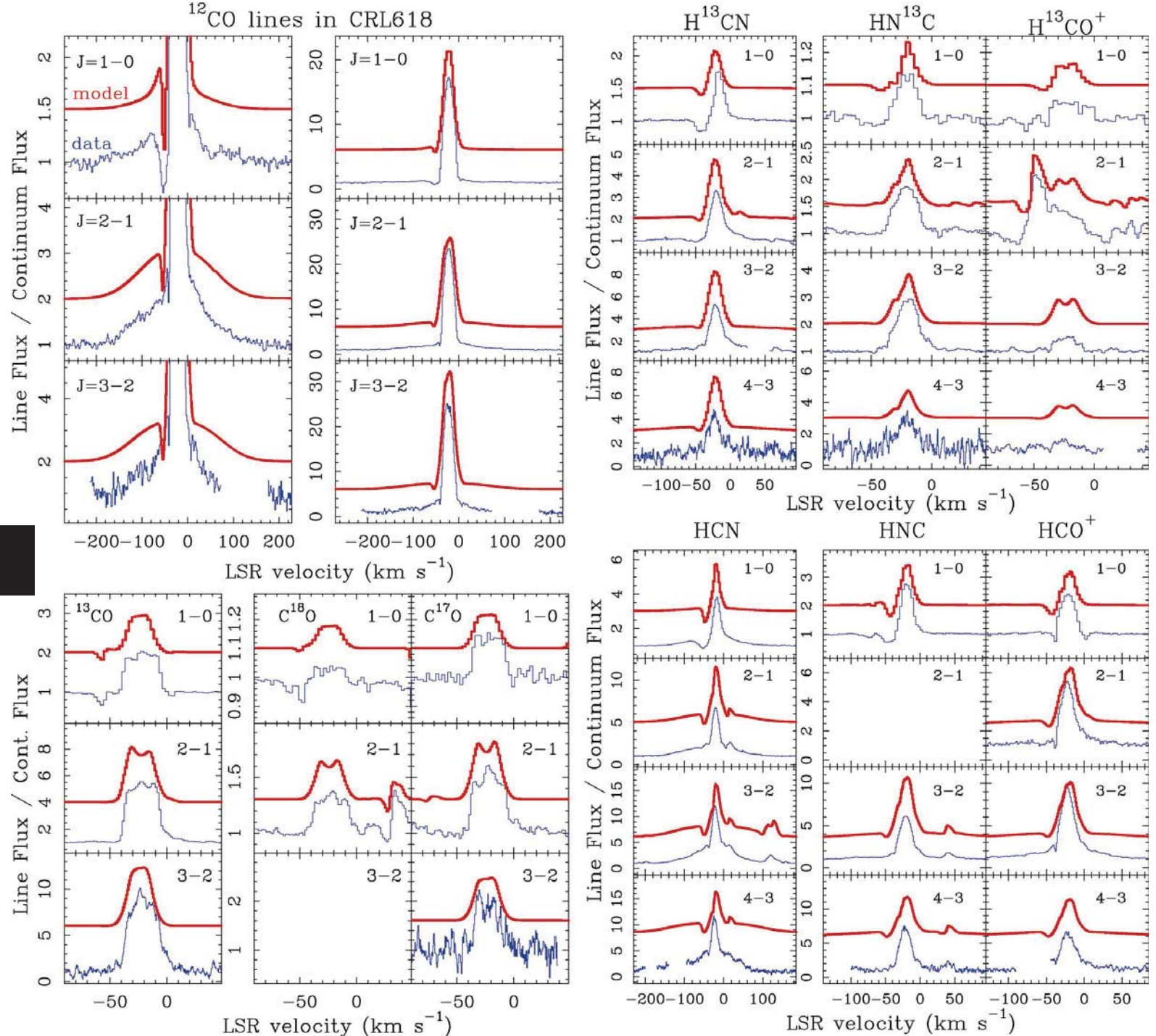

Pardo et al.
ApJ

High-angular resolution CO mapping

OVRO 1” resolution CO *J*=2-1 mapping of the PPN CRL618

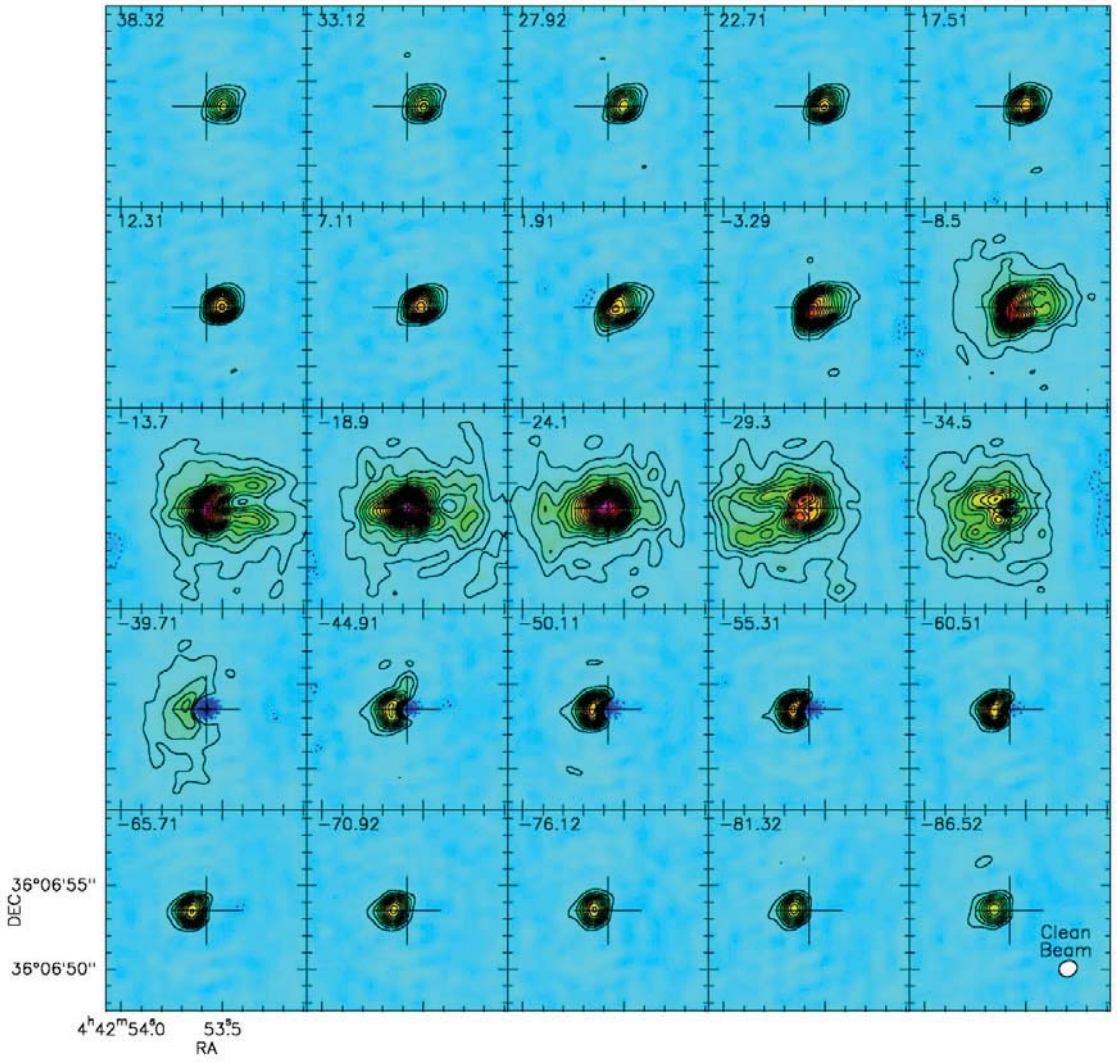

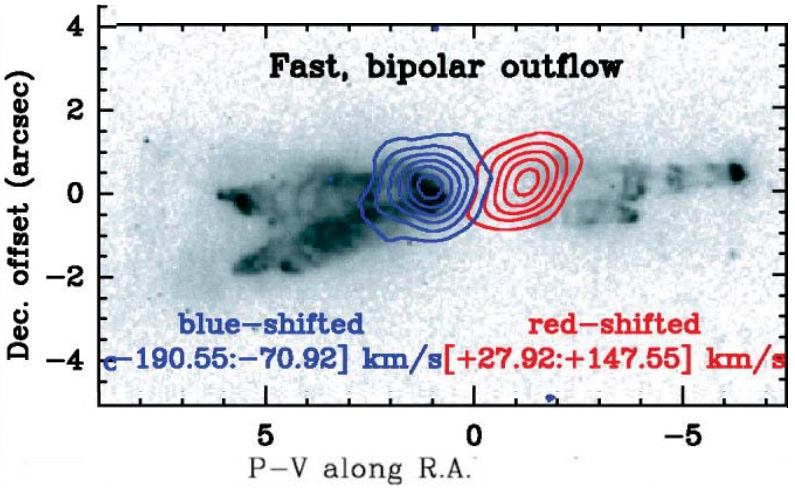

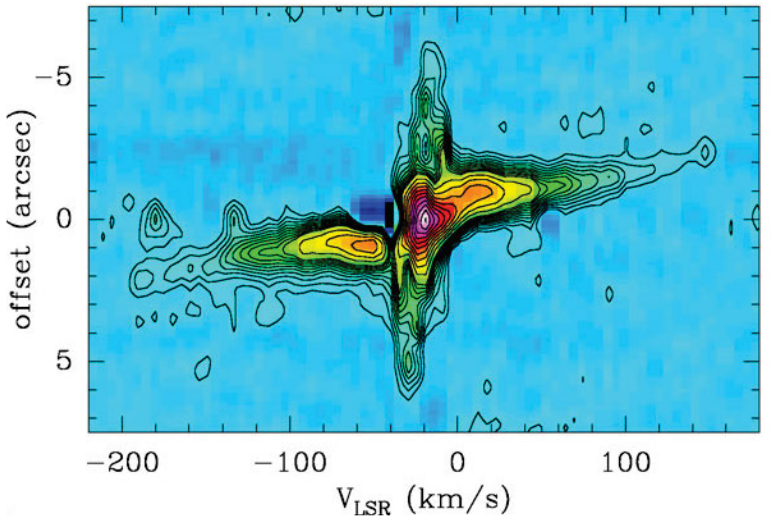

L+H ~1” Δv~5km/s

~3 tracks

Sánchez Contreras et al. 2004, ApJ 617,1142

Probing CRL618 step by step - CHEMICAL ABUNDANCES

Introducing all detected molecules in the model stablished with the previous analysis, we can try to fit the data using only the chemical abundances as free parameter.

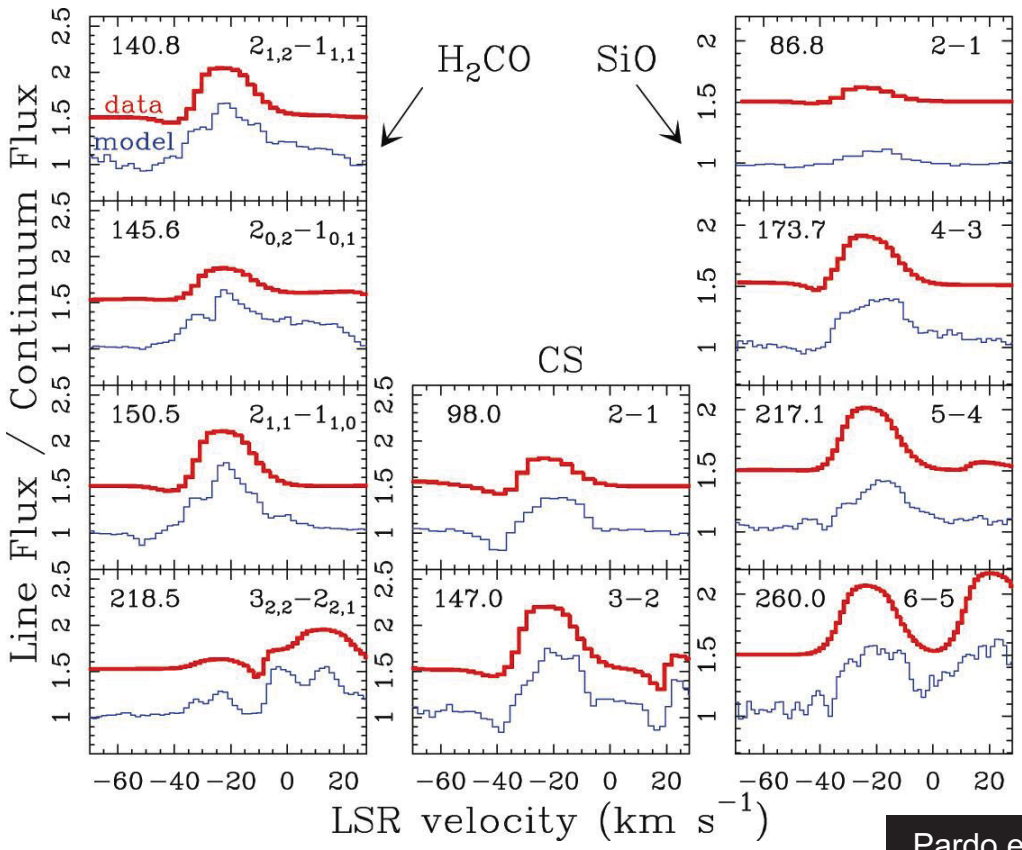

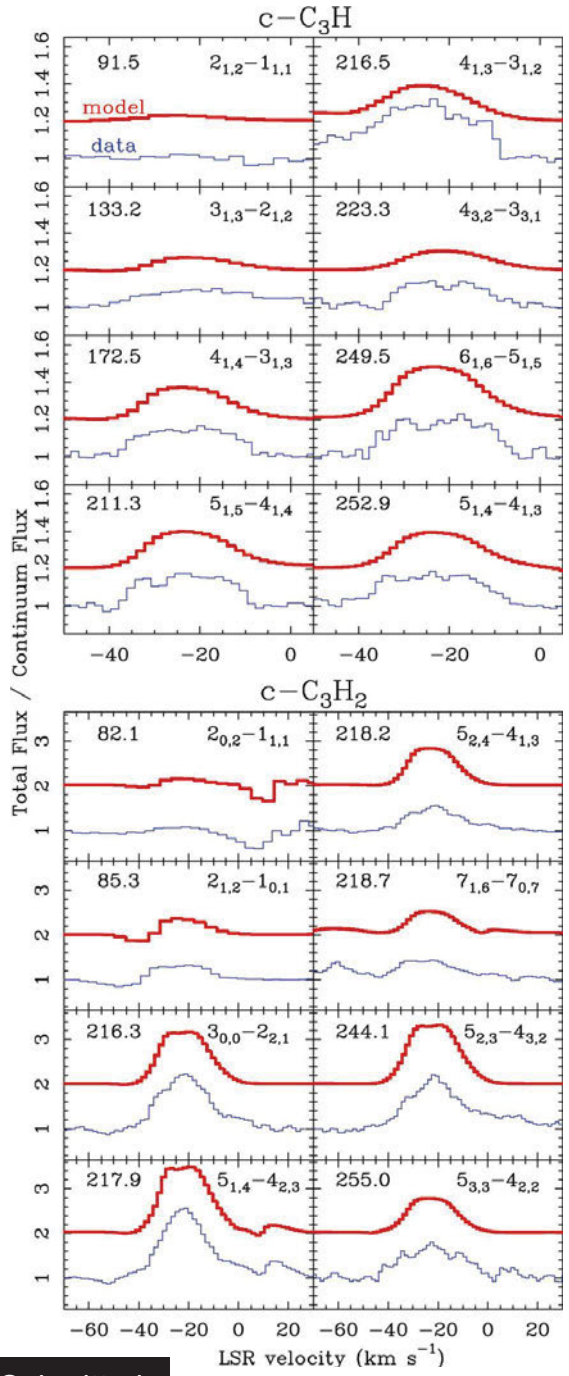

Pardo et al. ApJ Submitted

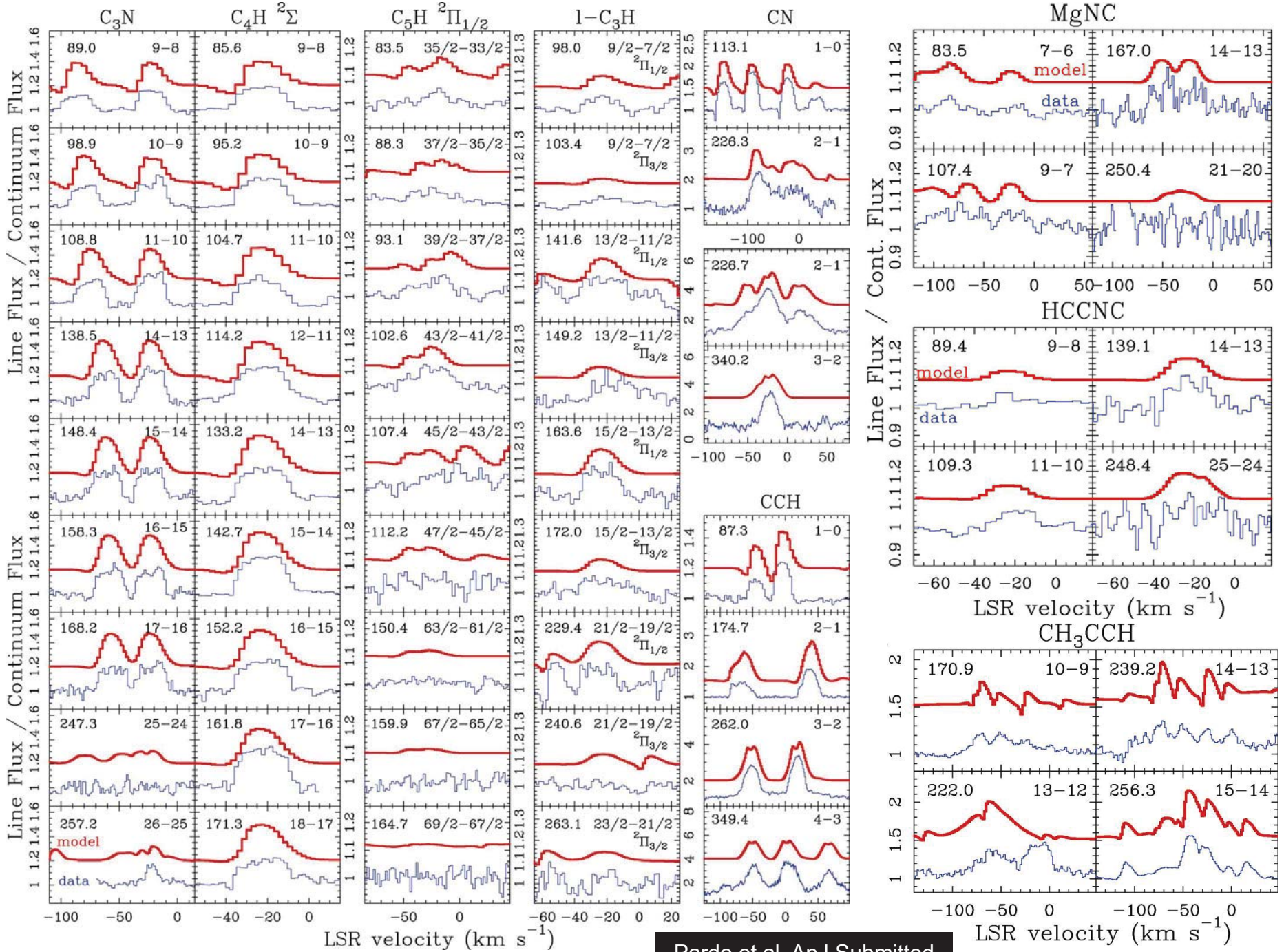

Pardo et al. ApJ Submitted

Molecule and vib. state	E_{vib} (cm^{-1})	J_{up} range	Range E_{rot} (cm^{-1})	Total Num. of lines	[X]/[HC_3N] in SEE	[X]/[HC_3N] in HVW	[X]/[HC_3N] in CCS
HC_3N v=0		9-30	15-205	17	0.4092	0.2325	0.9905
HC_3N ν_7	223	9-30	15-205	34	0.2412	0.1859	0.0095
HC_3N $2\nu_7$	446	9-30	15-205	51	0.1065	0.1115	-
HC_3N ν_6	499	9-30	15-205	34	0.0531	0.0598	-
HC_3N ν_5	663	9-30	15-205	34	0.0216	0.0304	-
HC_3N $3\nu_7$	669	9-30	15-205	68	0.0418	0.0594	-
HC_3N $\nu_7+\nu_6$	721	9-30	15-205	68	0.0313	-	-
HC_3N ν_4	880	9-30	15-205	17	0.0033	-	-
HC_3N $\nu_7+\nu_5$	886	9-30	15-205	68	0.0127	-	-
HC_3N $4\nu_7$	892	9-30	15-205	85	0.0154	-	-
HC_3N $2\nu_7+\nu_6$	944	9-30	15-205	102	0.0138	-	-
HC_3N $2\nu_6$	998	9-30	15-205	51	0.0052	-	-
HC_3N $\nu_7+\nu_4$	1103	11-30	15-205	34	0.0019	-	-
HC_3N $2\nu_7+\nu_5$	1109	11-30	15-205	102	0.0056	-	-
HC_3N $5\nu_7$	1115	11-30	15-205	102	0.0054	-	-
$H^{13}CCN$		10-31	20-218	18	0.0273	0.0155	0.0660
$HC^{13}CCN$		9-30	15-205	17	0.0273	0.0155	0.0660
$HCC^{13}CN$		9-30	15-205	17	0.0273	0.0155	0.0660
$H^{13}CCN$ ν_7	223	10-31	20-218	36	0.0161	-	-
$HC^{13}CCN$ ν_7	223	9-30	15-205	34	0.0161	-	-
$HCC^{13}CN$ ν_7	223	9-30	15-205	34	0.0161	-	-
$H^{13}CCN$ ν_6	499	10-31	20-218	36	0.0035	-	-
$HC^{13}CCN$ ν_6	499	9-30	15-205	34	0.0035	-	-
$HCC^{13}CN$ ν_6	499	9-30	15-205	34	0.0035	-	-
HCCNC		9-27	16-165	15	-	-	0.025
HC_5N v=0		31-104	39-485	56	0.0132	-	0.2794
HC_5N ν_{11}	105	31-104	39-485	112	0.0149	-	0.0451
HC_5N $2\nu_{11}$	210	31-104	39-485	168	0.0126	-	0.0055
HC_5N ν_{10}	230	31-104	39-485	224	0.0075	-	0.0023
HC_5N $3\nu_{11}$	315	31-95	39-402	188	0.0094	-	
HC_7N		72-85	96-134	14	-	-	0.056

Molecule and vib. state	E_{vib} (cm^{-1})	J_{up} range	Range E_{rot} (cm^{-1})	Total Num. of lines	[X]/[HC_3N] in SEE	[X]/[HC_3N] in HVW	[X]/[HC_3N] in CCS
CO		1-2	0-12	2	-	667	100
^{13}CO		1-2	0-11	2	2.5	-	2.5
$C^{17}O$		1-2	0-11	2	0.3	-	0.3
$C^{18}O$		1-2	0-11	2	0.2	-	0.2
HCO+		1-3	0-18	3	0.1	0.2	0.1
$H^{13}CO+$		1-3	0-18	3	-	-	0.003
HOC+				1			
HCN		1-3	0-18	3	2.0	2.0	1.5
HCN $\nu 2$	712	2-3	3-18	4			
$H^{13}CN$		1-3	3-17	3	0.133	0.133	0.033
HNC		1-3	0-18	2	0.2	0.2	0.167
HNC $\nu 2$	477	1-3	3-18	2			
$HN^{13}C$		1-3	0-18	3	0.013	0.01	0.004
H_2CO		-	0.64	10	-	-	0.125
SiO		2-6	1-30	5	-	-	0.013
CS		2-5	2-35	3	-	-	0.125
N_2H^+		1-1	0-3	1	-	-	0.025
c-C_3H_2			2-134	66	-	-	0.36
MgNC		7-14	8-36	12	-	-	0.10
CH_3CN		5-15	9-300	8*	0.067	0.100	0.033
CH_3CCH		5-16	6-315	10*	1.0	2.0	0.200
CH_2CHCN							0.067
CN		1-2	0-11	2*	-	-	4.0
^{13}CN		1-2	0-11	2*	-	-	0.25
CCH		1-3	0-18	3*	-	-	0.5
C_3N		9-22	14-77	10	-	-	0.118
c-C_3H			0-41	27	-	-	0.050
l-C_3H			5-52	31	-	-	0.017
C_4H		9-29	14-142	34	-	-	1.0
C_5H		-	23-100	40	-	-	0.005

3 mm WINDOW: Data and final model

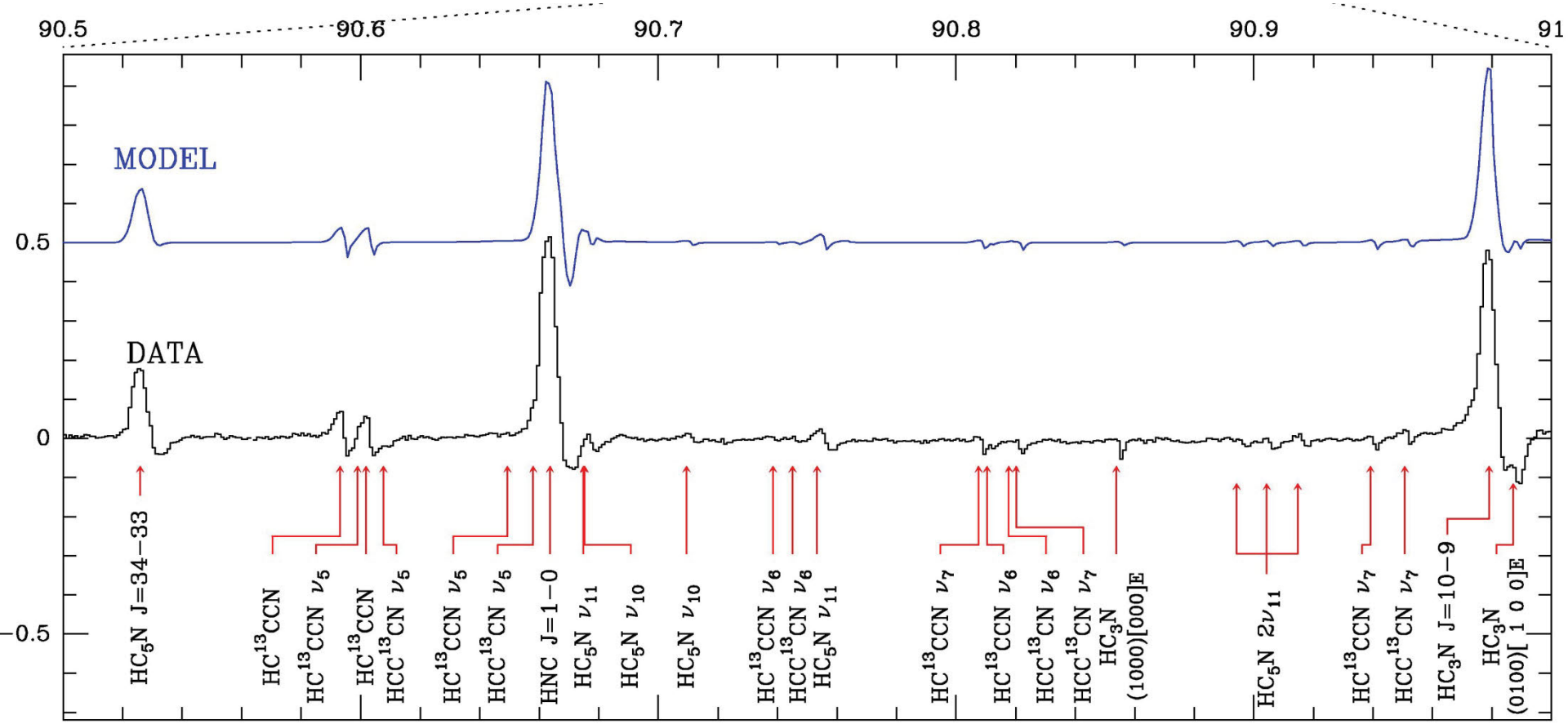

2 mm window: Data and final model

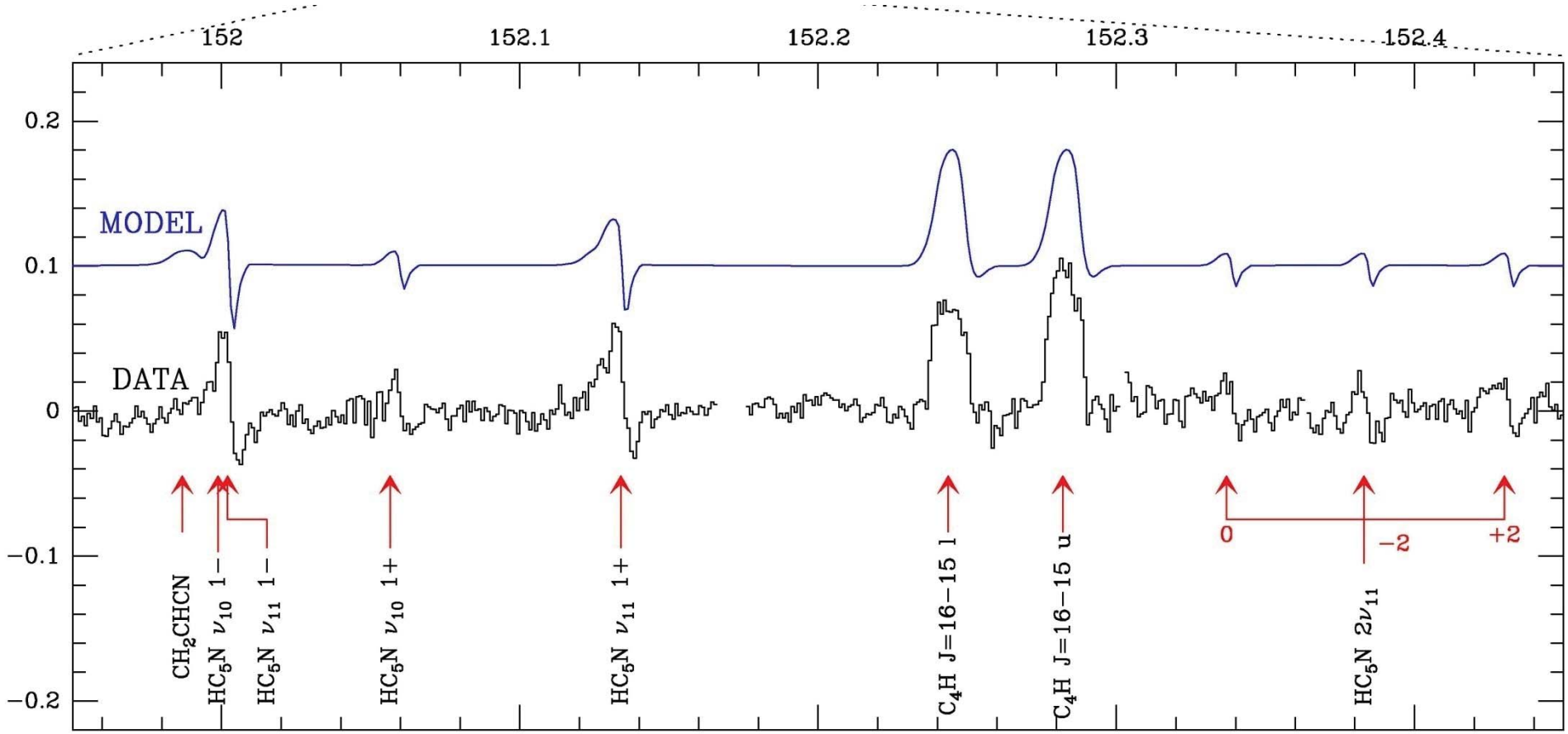

1.3 mm window: Data and final model

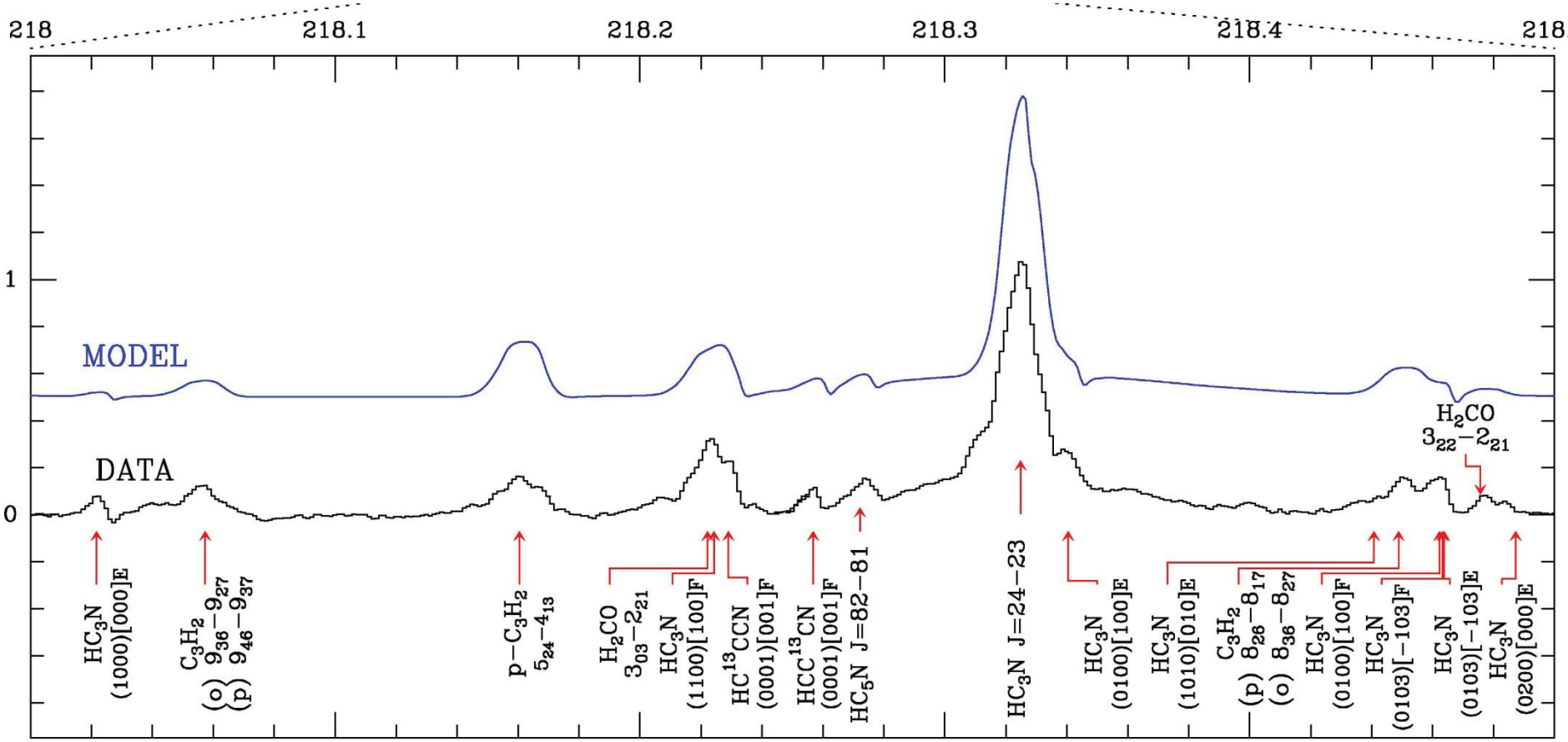

1 mm window: Data and final model

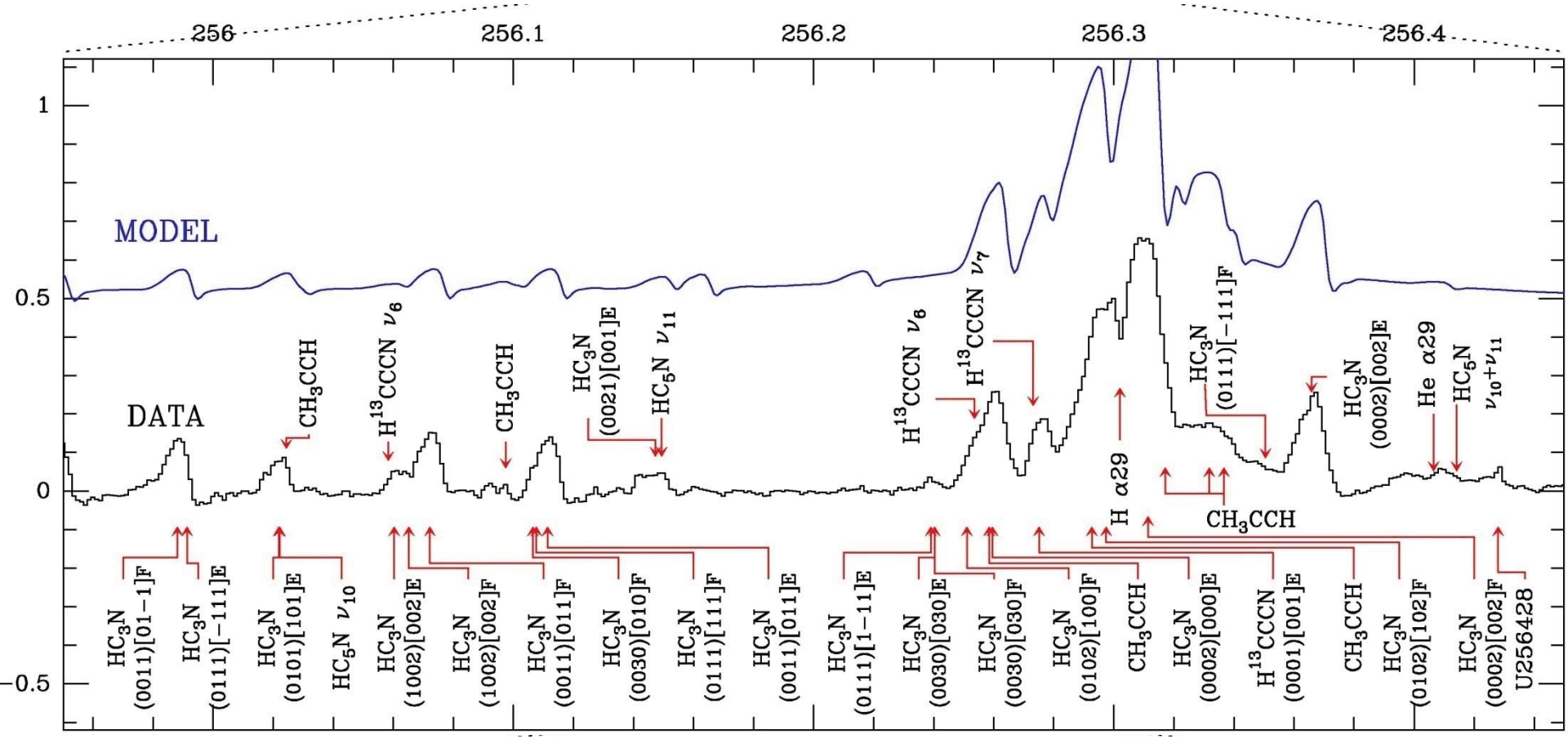

These results are complementary of our previous infrared studies with ISO

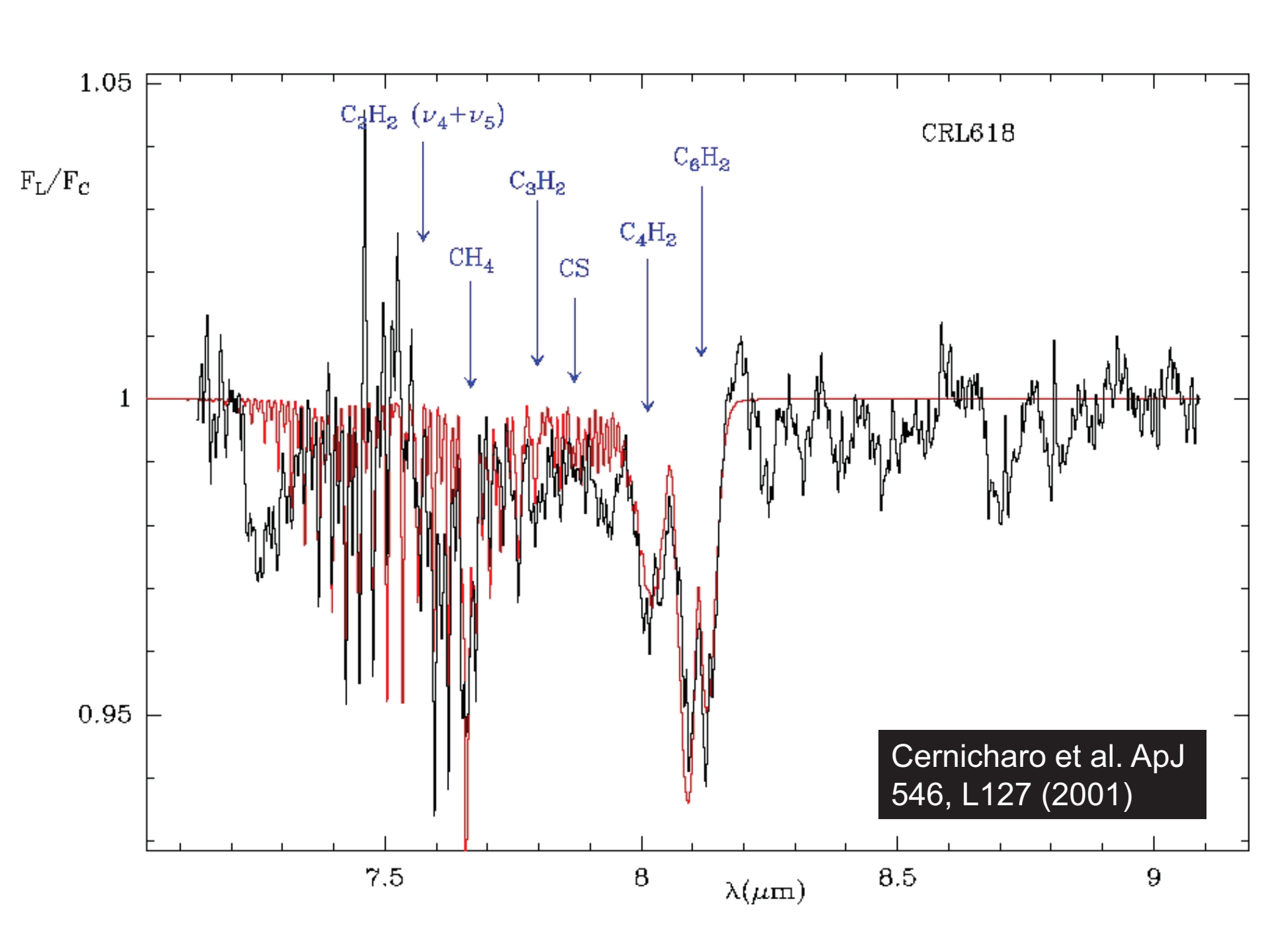
1.05
1
0.95
F_L/F_C
C_2H_2 ($\nu_4+\nu_5$)
CH_4
C_3H_2
CS
C_4H_2
C_6H_2
CRL618
7.5
8
8.5
9
$\lambda(\mu m)$
Cernicharo et al. ApJ 546, L127 (2001)

Growth of Carbon chains according to these schemes is very efficient in CRL618

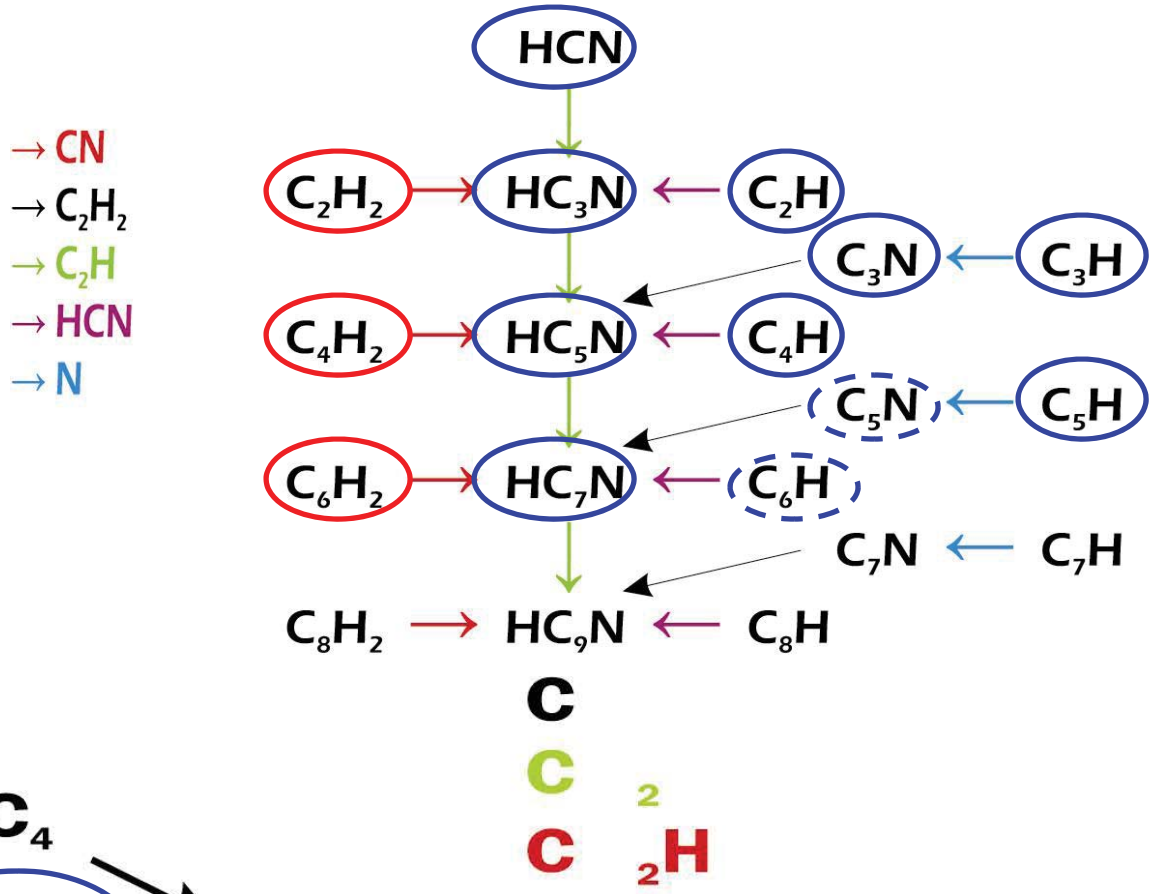

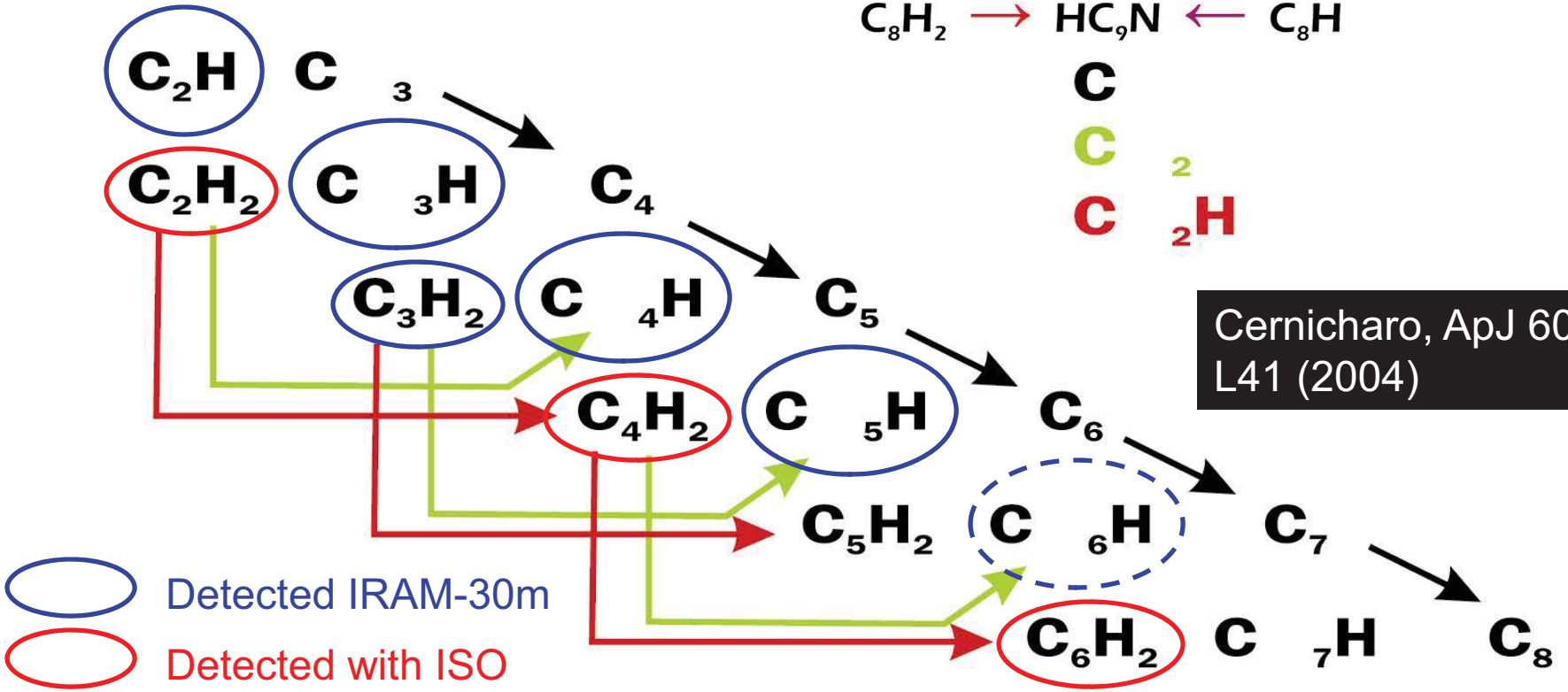

Cernicharo, ApJ 608, L41 (2004)

Summary: Steps forward in the understanding of CRL 618 achieved with this work

- Getting around the problem of the poor angular resolution, we have been able to establish with a great accuracy, :
  - The morphology.
  - The physical conditions.
  - The chemical abundances at least of the polar species.
- The results obtained are being used in chemical models to try to explain the formation of species of biological interest, such as benzene (already detected).
- The spectroscopic model obtained for this object is the most detailed up to date. Only 80 features in the data remain unknown. All the others are assigned and, for the most part, modelled.
- These results pave the way for future works with ALMA and Herschel, that should allow a much better angular resolution, and larger frequency coverage.

This work is the result of a long collaboration with :

M. Guélin
M. Agúndez
J.R. Goicoechea
J.R. Pardo
B. Tercero
P. Fonfría

L. Margules
I. Kleiner
M. Carvajal
J. Demaison
K. Demyck
G. Wlodarczak
J.L. Alonso
C. López
J. Pearson